

2014

AMPHIPHILIC CYCLIC CELL-PENETRATING PEPTIDES AS DRUG DELIVERY VEHICLES AND ANTIMICROBIAL PEPTIDES

Donghood Oh
University of Rhode Island, odh153@gmail.com

Follow this and additional works at: https://digitalcommons.uri.edu/oa_diss

Terms of Use

All rights reserved under copyright.

Recommended Citation

Oh, Donghood, "AMPHIPHILIC CYCLIC CELL-PENETRATING PEPTIDES AS DRUG DELIVERY VEHICLES AND ANTIMICROBIAL PEPTIDES" (2014). *Open Access Dissertations*. Paper 213.
https://digitalcommons.uri.edu/oa_diss/213

This Dissertation is brought to you by the University of Rhode Island. It has been accepted for inclusion in Open Access Dissertations by an authorized administrator of DigitalCommons@URI. For more information, please contact digitalcommons-group@uri.edu. For permission to reuse copyrighted content, contact the author directly.

AMPHIPHILIC CYCLIC CELL-PENETRATING
PEPTIDES AS DRUG DELIVERY VEHICLES AND
ANTIMICROBIAL PEPTIDES

BY

DONGHOON OH

A DISSERTATION SUBMITTED IN PARTIAL FULFILLMENT OF THE
REQUIREMENTS FOR THE DEGREE OF
DOCTOR OF PHILOSOPHY
IN
BIOMEDICAL AND PHARMACEUTICAL SCIENCES

UNIVERSITY OF RHODE ISLAND

2014

DOCTOR OF PHILOSOPHY DISSERTATION

OF

DONGHOON OH

APPROVED:

Dissertation Committee:

Major Professor Keykavous Parang

Roberta S. King

Geoffrey D. Bothun

Nasser H. Zawia
DEAN OF THE GRADUATE SCHOOL

UNIVERSITY OF RHODE ISLAND
2014

ABSTRACT

Cell membrane is a barrier to be overcome for efficient delivery of therapeutics into a target site in cytoplasm or nucleus. The hydrophobic phospholipids are major components of the cell membrane that obstruct the transportation of therapeutics. Thus, various delivery systems, such as liposomes, nanoparticles and viral vectors, have been developed to transfer small molecules, peptides, proteins, and oligonucleotides across the membrane.

Negatively charged phosphopeptides, oligonucleotides, and siRNAs have emerged as potential therapeutic agents. Phosphopeptides mimic phosphoproteins, which give on/off signal to many enzymes through interactions with protein kinases. For example, phosphopeptide pTyr-Glu-Glu-Ile (pYEEI) is an optimal peptide ligand for binding to the Src tyrosine kinase SH2 domain. Oligonucleotides have been introduced as antisense drugs to inhibit the translation of mRNA that transfers the coding information from genes. Small interfering RNA (siRNA)-based therapy has been also spotlighted since the discovery of RNA interference (RNAi) phenomenon. However, the cellular delivery of phosphopeptides, oligonucleotides, and siRNAs is a major obstacle despite many advantages of these compounds. Phosphopeptides contain negatively charged phosphate group, and/or negatively charged amino acids, such as glutamic acid or aspartic acid, in their sequences. Oligonucleotides and siRNAs are polymers composed of nucleosides, which are connected through negatively charged phosphodiester groups. These negatively charged molecules are hard to enter cancer cells by diffusion because cancer cell membranes are composed of negatively charged lipids. In addition, when a naked siRNA is administered *in vivo*, it

does not show efficient cellular uptake in most mammalian cells and is quickly disappeared in the blood. Thus, developing carriers to improve the cellular uptake delivery of negatively charged cell-impermeable compounds has become a subject of major interest. Novel strategies are urgently needed to circumvent the problems associated with the delivery of these compounds.

Cell-penetrating peptides (CPPs) have become one of the emerging vehicles for delivery of cargo drugs. CPPs are short hydrophilic or amphiphilic peptides that have plenty of positively charged amino acids, such as lysine or arginine, which can penetrate cell membranes. CPP-drug conjugates have been reported to help the cellular uptake of some drugs. Alternatively, they have been used as non-covalent drug delivery systems.

CPPs have been investigated for improving the intracellular delivery of negatively-charged molecules. By physical interaction between positive charges in CPPs and negative charges in phosphopeptides, oligonucleotides, and siRNAs, the cell penetration could be improved. Among many CPPs, arginine-rich peptides have been the subject of major focus because it has been known that the guanidine group of arginine side chain shows better interaction with the negatively charged phospholipid in the cell membrane. Tryptophan is also a key amino acid found in CPPs that enhances the interaction of peptides with lipids in the cell membrane.

Parang's laboratory has previously shown that monocyclic CPPs containing alternative arginine and tryptophan have potential applications for drug delivery. Cyclic peptides have several benefits compared to linear peptides, such as stability against proteolytic enzymes and rigidity of structure. The rigidity of the structure can

enhance the binding affinity of ligands toward receptors by reducing the freedom of possible structural conformations. Cyclic peptides are also present in nature and have been developed as therapeutics. Cyclosporin, gramicin S, polymyxin B, and daptomycin are well-known examples of cyclic peptides. Parang's laboratory designed amphiphilic cyclic CPPs containing alternative tryptophan and arginine residues as the hydrophobic and positively charged residues, respectively. The peptides were efficient in improving the cellular delivery of anticancer and antiviral drugs.

In this dissertation, we designed novel classes of amphiphilic cyclic peptides for improving the intracellular delivery of cell-impermeable phosphopeptides, and their antimicrobial activities were investigated. The **hypothesis** of this dissertation is that amphiphilic cyclic peptides, having positively charged arginines on one side of structures and hydrophobic tryptophan (or fatty acid) on the other side, can enhance intracellular drug delivery and/or act as antimicrobial agents having synergy with other antibiotics.

In **Manuscript I** (Submitted to *Angewandte Chemie International Edition*), we designed amphiphilic bicyclic peptides as cellular delivery agents. The objective of this manuscript was to design a novel class of bicyclic CPPs containing two monocyclic peptides of tryptophan and arginine amino acids. Two bicyclic peptides [W₅G]-(triazole)-[KR₅] and [W₅E]-(β -Ala)-[KR₅] were synthesized by conjugation of two monocyclic peptides using click chemistry and amide synthesis, respectively. A corresponding linear peptide, W₅G-(triazole)-KR₅, and a monocyclic peptide with a linear component, [W₅G]-(triazole)-KR₅, were synthesized as controls. Among all peptides, [W₅E]-(β -Ala)-[KR₅] improved the cellular delivery of fluorescein-labeled

phosphopeptide, F'-GpYEEI by 19.3-fold. Confocal microscopy showed that the corresponding fluorescein-labeled bicyclic peptide F'-[KW₄E]-(β-Ala)-[KR₅] was localized in the cytosol and nucleus in human ovarian adenocarcinoma (SK-OV-3) cells. Studying the cellular uptake of F'-[KW₄E]-(β-Ala)-[KR₅] in the presence of endocytosis inhibitors indicated that the clathrin- and caveolin-dependent endocytosis were the main pathways for cellular uptake. [W₅E]-(β-Ala)-[KR₅] enhanced the intracellular uptake of fluorescein-labeled phosphopeptide, F'-GpYEEI by 4.5- and 3.0-fold compared to those of well-known cell-penetrating peptides (CPPs), TAT and CR₇, respectively. The bicyclic peptide was able to improve antiproliferative activity of doxorubicin by 20%. Thus, this manuscript suggests that amphiphilic bicyclic peptides containing tryptophan and arginine can be utilized as a new class of cell-penetrating peptides and potential cellular delivery tools.

In **Manuscript II** (Submitted to *Molecular Pharmaceutics*), we investigated the role of fatty acylation and cyclization for intracellular transport of phosphopeptides in short-length polyarginine peptides. Most of the reported arginine-rich CPPs to enhance intracellular drug delivery are linear peptides, and have more than seven arginines to retain cell penetrating properties. Herein, we synthesized penta and hexaarginine peptides (R₅ and R₆), and explored the effect of acylation and cyclization on the cell penetrating properties of the peptides. The fluorescence-labeled acylated cyclic peptide dodecanoyl-[R₅] and linear peptide dodecanoyl-(R₅) showed approximately 13.7- and 10.2-fold higher cellular uptake than that of control 5(6)-carboxyfluorescein, respectively. The mechanism of the peptide internalization into cells was found to be energy-dependent endocytosis. The molecular transporter property of fatty acylated

cyclic peptides was compared with those of fatty acylated linear peptide and nonacylated cyclic peptide using flow cytometry. The combination of acylation and cyclization (dodecanoyl-[R₅]) enhanced intracellular delivery of a fluorescence-labeled phosphopeptide (F'-GpYEEI) in human SK-OV-3 cancer cell line. Dodecanoyl-[R₅] and dodecanoyl-[R₆] enhanced the intracellular uptake of a fluorescence-labeled cell impermeable negatively charged phosphopeptide (F'-GpYEEI) in human ovarian cancer cells (SK-OV-3) by 3.4-fold and 5.5-fold, respectively. The cellular uptake of F'-GpYEEI in the presence of hexadecanoyl-[R₅] was 9.3- and 6.0-fold higher than that of in the presence of octanoyl-[R₅] and dodecanoyl-[R₅], respectively. A comparative FACS results showed that dodecanoyl-[R₅] enhanced the cellular uptake of the phosphopeptide by 1.4-2.5 fold higher than the corresponding linear peptide dodecanoyl-(R₅) and those of representative CPPs, such as hepta-arginine (CR₇) and TAT peptide. In this manuscript, we found that a combination of acylation by long chain fatty acids and cyclization on short arginine-containing peptides can improve their cell-penetrating property, possibly through efficient interaction of rigid positively charged R and hydrophobic dodecanoyl moiety with the corresponding residues in the cell membrane phospholipids.

In **Manuscript III** (to be submitted to *Molecular Pharmaceutics*), the antimicrobial activities of cyclic CPPs were investigated against multidrug resistant pathogens. Antimicrobial peptides and CPPs share similar structural features. Based on the intracellular delivery property of amphiphilic cyclic peptides in manuscript II, we synthesized several amphiphilic cyclic CPPs and their analogs, and investigated antibacterial activities against multidrug resistant pathogens. [R₄W₄] exhibited a

potent antibacterial activity, exhibiting MIC value of 2.67 $\mu\text{g}/\text{mL}$ against methicillin-resistant *Staphylococcus aureus* (MRSA). Cyclic [R₄W₄] and the linear counterpart R₄W₄ exhibited MIC values of 42.8 and 21.7 $\mu\text{g}/\text{mL}$, respectively, against *Pseudomonas aeruginosa*. [R₄W₄] in combination with tetracycline enhanced the potency, by decreasing the MIC 4 fold (0.12 $\mu\text{g}/\text{mL}$), suggesting partial synergistic effect of the combination between [R₄W₄] and tetracycline against MRSA. Twenty-four hour time-kill studies evaluating [R₄W₄] in combination with tetracycline demonstrated bactericidal activity against MRSA and *E. coli*. [R₄W₄] showed cell-penetrating properties as expected, and exhibited more than 84% cell viability at 15 μM (20.5 $\mu\text{g}/\text{mL}$) concentration against three different human cell lines. This study suggests that amphiphilic cyclic CPPs, when used in combination with antimicrobials could provide additional benefit to defeat multi-drug resistant pathogens.

In summary, the studies in this dissertation provided insights and a deep understanding of applications of cyclic cell-penetrating peptides to enhance intracellular uptake of cargo drugs, and their antimicrobial activities as drug alone or combination with other antibiotics. Amphiphilic bicyclic peptides are the first reported bicyclic peptides as CPPs and molecular transporters. Acylated cyclic polyarginines showed that short polyarginines can be utilized as CPPs to have cell-penetrating properties by combining fatty acylation and cyclization. Moreover, this study provided a potential of amphiphilic cyclic CPPs as antimicrobial agents that their potency could be maximized by the combination with other antibiotics possibly through their drug delivery properties. Overall, these findings will be beneficial for the scientific

community in academia and industry working in the area of designing molecular transporters of cell impermeable compounds, and cellular delivery.

ACKNOWLEDGMENTS

This doctoral dissertation has been completed by the support of many people around me. I would like to express my deep appreciation to all of them. First and foremost, I appreciate my major professor, **Dr. Keykavous Parang** for giving me an opportunity to study at College of Pharmacy, University of Rhode Island. He has supported me with his best during my dissertation research. This dissertation would not have been completed without his encouragement, patience, and guidance. I am also grateful to my dissertation committee members, Dr. Roberta S. King, Dr. Geoffrey D. Bothun, Dr. Navindra Seeram, and Dr. Yana Reshetnyak, for their participation. I would like to thank Dr. David Rowley and Dr. Kerry LaPlante for their discussion and thoughtful comments. I would like to thank my colleagues for helping me a lot to finish my research. Dr. Rakesh K. Tiwari always shared his ideas and experience whenever I needed help.

There are so many people who helped me a lot outside of my research world. First of all, I owe a debt of gratitude to my parents and parents-in-law. They have been praying day and night for me in my country South Korea. My wife, **Jee Young Park**, and my children, **Juhyung** and **Jueun**, are endless sources of inspiration. They have been supporting me with great love and confidence. I was able to complete my doctorate course thanks to their devotion. I really appreciate Pastor Seongwoo Chang and church members of The Way of Life Presbyterian Church for their prayers and support.

Above all, I give thanks to my heavenly father with my grateful heart. I know that this is not the end, but a new start. I do not know where I am going, but He only knows the way. Lastly, I would like to share a poem:

The LORD is my shepherd, I shall not be in want.

He makes me lie down in green pastures, he leads me beside quiet waters,

he restores my soul.

He guides me in paths of righteousness for his name's sake.

Even though I walk through the valley of the shadow of death, I will fear no evil,

for you are with me; your rod and your staff, they comfort me.

You prepare a table before me in the presence of my enemies.

You anoint my head with oil; my cup overflows.

Surely goodness and love will follow me all the days of my life,

and I will dwell in the house of the LORD forever.

- Psalm 23 -

PREFACE

This dissertation was prepared based on the University of Rhode Island “Guidelines for the Format of Theses and Dissertations” standards for Manuscript format. This dissertation consists of three manuscripts that have been combined to satisfy the requirements of the department of Biomedical and Pharmaceutical Sciences, College of Pharmacy, University of Rhode Island.

MANUSCRIPT I: Amphiphilic bicyclic peptides as cellular delivery agents.

This manuscript was submitted to *Angewandte Chemie International Edition* in March 2014.

MANUSCRIPT II: Enhanced cellular uptake of short polyarginine peptides through fatty acylation and cyclization.

This manuscript was submitted to *Molecular Pharmaceutics* in March 2014.

MANUSCRIPT III: Antibacterial activities of amphiphilic cyclic cell-penetrating peptides against multidrug resistant pathogens

This manuscript was prepared for submission to *Molecular Pharmaceutics* for publication.

TABLE OF CONTENTS

ABSTRACT	ii
ACKNOWLEDGMENTS	ix
PREFACE.....	xi
TABLE OF CONTENTS.....	xii
LIST OF TABLES	xiii
LIST OF FIGURES	xiv
LIST OF SCHEMES	xviii
MANUSCRIPT I	1
MANUSCRIPT II	43
MANUSCRIPT III.....	81

LIST OF TABLES

MANUSCRIPT I

There are no Tables in Manuscript I.

MANUSCRIPT II

There are no Tables in Manuscript II.

MANUSCRIPT III

PAGE

Table 1. Synthetized peptides list used for antimicrobial activity 109

Table 2. Antibacterial activities of synthetic peptides against Gram-positive and
Gram-negative strains 110

Table 3. Antimicrobial activity of peptides in combination with tetracycline against
MRSA 111

LIST OF FIGURES

MANUSCRIPT I	PAGE
Figure 1. (a) The chemical structures of amphiphilic linear, monocyclic, and bicyclic peptides. (b) Cellular uptake of F ⁷ -GpYEEI (F ⁷ -PP, 5 μM) in SK-OV-3 cells in the presence of bicyclic peptides (10 μM) and their derivatives 13	13
Figure 2. (a) Confocal Laser Scanning (CLSM) images of SK-OV-3 cells treated with bicyclic peptide F ⁷ -[KW ₄ E]-(β -Ala)-[KR ₅] (10 μM, upper) and FAM (10 μM, lower) for 1 h; (b) FACS analysis of SK-OV-3 cells incubated with F ⁷ -[KW ₄ E]-(β -Ala)-[KR ₅] (5 μM) or F ⁷ -[W ₅ R ₄ K] (5 μM) for 1 h 15	15
Figure 3. Cellular uptake of F ⁷ -[KW ₄ E]-(β -Ala)-[KR ₅] (5 μM) in SK-OV-3 cells incubated (a) at 37 °C and 4 °C, (b) with 10 mM NaN ₃ and 50 mM 2-deoxy-D-glucose, and (c) with endocytic inhibitors (CQ: chloroquine; CPZ: chlorpromazine; MCD: methyl β -cyclodextrin; NYS: nystatin; EIPA: 5-(<i>N</i> -ethyl- <i>N</i> -isopropyl) amiloride) analyzed by flow cytometry 16	16
Figure 4. (a) The effect of [W ₅ E]-(β -Ala)-[KR ₅] (10 μM) on cellular uptake of DOX (5 μM) in SK-OV-3 cells. After 1 h incubation with compounds, the media were replaced with fresh complete media and kept for 24 h; (b) The antiproliferative assay of DOX (1 μM) in the presence of [W ₅ E]-(β -Ala)-[KR ₅] (10 μM) in SK-OV-3 cells for 72 h. After 24 h incubation, the treatment was replaced by fresh media. The cells were kept in an incubator for 24-72 h 17	17
Figure S1. Cytotoxicity of amphiphilic peptides in human ovarian adenocarcinoma SK-OV-3 and human embryonic kidney HEK 293T cells after 24 h incubation 32	32

Figure S2. Cytotoxicity of [W ₅ E]-(β -Ala)-[KR ₅] against human leukemia CCRF-CEM cell after 24 h incubation	33
Figure S3. Cellular uptake of F'-GpYEEI (F'-PP, 5 μ M) in SK-OV-3 cells in the presence of cell-penetrating peptides (10 μ M). The sequences of CR ₇ and TAT are CRRRRRRR-NH ₂ and YGRKKRRQRRR-NH ₂ , respectively	34

MANUSCRIPT II	PAGE
Figure 1. Chemical structures of synthetic peptides used in this study. (F': fluorescein-labeled; []: cyclic peptide; (): linear peptide).....	71
Figure 2. Comparison of cytotoxicity between cyclic and linear acylated polyarginine peptides, and non-acylated cyclic peptide [R ₅] at various concentrations against CCRF-CEM, SK-OV-3, and HEK 293T after 24 h ..	72
Figure 3. Comparative cellular uptake of F'-dodecanoyl-[R ₅] and F'-dodecanoyl-(R ₅) (5 μ M) in SK-OV-3 cells (1 h).....	73
Figure 4. Confocal laser scanning microscope image of (A) F'-dodecanoyl-[R ₅] and (B) F'-dodecanoyl-(R ₅). The peptides were incubated for 1 h in SK-OV-3 cells at 10 μ M concentration ..	74
Figure 5. Cellular uptake of F'-dodecanoyl-[R ₅] (5 μ M) in SK-OV-3 cells in temperature control assay at 37 °C and 4 °C, and ATP depletion assay with NaN ₃ (10 mM) and 2-deoxy-D-glucose (50 mM) analyzed by flow cytometry	75
Figure 6. Cellular uptake of F'-GpYEEI (5 μ M) in the presence of dodecanoyl-[R ₅], [R ₅], dosecanoyl-(R ₅), and dodecanoyl-[R ₆] (10 μ M) in SK-OV-3 cell line. Phosphopeptide delivery efficiency of dodecanoyl-[R ₅] were compared with known	

CPPs (R ₇ : CRRRRRRR; TAT: YGRKKRRQRRR). The mean fluorescence of F'-GpYEEI taken by dodecanoyl-[R ₅] was set as 100%.	76
Figure 7. Chemical structures of ACPs with different length of fatty acid chains (C ₈ , C ₁₂ , and C ₁₆)	77
Figure 8. (A) Cytotoxicity assay of cyclic polyarginine peptide-fatty acid conjugates against SK-OV-3 cells (24 h incubation). (B) Cellular uptake of a phosphopeptide, F'-GpYEEI (5 μM) in the presence of peptide-fatty acid conjugates (10 μM) in SK-OV-3 cells	78
Figure 9. Cellular uptake assay of a phosphopeptides, F'-GpYEEI (5 μM) in the presence of W ₄ -[R ₅] and W-dodecanoyl-[R ₅] (10 μM) against SK-OV-3 and CCRF-CEM cell lines (1 h incubation). The mean fluorescence of F'-GpYEEI by W ₄ -[R ₅] was set as 100%	79

MANUSCRIPT III	PAGE
Figure 1. Chemical structures of synthetic peptides examined for antimicrobial activity	112
Figure 2. Time-kill curves of peptide 1, tetracycline, and combination for MRSA (ATCC 43300) and <i>E. coli</i> (ATCC 35218) at 37 °C for 24 h. Peptide 1 at two times the MIC was combined with tetracycline at one, two, four and eight times (MICs of peptide 1: 4 μg/mL for MRSA and 16 μg/mL for <i>E. coli</i> ; tetracycline (TC): 0.5 μg/mL for MRSA and 2 μg/mL for <i>E. coli</i>)	113
Figure 3. Cytotoxicity assay of peptide 1 by MTS-PMS assay (24 h incubation)	114
Figure 4. Confocal laser scanning microscope image of F'-[KR ₄ W ₄] (10 μM) in SK-	

OV-3 cells (1 h incubation)	115
Figure 5. Energy-dependent mechanistic study of intracellular uptake for F'-[KW ₄ R ₄].	
Cellular uptake was investigated under 4 °C and ATP depletion conditions ..	116

LIST OF SCHEMES

MANUSCRIPT I	PAGE
Scheme S1. The synthesis of monocyclic peptide [W ₅ G(propargyl)].....	35
Scheme S2. The synthesis of monocyclic peptide [W ₅ E]	36
Scheme S3. The synthesis of monocyclic peptide [K(N ₃)R ₅]	37
Scheme S4. The synthesis of monocyclic peptide (β -Ala)-[KR ₅] ..	38
Scheme S5. The conjugation of two monocyclic peptides for the synthesis of [W ₅ G]- (triazole)-[KR ₅] peptide	39
Scheme S6. The conjugation of two monocyclic peptides for the synthesis of [W ₅ E]- (β -Ala)-[KR ₅] peptide ..	40
Scheme S7. The synthesis of monocyclic F'-[KW ₄ E] peptide	41
Scheme S8. The synthesis of fluorescein-labeled bicyclic peptide F'-[KW ₄ E]-(β -Ala)- [KR ₅] ..	42
MANUSCRIPT II	PAGE
Scheme 1. Synthesis of dodecanoyl-[R ₅] as a representative example	80
MANUSCRIPT III	PAGE
Scheme 1. The synthesis of peptide 1 ([R ₄ W ₄])	117

MANUSCRIPT I

Submitted to *Angewandte Chemie International Edition* in March 2014

Amphiphilic Bicyclic Peptides as Cellular Delivery Agents**

Donghoon Oh,⁺ Shaban Anwar Darwish,⁺ Amir Nasrolahi Shirazi, Rakesh Kumar
Tiwari, and Keykavous Parang*

[*] D. Oh, Dr. S. A. Darwish, Dr. A. Nasrolahi Shirazi, Prof. R. Tiwari, Prof. K.

Parang

Department of Biomedical and Pharmaceutical Sciences

University of Rhode Island

7 Greenhouse Road, Kingston, RI 02881 (USA)

E-mail: kparang@uri.edu

Dr. A. Nasrolahi Shirazi, Prof. R. Tiwari, Prof. K. Parang

Chao Family Comprehensive Cancer Center, School of Medicine, University of

California, Irvine, Shanbrom Hall, 101 The City Drive, Orange, CA 92868; School of

Pharmacy, Chapman University

9401 Jeronimo Road, Irvine, CA 92618 (USA)

[⁺] These authors contributed equally to this work.

[**] We acknowledge the American Cancer Society, Grant No. RSG-07-290-01-CDD for the financial support. We thank National Center for Research Resources, NIH, and Grant Number 8 P20 GM103430-12 for sponsoring the core facility. This material is based upon work conducted at a research facility at the University of Rhode Island supported in part by the National Science Foundation EPSCoR Cooperative Agreement #EPS-1004057.

Supporting information for this article is available on the WWW under <http://dx.doi.org/10.1002/anie.201xxxxxx>.

Abstract

Two bicyclic peptides [W₅G]-(triazole)-[KR₅] and [W₅E]-(β -Ala)-[KR₅] composed of tryptophan and arginine residues were synthesized from monocyclic peptide building blocks and evaluated as cellular delivery agents. [W₅G]-(triazole)-[KR₅] and [W₅E]-(β -Ala)-[KR₅] containing triazole and β -alanine linkers improved the cellular delivery of fluorescein-labeled phosphopeptide, F'-GpYEEI by 7.6 and 19.3-fold, respectively, in human ovarian adenocarcinoma (SK-OV-3) cells. Confocal microscopy showed that the corresponding fluorescein-labeled bicyclic peptide F'-[KW₄E]-(β -Ala)-[KR₅] was localized in the cytosol and nucleus. Studying the cellular uptake of F'-[KW₄E]-(β -Ala)-[KR₅] in the presence of endocytosis inhibitors indicated that the clathrin- and caveolin-dependent endocytosis were the main pathways for cellular uptake. The bicyclic peptide was able to improve antiproliferative activity of doxorubicin by 20%. These data suggest that amphiphilic bicyclic peptides containing tryptophan and arginine can be utilized as a new class of cell-penetrating peptides and potential cellular delivery tools.

Cell-penetrating peptides (CPPs) have been studied as molecular transporters because of their cellular translocation properties.^[1] Covalent or non-covalent CPP-drug conjugates have been designed to deliver cell-impermeable drugs, such as negatively charged phosphopeptides, oligonucleotides, and siRNAs.^[2] Various CPPs, such as TAT peptide, antennapedia, or polyarginines, have been used as molecular transporters for a wide range of molecular cargos.^[3,4]

Among CPPs, cyclic peptides take advantage of their higher serum stability compared to the linear counterparts.^[5] In addition, the presence of positively charged arginine and hydrophobic tryptophan amino acids were found to be critical due to their characteristic interactions with phospholipid membranes.^[6-8] We have previously reported the development of homochiral cyclic peptides containing arginine and tryptophan [WR]₄ and [WR]₅ as nuclear-targeting CPPs.^[9] These monocyclic peptides were found to be effective tools as covalent and non-covalent molecular transporters.^[10,11] Our findings showed that in addition to the cyclic nature, the sequence of the peptide contributes significantly to the molecular transporter property of the peptide by keeping a balance between both hydrophobic and positively charged properties.

To the best of our knowledge, bicyclic peptides have not been explored as CPPs and molecular transporters. We hypothesized that an amphiphilic bicyclic peptide containing two hydrophobic and positively charged cyclic peptides could act an alternative cellular delivery tool. Amphiphilic bicyclic peptides containing tryptophan and arginine amino acids and appropriate controls were synthesized and evaluated as

CPPs and molecular transporters of a cell-impermeable negatively charged phosphopeptide.

Two bicyclic peptides containing triazole and β -alanine linkers were synthesized to determine the effect of spacers in cellular delivery. First, a monocyclic peptide containing five arginine residues and one lysine azide [K(N₃)R₅] and a cyclic peptide [W₅G(propargyl)] containing five tryptophans and one propargylglycine (G(propargyl)) were prepared and conjugated by click chemistry to generate [W₅G]-(triazole)-[KR₅] containing a triazole linker (Figure 1a). Alternatively, bicyclic peptide [W₅E]-(β -Ala)-[KR₅] was synthesized through linking two monocyclic peptides, [W₅E] and (β -Ala)-[KR₅], through a β -alanine (β -Ala) spacer (Figure 1a) (See Supporting Information for experimental details).

Furthermore, a corresponding linear peptide containing tryptophan and arginine residues, W₅G-(triazole)-KR₅, and a monocyclic peptide with a linear component, [W₅G]-(triazole)-KR₅, were synthesized as controls (Figure 1a) to determine the effect of the cyclic nature of the peptide.

First, we examined the cytotoxicity of these peptides by MTS proliferation assay against human ovarian adenocarcinoma SK-OV-3 cell lines and human embryonic kidney HEK 293T cell lines. In both cancer and normal cell lines, all four peptides showed more than 80% cell viability at 10 μ M concentration (Supporting Information). Further cytotoxicity of [W₅E]-(β -Ala)-[KR₅] was determined against a non-adherent cell line (human leukemia CCRF-CEM) after 24 h. The data showed that cell viability at 15 μ M peptide concentration was remained up to 88% in non-adherent CCRF-CEM

cell line. Thus, a noncytotoxic concentration of 5-10 μM was selected for further cellular uptake studies.

To determine the ability of these amphiphilic peptides as molecular transporters, we used a negatively charged fluorescein-labeled phosphopeptide, F'-GpYEEI (F' = fluorescein), as a model cell-impermeable compound, which is known as a substrate of Src kinase SH2 domain.^[12,13] F'-GpYEEI (5 μM) was incubated in SK-OV-3 cells in the presence of these four peptides (10 μM) for 1 h, and the cellular uptake was evaluated by flow cytometry. All four peptides enhanced the intracellular uptake of F'-GpYEEI. The cellular uptake of the phosphopeptide was increased 2.9-, 7.2-, 7.6-, and 19.3-fold for linear W₅G-(triazole)-KR₅, monocyclic [W₅G]-(triazole)-KR₅, bicyclic [W₅G]-(triazole)-[KR₅], and bicyclic [W₅E]-(β -Ala)-[KR₅], respectively. Thus, [W₅E]-(β -Ala)-[KR₅] showed significantly higher cellular delivery of the phosphopeptide among all peptides (Figure 1b). These data showed that amphiphilic peptides containing tryptophan and arginine residues can enhance the transportation of a cell impermeable phosphopeptide. Moreover, cyclic nature of the peptide contributes significantly to the intracellular uptake since all the peptides containing one or two cyclic peptides showed higher molecular transporter property. In addition, the bicyclic peptide containing β -alanine linker, [W₅E]-(β -Ala)-[KR₅], exhibited 2.5-fold higher uptake of the cell-impermeable phosphopeptide than that of bicyclic peptide [W₅G]-(triazole)-[KR₅]. [W₅E]-(β -Ala)-[KR₅] has a more flexible linker between two cyclic peptides. Thus, the nature and the length of the linker between two cyclic peptides are critical in generating an appropriate conformation for interaction with the cell membrane phospholipid and molecular transporter property of the compound. Thus,

bicyclic peptide [W₅E]-(β -Ala)-[KR₅] was selected for further study and evaluation as a CPP.

A corresponding fluorescein-labeled bicyclic peptide of [W₅E]-(β -Ala)-[KR₅], F'-[KW₄E]-(β -Ala)-[KR₅] (F' = fluorescein) (Figure 2), was synthesized (See Supporting Information for experimental details) for cell permeability studies. SK-OV-3 cells were incubated with the fluorescein-labeled bicyclic peptide (10 μ M) for 1 h at 37 °C. Confocal laser scanning microscope (CLSM) images showed that the fluorescein-labeled bicyclic peptide was dispersed into the nucleus and cytosol (upper panel in Figure 2a), but no significant fluorescence was observed in the cells treated with fluorescein (FAM) alone under the same condition (lower panel in Figure 2a). The diffusion of fluorescence was observed in both cytoplasm and nucleus even though the punctate fluorescence was detected in FITC image. These data indicate that the bicyclic peptide is localized in cellular organelles possibly via endocytosis, and the peptide escapes from endosomes into the cytosol and nucleus.

Flow cytometry analysis was further confirmed the cellular uptake of F'-[KW₄E]-(β -Ala)-[KR₅]. SK-OV-3 cells were incubated for 1 h with the fluorescence-labeled peptides. The bicyclic peptide showed 2.9-fold more uptake when compared with fluorescein (FAM) (Figure 2b). The cellular uptake of the bicyclic peptide, F'-[KW₄E]-(β -Ala)-[KR₅] was found to be 1.8-fold more in comparison to our previously reported monocyclic F'-[W₅R₄K] peptide^[9] at 5 μ M concentration. These data indicate that the bicyclic peptide has higher cellular uptake when compared to the corresponding monocyclic peptide. Thus, this new bicyclic peptide could be used as an alternative CPP with more efficiency compared to the monocyclic peptide.

To examine the cellular uptake mechanism of F'-[KW₄E]-(β-Ala)-[KR₅], a temperature control assay was carried out at 4 °C to inhibit the energy-dependent endocytosis. The uptake of the bicyclic peptide was significantly reduced at 4 °C, indicating that the cellular uptake mechanism was dependent on the endocytosis (Figure 3a).^[14] To further confirm the energy-dependent cellular uptake of the bicyclic peptide, SK-OV-3 cells were incubated with sodium azide (10 mM) and 2-deoxy-D-glucose (50 mM) for 1 h before and 1 h after adding the bicyclic peptide to induce ATP depletion. The result showed that there was inhibition by ATP depletion (Figure 3a), which is consistent with the result of the temperature control assay at 4 °C, suggesting that endocytosis is the major pathway for the cellular uptake of the bicyclic peptide as shown for other systems.^[15]

The cellular uptake studies were also conducted in the presence of several endocytosis inhibitors, such as chloroquine, chlorpromazine, methyl β-cyclodextrin, nystatin, and 5-(N-ethyl-N-isopropyl)amiloride (EIPA), to determine the specific endocytosis mechanism. SK-OV-3 cells were incubated with each inhibitor for 30 min before 1 h incubation with F'-[KW₄E]-(β-Ala)-[KR₅]. The results showed that only chlorpromazine and nystatin significantly reduced the cellular uptake of the bicyclic peptide (Figure 3b). Since chlorpromazine is a clathrin-dependent endocytosis inhibitor and nystatin blocks the lipid raft-caveolae endocytosis,^[16,17] we suggest that the cellular uptake mechanism of F'-[KW₄E]-(β-Ala)-[KR₅] is a clathrin- and caveolin-dependent endocytosis. These data indicate that the cellular uptake of the bicyclic peptide as a CPP follows a different pattern from that of cyclic peptide [WR]₅, which showed endocytosis-independent cellular uptake.^[9]

Bicyclic [W₅E]-(β -Ala)-[KR₅] improved the uptake of F'-GpYEEI by 19.3-fold as shown in Figure 1b. To evaluate the molecular transporter property of the bicyclic peptide compared to a number of other CPPs, such as linear polyarginine (CR₇), TAT, and monocyclic peptide [WR]₅, we carried out the cellular uptake assay using a fluorescein-labeled phosphopeptide, F'-GpYEEI. Negatively charged F'-GpYEEI was used as a model cell impermeable cargo. It was expected that the interaction between negatively charged phosphopeptides and positively charged bicyclic peptide could improve the cellular uptake of the phosphopeptide. For cellular uptake assay, we used a non-cytotoxic concentration of the bicyclic peptide (10 μ M). For comparative studies, F'-GpYEEI was co-incubated using typical CPPs, such as linear polyarginine (CR₇) and TAT peptides, and monocyclic [WR]₅. After incubation of F'-GpYEEI with or without the peptides in SK-OV-3 cells, FACS analysis was carried out to quantify the F'-GpYEEI enhanced by CPPs. The intracellular uptake of F'-GpYEEI in the presence of the bicyclic peptide was enhanced by 4.5- and 3.0-fold higher than those of TAT and CR₇ peptide, and 1.8-fold over [WR]₅ cyclic CPP (See Supporting Information). Thus, [W₅E]-(β -Ala)-[KR₅] was found to be a more efficient molecular transporter for the negatively-charged phosphopeptide compared to commonly used CPPs and our previous reported cyclic CPP.^[9] We have previously reported the binding affinity between monocyclic [WR]₅ and the negatively charged phosphopeptide. Improved uptake in the presence of the bicyclic peptide could be due to the higher binding affinity with the phosphopeptide because of the presence of all positively-charged amino acids at one side and/or higher efficiency of the bicyclic peptide as a molecular transporter.

Next, an intracellular retention of a commercially available anticancer drug, doxorubicin (DOX), was determined in the presence and absence of the bicyclic peptide. SK-OV-3 cells were incubated with doxorubicin (5 μM) and $[\text{W}_5\text{E}]-(\beta\text{-Ala})-[\text{KR}_5]$ (10 μM) containing medium for 1 h. Then all compounds and media were removed, and fresh complete media was added and kept for 24 h. We found that the bicyclic peptide did not increase the cellular uptake of DOX compared to the free DOX after 1 h incubation. However, 1.7-fold higher retention of DOX was observed intracellularly in the presence of the bicyclic peptide after 24 h (Figure 4a).

To determine whether $[\text{W}_5\text{E}]-(\beta\text{-Ala})-[\text{KR}_5]$ can be exploited for the delivery of biologically relevant doses of DOX to cells, the antiproliferative activity of DOX was evaluated in SK-OV-3 cells in the presence and absence of the bicyclic peptide. The antiproliferative activity of DOX (1 μM) in the presence of the $[\text{W}_5\text{E}]-(\beta\text{-Ala})-[\text{KR}_5]$ (10 μM) was improved by approximately 20% compared to that of DOX alone after 72 h incubation (Figure 4b). An inhibitory effect on the cell proliferation of SK-OV-3 cells suggests improved efficacy of DOX. $[\text{W}_5\text{E}]-(\beta\text{-Ala})-[\text{KR}_5]$ alone did not show any toxicity in SK-OV-3 cells under similar conditions, suggesting that the higher antiproliferative is possibly related to the efflux inhibition of the drug in the presence of the bicyclic peptide or the time-delayed release of DOX from the endosome after cellular uptake.

In conclusion, we report synthesized bicyclic peptides, $[\text{W}_5\text{G}]-(\text{triazole})-[\text{KR}_5]$ and $[\text{W}_5\text{E}]-(\beta\text{-Ala})-[\text{KR}_5]$, as a new class of CPPs. To the best of our knowledge, this is the first bicyclic peptides as a cellular delivery tool. $[\text{W}_5\text{E}]-(\beta\text{-Ala})-[\text{KR}_5]$ was internalized through a clathrin-mediated and lipid raft-caveolin-dependent endocytic

mechanism, and worked as a molecular transporter for delivery of a negatively-charged phosphopeptide. [W₅E]-(β -Ala)-[KR₅] also enhanced the retention of DOX in SK-OV-3 cells. Thus, an amphiphilic bicyclic peptide containing two monocyclic peptides can be used as a CPP and potential cellular delivery vehicle.

Keywords: amphiphiles • bicyclic peptide • cell-penetrating • drug delivery • endocytosis

- [1] S. B. Fonseca, M. P. Pereira, S. O. Kelley, *Adv. Drug Deliv. Rev.* **2009**, *61*, 953–964.
- [2] F. Heitz, M. C. Morris, G. Divita, *Br. J. Pharmacol.* **2009**, *157*, 195–206.
- [3] H. Brooks, B. Lebleu, E. Vivès, *Adv. Drug Deliv. Rev.* **2005**, *57*, 559–577.
- [4] S. W. Jones, R. Christison, K. Bundell, C. J. Voyce, S. M. V. Brockbank, P. Newham, M. A. Lindsay, *Br. J. Pharmacol.* **2005**, *145*, 1093–1102.
- [5] L. T. Nguyen, J. K. Chau, N. A. Perry, L. de Boer, S. A. J. Zaat, H. J. Vogel, *PLoS ONE* **2010**, *5*, e12684.
- [6] I. Nakase, M. Niwa, T. Takeuchi, K. Sonomura, N. Kawabata, Y. Koike, M. Takehashi, S. Tanaka, K. Ueda, J. C. Simpson, et al., *Mol. Ther.* **2004**, *10*, 1011–1022.
- [7] G. Lättig-Tünnemann, M. Prinz, D. Hoffmann, J. Behlke, C. Palm-Apergi, I. Morano, H. D. Herce, M. C. Cardoso, *Nat. Commun.* **2011**, *2*, 453.
- [8] D. I. Chan, E. J. Prenner, H. J. Vogel, *Biochim. Biophys. Acta* **2006**, *1758*, 1184–1202.

- [9] D. Mandal, A. Nasrolahi Shirazi, K. Parang, *Angew. Chem. Int. Ed.* **2011**, *50*, 9633–9637.
- [10] A. Nasrolahi Shirazi, R. Tiwari, B. S. Chhikara, D. Mandal, K. Parang, *Mol. Pharm.* **2013**, *10*, 488–499.
- [11] A. Nasrolahi Shirazi, R. K. Tiwari, D. Oh, A. Banerjee, A. Yadav, K. Parang, *Mol. Pharm.* **2013**, *10*, 2008–2020.
- [12] Z. Songyang, S. E. Shoelson, J. McGlade, P. Olivier, T. Pawson, X. R. Bustelo, M. Barbacid, H. Sabe, H. Hanafusa, T. Yi, *Mol. Cell. Biol.* **1994**, *14*, 2777–2785.
- [13] G. Waksman, D. Kominos, S. C. Robertson, N. Pant, D. Baltimore, R. B. Birge, D. Cowburn, H. Hanafusa, B. J. Mayer, M. Overduin, et al., *Nature* **1992**, *358*, 646–653.
- [14] J. Saraste, G. E. Palade, M. G. Farquhar, *Proc. Natl. Acad. Sci.* **1986**, *83*, 6425–6429.
- [15] J. P. Richard, K. Melikov, E. Vives, C. Ramos, B. Verbeure, M. J. Gait, L. V. Chernomordik, B. Lebleu, *J. Biol. Chem.* **2003**, *278*, 585–590.
- [16] L. H. Wang, K. G. Rothberg, R. G. Anderson, *J. Cell Biol.* **1993**, *123*, 1107–1117.
- [17] K. G. Rothberg, J. E. Heuser, W. C. Donzell, Y. S. Ying, J. R. Glenney, R. G. Anderson, *Cell* **1992**, *68*, 673–682.

Figures

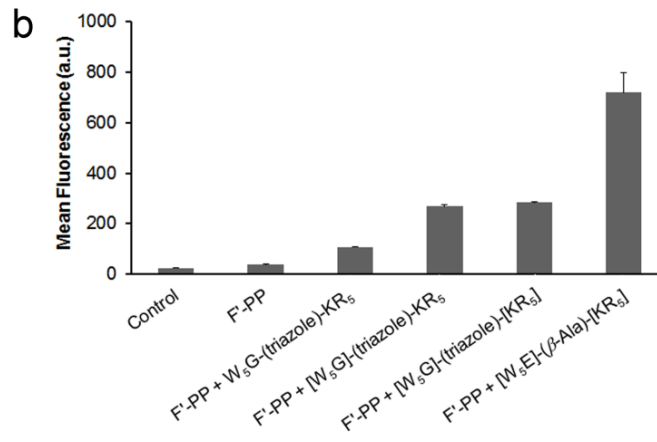
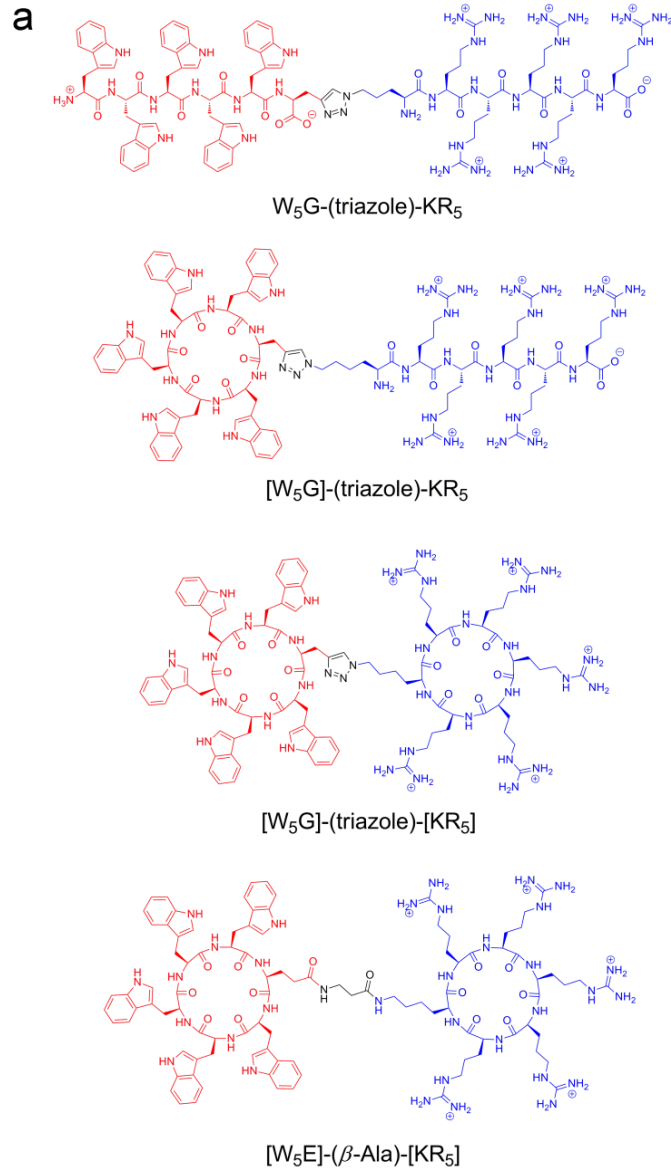


Figure 1. (a) The chemical structures of amphiphilic linear, monocyclic, and bicyclic peptides. (b) Cellular uptake of F'-GpYEEI (F'-PP, 5 μM) in SK-OV-3 cells in the presence of bicyclic peptides (10 μM) and their derivatives.

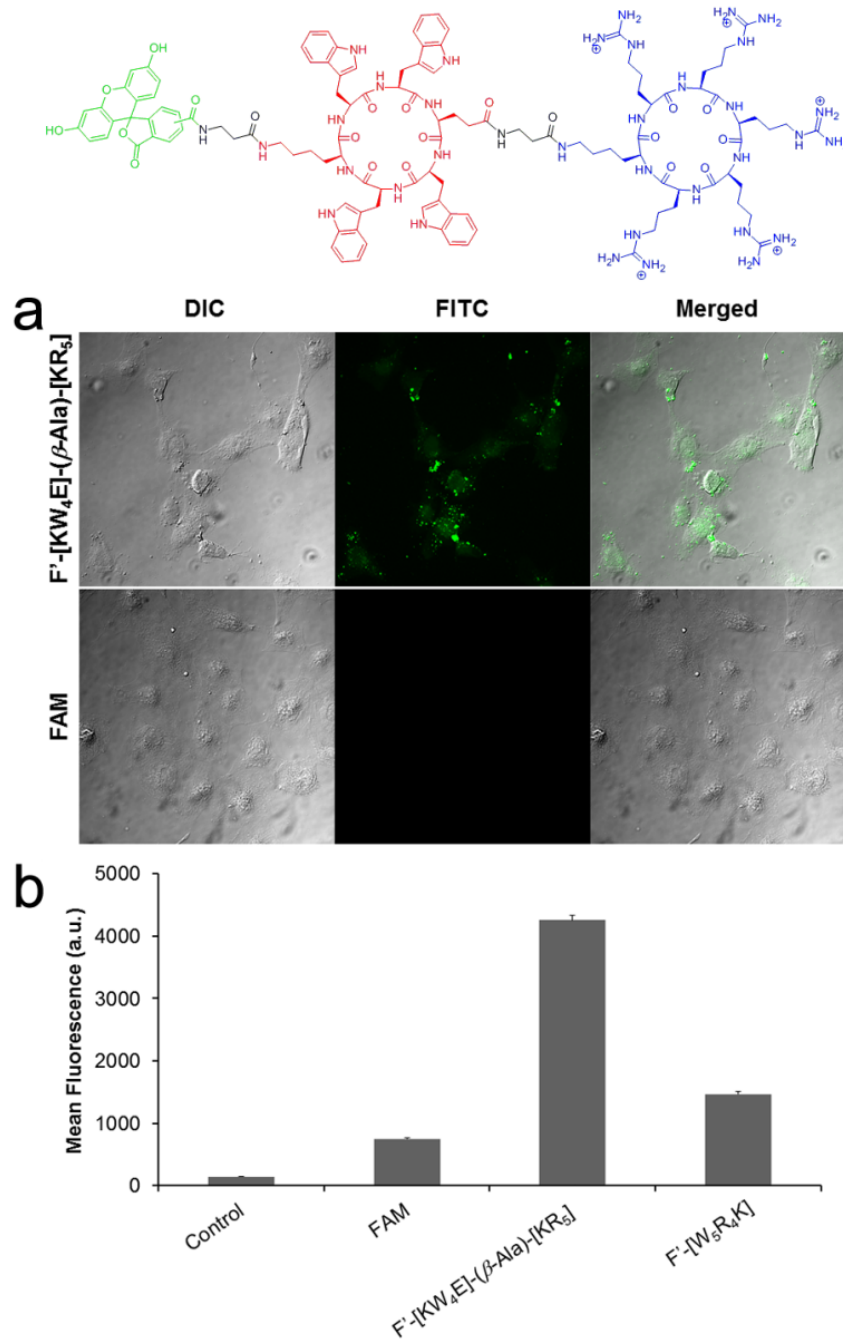


Figure 2. (a) Confocal Laser Scanning (CLSM) images of SK-OV-3 cells treated with bicyclic peptide F'-[KW₄E]-(β -Ala)-[KR₅] (10 μ M, upper) and FAM (10 μ M, lower) for 1 h; (b) FACS analysis of SK-OV-3 cells incubated with F'-[KW₄E]-(β -Ala)-[KR₅] (5 μ M) or F'-[W₅R₄K] (5 μ M) for 1 h.

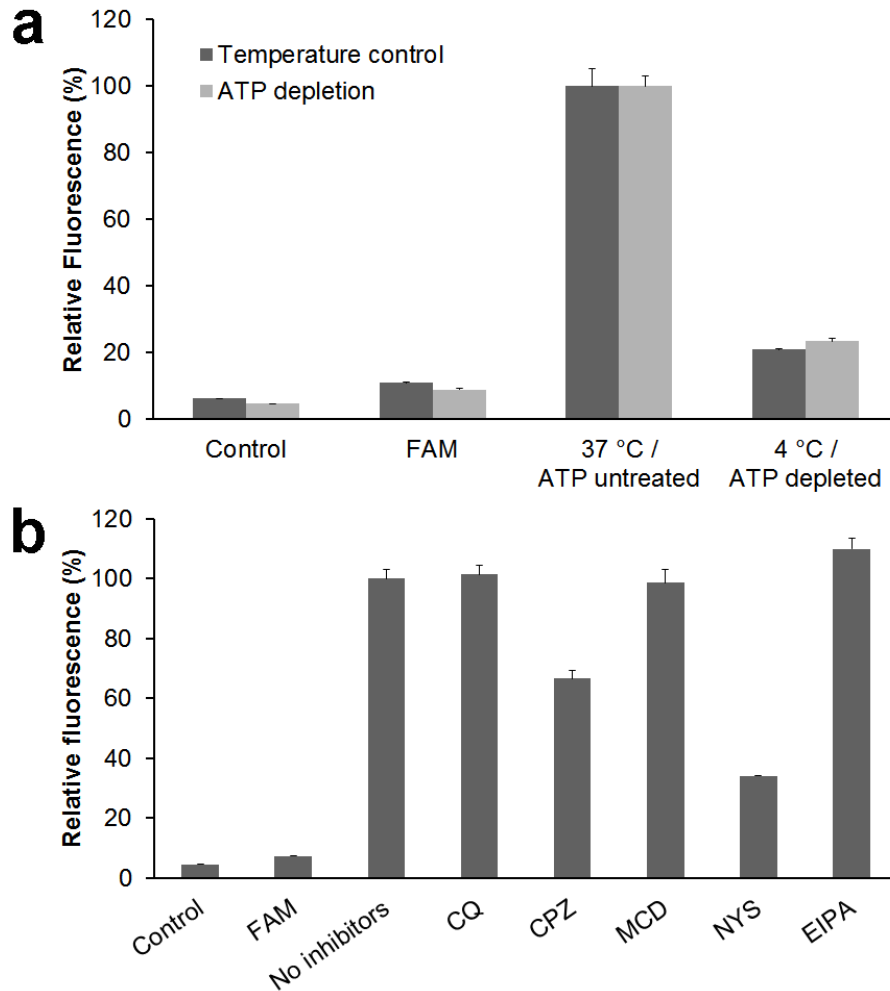


Figure 3. Cellular uptake of F'-[KW₄E]-(β-Ala)-[KR₅] (5 μM) in SK-OV-3 cells incubated (a) at 37 °C and 4 °C, (b) with 10 mM NaN₃ and 50 mM 2-deoxy-D-glucose, and (c) with endocytic inhibitors (CQ: chloroquine; CPZ: chlorpromazine; MCD: methyl β-cyclodextrin; NYS: nystatin; EIPA: 5-(N-ethyl-N-isopropyl) amiloride) analyzed by flow cytometry.

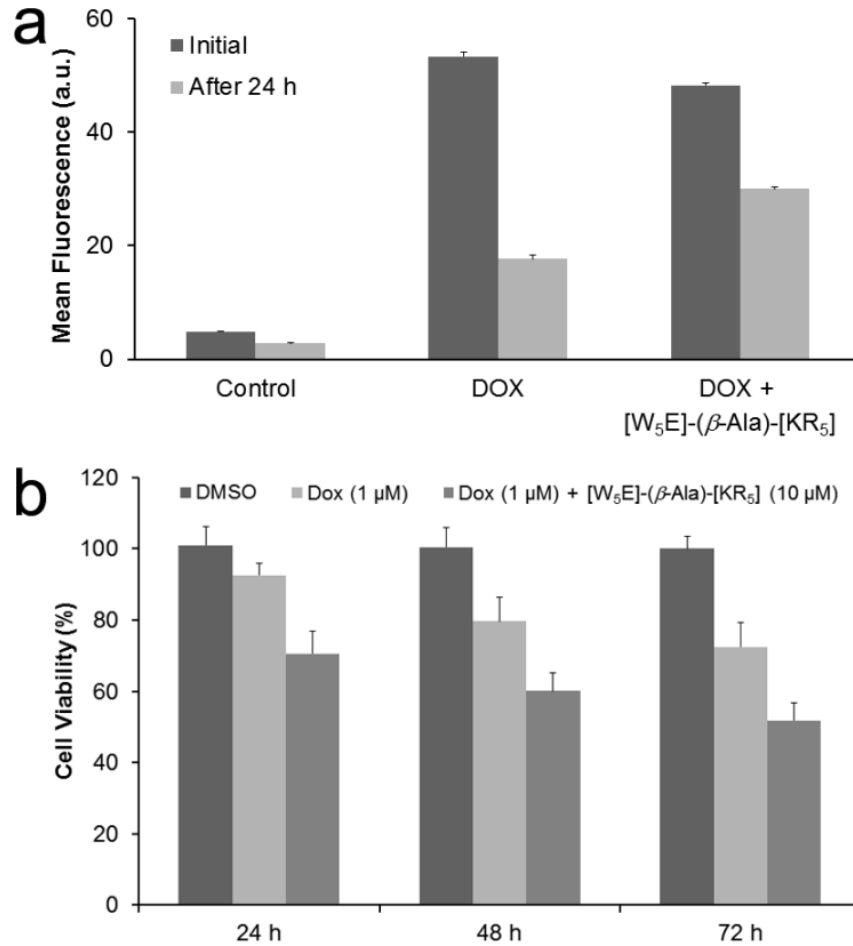


Figure 4. (a) The effect of [W₅E]-(β-Ala)-[KR₅] (10 μM) on cellular uptake of DOX (5 μM) in SK-OV-3 cells. After 1 h incubation with compounds, the media were replaced with fresh complete media and kept for 24 h; (b) The antiproliferative assay of DOX (1 μM) in the presence of [W₅E]-(β-Ala)-[KR₅] (10 μM) in SK-OV-3 cells for 72 h. After 24 h incubation, the treatment was replaced by fresh media. The cells were kept in an incubator for 24-72 h.

Supporting Information

Experimental Section

1. General procedure

Materials. The resins for peptide synthesis, coupling reagents, and Fmoc-protected amino acid building blocks were purchased from Chem-Impex International, Inc. 2-(1*H*-Benzotriazole-1-yl)-1,1,3,3-tetramethyluronium hexafluorophosphate (HBTU) was purchased from Oakwood products, Inc. Other chemicals and reagents were purchased from Sigma-Aldrich Chemical Co.

Solid-phase peptide synthesis. All reactions were carried out manually in a glass reaction vessel with a sintered glass frit by mixing under nitrogen bubbling at room temperature, unless otherwise stated. Generally, all linear and monocyclic peptides were synthesized by the Fmoc/*t*Bu solid phase synthesis strategy, employing *N*-(9-fluorenyl)methoxycarbonyl (Fmoc)-based chemistry and Fmoc-L-amino acid building blocks, and head-to-tail cyclization method as described previously by us.^[9] Single amino acid loaded 2-chlorotrityl resins were used for conjugation with Fmoc-L-amino acid building blocks. HBTU and *N,N*-diisopropylethylamine (DIPEA) in *N,N*-dimethylformamide (DMF) were used as coupling and activating reagents, respectively. Fmoc-deprotection at each step was carried out in the presence of piperidine in DMF (20%) followed by washing with DMF. The linear peptides were cleaved from the resins and the side chains were deprotected by shaking with freshly prepared cleavage cocktail of trifluoroacetic acid (TFA)/triisopropylsilane (TIS)/water (92.5/5/2.5, v/v/v) for 2-3 h. The crude peptides were filtered, and the resins were

washed again with 2-3 mL of cleavage cocktail. The crude peptides were precipitated and washed with cold diethyl ether.

For cyclization, a cleavage cocktail, 2,2,2-trifluoroethanol (TFE)/acetic acid/dichloromethane (DCM) (2:1:7, v/v/v) was used for 1 h to cleave side-chain protected linear peptides from resins. The resins were filtered off, and the filtrate was repeatedly evaporated and dissolved in a small portion of DCM and hexane. The obtained side-chain protected linear peptides were kept in vacuum for overnight and used directly for the cyclization. Cyclization of linear peptides was carried out in the presence of a mixture of 1-hydroxy-7-azabenzotriazole (HOAT) and *N,N'*-diisopropylcarbodiimide (DIC) in anhydrous DMF/DCM for 24 h. The solvents were evaporated and the side-chain deprotection groups of cyclic peptide were removed by cleavage cocktails, TFA/thioanisole/1,2-ethanedithiol (EDT)/anisole (90:5:3:2, v/v/v/v) or TFA/TIS/water (92.5/5/2.5, v/v/v) for 2-3 h reaction. The crude monocyclic peptides were precipitated and washed with cold diethyl ether.

The crude peptides were purified on a reversed-phase high pressure liquid chromatography (RP-HPLC) system using Shimadzu LC-8A preparative liquid chromatography on a Phenomenex Gemini C18 column (10 μ m, 250 \times 21.2 mm) with a gradient 0-100% of acetonitrile (CH₃CN) containing 0.1% TFA (v/v) and water containing 0.1% (v/v) for 1 h with a flow rate between 9 to 18 mL/min at 214 nm wavelength. Purity of some compounds was confirmed by analytical HPLC using an RP-C18 column (Shimadzu Premier C18, 3 μ m, 150 \times 4.6 mm). The chemical structures of final products were confirmed by an AXIMA performance matrix-

assisted laser desorption/ionization-time of flight (MALDI-TOF) mass spectrometer (Shimadzu Corporation).

2. Synthesis of linear $\mathbf{K(N_3)R_5}$. H-Arg(Pbf)-2-chlorotrityl resin (1389 mg, 0.5 mmol, 0.36 mmol/g) was swelled in DMF for 30 min by N_2 . Fmoc-Arg(Pbf)-OH (1298 mg, 2 mmol, 4 equiv) was coupled to the *N*-terminal of H-Arg(Pbf)-2-chlorotrityl resin, using HBTU (758 mg, 2 mmol, 4 equiv) and DIPEA (697 μ L, 4 mmol, 8 equiv) in DMF (7 mL) by agitating the resin for 1 h using N_2 . After the coupling, the resin was washed with DMF, followed by Fmoc-deprotection. The subsequent three Fmoc-Arg(Pbf)-OH couplings and one Fmoc-Lys(N_3)-OH (789 mg, 2 mmol, 4 equiv) coupling was carried out in the same manner, respectively. The terminal Fmoc group was deprotected, followed by washing with DMF, DCM, and methanol. The crude *N*-azido $\mathbf{KR_5}$ was cleaved by shaking with a freshly prepared cleavage cocktail, TFA/TIS/water (92.5:5:2.5, v/v/v, 15 mL) for 3 h, and purified by a method described in general procedure. $\mathbf{K(N_3)R_5}$: HPLC (R_t) = 9.30 min; MALDI-TOF (*m/z*): $C_{36}H_{72}N_{24}O_7$ calcd. 952.6016; found 952.9263 [M]⁺.

3. Synthesis of linear $\mathbf{W_5G(propargyl)}$. H-Trp(Boc)-2-chlorotrityl resin (769 mg, 0.6 mmol, 0.78 mmol/g) was swelled using DMF, and coupled with Fmoc-Trp(Boc)-OH (1264 mg, 2.4 mmol, 4 equiv) using HBTU (910 mg, 2.4 mmol, 4 equiv) and DIPEA (836 μ L, 4.8 mmol, 8 equiv) with DMF (10 mL) for 1 h, followed by Fmoc-deprotection. The coupling and deprotection cycle was repeated 3 more times followed by coupling with Fmoc-L-Gly(propargyl)-OH (804 mg, 2.4 mmol, 4 equiv)

using HBTU (910 mg, 2.4 mmol, 4 equiv), and DIPEA (836 μ L, 4.8 mmol, 8 equiv) in DMF (10 mL). The crude W₅G(propargyl) was obtained by TFA/TIS/water cleavage and precipitation using cold diethyl ether as described above. **W₅G(propargyl)**: ¹H NMR (DMSO-*d*₆, 300 MHz, δ ppm): 12.63 (s, 1H, COOH), 10.60-10.89 (m, 5H, NH Trp), 7.94-8.34 (m, 5H, NH), 6.84-7.68 (m, 25H, ArH), 4.42-4.74 (m, 6H, α CH Trp and Gly(propargyl)), 2.85-3.22 (m, 10H β CH₂ Trp), 2.56-2.67 (m, 2H, β CH₂ Gly(propargyl)), 1.88 (m, 1H, δ CH Gly(propargyl)), 1.00 (d, *J* = 6.5, 2H, NH₂); HPLC (R_t) = 14.00 min; MALDI-TOF (m/z): C₆₀H₅₇N₁₁O₇ calcd. 1043.4442; found 1066.6016 [M + Na]⁺, 1082.1667 [M + K]⁺.

4. Synthesis of monocyclic peptides. The synthetic procedure is same as the linear peptide except the cleavage and additional cyclization step as described in the general procedure. As a representative example, the synthesis of [W₅G(propargyl)] is described here (Scheme S1). The side-chain protected linear W₅G(propargyl) was synthesized as described above. The side chain protected linear peptide was cleaved from the resin with TFE/acetic acid/DCM mixture and cyclized in the presence of HOAT (326 mg, 2.4 mmol, 4 equiv) and DIC (371 μ L, 2.4 mmol, 4 equiv) in dilute anhydrous DMF/DCM (5:1, v/v, 250 mL) under N₂ with stirring for 24 h. **[W₅G(propargyl)]**: ¹H NMR (DMSO-*d*₆, 300 MHz, δ ppm): 10.66-10.84 (m, 5H, NH Trp), 7.90-8.31 (m, 6H, NH), 6.86-7.55 (m, 25H, ArH), 4.01-4.33 (m, 5H, α CH Trp), 3.70-3.70(s broad, 1H, α CH Gly(propargyl)), 2.98-3.23 (m, 10H β CH₂ Trp), 2.54-2.65 (m, 2H, β CH₂ Gly(propargyl)), 1.75 (s, 1H, δ CH Gly(propargyl)); HPLC (R_t) = 28.30

min; MALDI-TOF (m/z): C₆₀H₅₅N₁₁O₆ calcd. 1025.4337; found 1048.1293 [M + Na]⁺, 1064.1329 [M + K]⁺.

[K(N₃)R₅]: ¹H NMR (DMSO-*d*₆, 300 MHz, δ ppm): 7.81-8.10 (m, 6H, *NH*), 6.88-7.24 (s broad, 20H, *NH* guanidinium), 4.10-4.34 (m, 6H, α CH Arg and Lys), 3.18-3.35(m, 10H, δ CH Arg), 1.82-1.88 (m, 12H β CH₂ Arg and Lys), 1.40-1.60 (m, 16H, γ CH₂ Arg and γ,δ,ϵ CH₂ Lys); HPLC (R_t) = 9.20 min; MALDI-TOF (m/z): C₃₆H₇₀N₂₄O₆ calcd. 934.5910; found 935.2969 [M + H]⁺.

[W₅E]: HPLC (R_t) = 24.00 min; ¹H NMR (DMSO-*d*₆, 300 MHz, δ ppm): 12.00 (s, 1H, COOH), 10.70-10.85 (m, 5H, *NH* Trp), 7.92-8.25 (m, 6H, *NH*), 6.90-7.60 (m, 25H, *ArH*), 4.18-4.32 (m, 5H, α CH Trp), 3.95-4.05 (m, 1H, α CH Glu), 2.90-3.13 (m, 10H β CH₂ Trp), 2.65-2.77 (m, 4H, β,γ CH₂ Glu); MALDI-TOF (m/z): C₆₀H₅₇N₁₁O₈ calcd. 1059.4392; found 1082.2554 [M + Na]⁺, 1098.2372 [M + K]⁺.

(β -Ala)-[KR₅]: HPLC (R_t) = 9.28 min; MALDI-TOF (m/z): C₃₉H₇₇N₂₃O₇ calcd. 979.6376; found 980.4063 [M + H]⁺.

The synthetic Schemes for [W₅G(propargyl)], [W₅E], [K(N₃)R₅], and (β -Ala)-[KR₅] are depicted in Schemes S1-S4, respectively.

5. Conjugation of linear or monocyclic peptides by click chemistry. In general, the alkyne (1 equiv) and the azide (1 equiv) were dissolved in methanol/water. To this solution, pentahydrated copper sulphate (1 equiv), copper powder (Cu, 10 equiv), sodium ascorbate (10 equiv), and DIPEA (2 equiv) were added. The reaction mixture was stirred at room temperature under N₂ and monitored by MALDI-TOF mass spectra. As a representative example, the synthesis of [W₅G]-(click)-[KR₅] is

described here (Scheme S5). [W₅G(propargyl)] (7.00 mg, 0.0068 mmol, 1 equiv) and [K(N₃)R₅] (6.36 mg, 0.0068 mmol, 1 equiv) were dissolved in CH₃OH/H₂O (1:1, v/v, 2 mL), and CuSO₄·5H₂O (1.7 mg, 0.0068 mmol, 1 equiv), Cu (4.32 mg, 0.068 mmol, 10 equiv), sodium ascorbate (13.47 mg, 0.068 mmol, 10 equiv) and DIPEA (2.26 μL, 0.013 mmol, 2 equiv) were added, and the mixture was stirred for 3 h. The mixture was filtered and the filtrate was dried using rotatory evaporator. The crude peptide [W₅G]-(triazole)-[KR₅] was purified using a preparative RP-HPLC and lyophilized to give 3 mg fluffy brown product. **[W₅G]-(triazole)-[KR₅]**: Yield 22% (fluffy brown solid 3 mg); ¹H NMR (DMSO-*d*₆, 300 MHz, δ ppm): 10.69-10.92 (m, 5H, *NH* Trp), 7.98-8.36 (m, 12H, *NH*), 6.77-7.74 (m, 46H, *ArH* and *NH* guanidinium), 4.00-4.40 (m, 6H, *αCH* Trp and Gly(propargyl)), 3.58-3.95 (broad peak, 6H, *αCH* Arg and Lys), 2.73-3.29 (m, 24H, *βCH* Arg and *εCH* Lys, *βCH* Trp and Gly(propargyl)), 1.25-1.96 (m, 26H, *β,γCH* Arg and *β,γ,δCH* Lys). HPLC (*R*_t) = 10.60 min; MALDI-TOF (*m/z*): C₉₆H₁₂₅N₃₅O₁₂ calcd. 1960.0247; found 1961.7063 [M + H]⁺.

[W₅G]-(triazole)-KR₅: Yield 26% (brown solid, 3.5 mg); HPLC (*R*_t) = 10.30 min; MALDI-TOF (*m/z*): C₉₆H₁₂₇N₃₅O₁₃ calcd. 1978.0353; found 1979.7148 [M + H]⁺.

W₅G-(triazole)-KR₅: Yield 15% (brown solid, 4.0 mg); HPLC (*R*_t) = 10.30 min; MALDI-TOF (*m/z*): C₉₆H₁₂₉N₃₅O₁₄ calcd. 1996.0458; found 1996.7783 [M]⁺.

6. Conjugation of monocyclic peptides by peptide bond. The dry powdered monocyclic peptides, [W₅E] (12.7 mg, 0.012 mmol, 1 equiv) and (β-Ala)-[R₅K] (11.8mg, 0.012 mmol, 1 equiv), were added to 5 mL glass vial and dissolved in anhydrous DMF (1 mL) using magnetic bead with stirring at room temperature under

N₂ gas. The coupling and activating reagents, 1-hydroxybenzotriazole (HOBT, 4.21 mg, 0.031 mmol, 2.6 equiv), (Benzotriazol-1-yloxy)tripyrrolidinophosphonium hexafluorophosphate (PyBOP, 8.11 mg, 0.015 mmol, 1.3 equiv), and DIPEA (16.70 μL, 0.096 mmol, 8 equiv) were added. The mixture was stirred for 1 h. After 1 h reaction, the bicyclic peptide was precipitated using cold diethyl ether and separated by centrifugation. The crude peptide was purified by RP-HPLC as described above (Scheme S6). **[W₅E]-(β-Ala)-[KR₅]**: Yield 15% (white fluffy solid, 3.70 mg); ¹H NMR (DMSO-*d*₆, 300 MHz, δ ppm): 10.70-10.90 (m, 5H, *NH* Trp), 7.84-8.30 (m, 14H, *NH*), 6.80-7.84 (m, 45H, *ArH* and *NH*, *NH*₂ Arg), 4.14-4.37 (m, 5H, *αCH* Trp), 3.97-4.16 (m, 7H, *αCH* Arg and Glu), 3.35-3.57 (m, 4H, *βCH* β-Ala and *εCH* Lys), 2.90-3.20 (m, 10H, *βCH* Trp), 2.20-2.35 (m, 6H, *β,γ* *CH* Glu and *αCH* β-Ala), 2.52-2.65 (m, 10H, *δCH* Arg), 1.75-1.93 (m, 12H, *βCH* Arg and Lys), 1.52-1.72 (m, 14H, *γ,δCH* Lys and *γCH* Arg); HPLC (*R*_t) = 32.30 min; MALDI-TOF (*m/z*): C₉₉H₁₃₂N₃₄O₁₄ calcd. 2021.0662; found 2022.6672 [*M* + *H*]⁺, 2043.5676 [*M* + *Na*]⁺.

7. Synthesis of fluorescein-labeled monocyclic peptide (F'-[KW₄E]). H-Trp-(Boc)-2-chlorotrityl chloride resin (0.3 mmol, 384 mg, 0.78 mmol/g) was swelled in DMF for 30 min under N₂. Fmoc-Trp(Boc)-OH (632 mg, 1.2 mmol, 4 equiv) was coupled to *N*-terminal the resin using HBTU (455 mg, 1.2 mmol, 4 equiv) and DIPEA (418 μL, 2.4 mmol, 8 equiv) in DMF (12 mL) by agitating the resin for 1 h. After completion of the coupling, the resin was washed with DMF (20 mL × 3) followed by Fmoc-deprotection with piperidine in DMF (20% v/v) and again washed with DMF (20 mL × 3). The subsequent amino acids, Fmoc-Glu(OtBu)-OH (511 mg, 1.2 mmol, 4 equiv),

Fmoc-Trp(Boc)-OH, Fmoc-Trp(Boc)-OH, (Dde)-Lys(Fmoc)-OH (Dde: *N*-(1-(4,4-dimethyl-2,6-dioxocyclohexylidene)ethyl)) (639 mg, 1.2 mmol, 4 equiv) and Fmoc- β -Ala-OH (374 mg, 1.2 mmol, 4 equiv) were coupled in a similar manner, followed by each cycle of deprotection of Fmoc group after each coupling. Then a mixture of 5(6)-carboxyfluorescence diisobutyrate (CFDI, 465 mg, 0.9 mmol, 3 equiv), 1-hydroxy-7-azabenzotriazole (HOAT, 122 mg, 0.9 mmol, 3 equiv), 7-azabenzotriazol-1-yl-oxytris(pyrrolidino)phosphonium hexafluorophosphate (PyAOP, 469 mg, 0.9 mmol, 3 equiv), and DIPEA (314 μ L, 1.8 mmol, 6 equiv) in anhydrous DMF/DCM (5:1 v/v, 12 mL) was added to the resin-bound linear peptide. The coupling reaction was carried out for 3 h at room temperature, and the resin was washed with DMF (20 mL \times 3). The Dde protection at *N*-terminal was deprotected by agitating with hydrazine monohydrate in DMF (2% v/v, 15 mL \times 3, 5 min). The CFDI protection was deprotected by incubating peptidyl resin with 20% piperidine in DMF (15 mL \times 2, 10 min. each) with final washing with DMF (20 mL \times 3). Finally, the side chain protected peptide was cleaved from the resin by shaking the resin with a mixture of TFE/acetic acid/DCM (2:1:7, v/v/v, 50 mL) for 1 h. The solution was evaporated, and the residue was dried overnight in a vacuum. The crude peptide was used directly for the cyclization under a dilute condition with DMF/DCM (5:1, v/v, 250 mL), using HOAT (163 mg, 1.2 mmol, 4 equiv) and DIC (185 μ L, 1.2 mmol, 4 equiv), and stirred for 24 h under nitrogen atmosphere. After cyclization, the solvent was evaporated, and the side-chain deprotection was carried out by the addition of cleavage cocktail, TFA/thioanisole/EDT/anisole (90:5:3:2, v/v/v/v, 15 mL) for 2 h. The crude bicyclic peptide was precipitated and purified as describe above. The synthetic method of F'-

[KW₄E] is presented in Scheme S7. **F'-[KW₄E]**: ¹H NMR (DMSO-*d*₆, 300 MHz, δ ppm): 11.58 (s, 1H, COOH), 10.62-10.92 (m, 4H, NH Trp) 7.80-8.26 (m, 8H, NH), 6.44-7.66 (m, 29H, ArH), 5.75 (s, 2H, OH), 4.10-4.45 (m, 4H, α CH Trp), 4.92-4.06 (m, 2H, α CH Glu and Lys), 2.58-3.19 (m, 8H, β CH Trp), 1.45-2.30 (m, 16H, α,β CH β -Ala, β,γ CH Glu, and $\beta,\gamma,\delta,\epsilon$ CH Lys); HPLC (R_t) = 18.20 min; MALDI-TOF (m/z): C₇₉H₇₄N₁₂O₁₅, calcd. 1430.5397; found 1469.4227 [M + K]⁺.

8. Synthesis of fluorescein-labeled bicyclic peptide (F'-[KW₄E]-(β -Ala)-[KR₅]).

The dry powdered fluorescein-labeled cyclic peptide F'-[KW₄E] (8.9 mg, 0.0062 mmol, 1 equiv), 1-hydroxybenzotriazole (HOBT, 2.16 mg, 0.016 mmol, 2.6 equiv), and PyBOP (4.19 mg, 0.080 mmol, 1.3 equiv) were dissolved in DMF (1.5 mL). DIPEA (8.53 μ L, 0.049 mmol, 8 equiv) was added dropwise with stirring using magnetic bead under N₂ condition for 10 min. to preactivate COOH group of glutamic acid followed by dropwise addition of a solution of cyclic peptide (β -Ala)-[KR₅] (6.00 mg, 0.0062 mmol, 1 equiv) in DMF (0.5 mL) (Scheme S8). The reaction was monitored by MALDI-TOF, showing completion of the reaction after 40 min. The crude fluorescein-labeled bicyclic peptide was precipitated by adding cold diethyl ether. The crude peptide was purified using RP-HPLC method described above. **F'-[KW₄E]-(β -Ala)-[KR₅]**: HPLC (R_t) = 10.30 min; MALDI-TOF (m/z): C₁₁₈H₁₄₉N₃₅O₂₁, calcd. 2392.1667; found 2393.7971 [M + H]⁺.

9. Cell culture. Human ovarian carcinoma cell line SK-OV-3, human leukemia cell line CCRF-CEM, and human embryonic kidney cell line HEK 293T were purchased

from American Type Culture Collection. The cells were grown in eagle's minimum essential medium (EMEM) for SK-OV-3 and HEK 293T, and RPMI-1640 medium (ATCC, Manassas, VA) for CCRF-CEM, supplemented with 10% fetal bovine serum (FBS) and 1% penicillin-streptomycin solution (10,000 units of penicillin and 10 mg of streptomycin in 0.9% NaCl) in a humidified atmosphere of 5% CO₂ at 37 °C.

10. Confocal laser scanning microscopy (CLSM)

10.1. Cellular uptake of F'-[KW₄E]-(β -Ala)-[KR₅] in SK-OV-3. SK-OV-3 cells were seeded with complete EMEM on coverslips in 6-well plate (1×10^5 cells/well) and kept until 50% confluency. The media were removed and cells were incubated with 10 μ M F'-[KW₄E]-(β -Ala)-[KR₅] in Gibco® Opti-MEM® I reduced serum medium (Life Technologies, Grand Island, NY) for 1 h at 37 °C. Then cells were washed with 1X phosphate buffered saline with calcium and magnesium (PBS⁺) three times. The coverslips were mounted on microscope slides, and images were obtained using Carl Zeiss LSM 700 system with a 488 nm argon ion laser excitation and a BP 505-530 nm band pass filter.

11. Flow cytometry

11.1. Cellular uptake of fluorescein-labeled bicyclic peptide. SK-OV-3 cells were grown in 6-well plates (2×10^5 cells/well) with complete EMEM media prior 24 h to add F'-[KW₄E]-(β -Ala)-[KR₅]. The 1 mM of fluorescein-labeled bicyclic peptide stock solution was prepared in water and diluted in Gibco® Opti-MEM® I reduced serum medium to generate 5 μ M concentration. The culture media were removed from 6-well

plates, and the prepared 5 μ M fluorescein-labeled bicyclic peptide solution was added. After 1 h incubation, trypsin-EDTA solution was added to detach cells from plate's surface and remove cell surface binding peptides. After 5 min of treatment with trypsin-EDTA, a portion of complete media was added to stop the activity of trypsin. The cell lines were collected and centrifuged at 2500 rpm. Then they were washed twice using PBS without calcium and magnesium, and prepared in FACS buffer for cell sorting. Finally, the cells were analyzed by BD FACSCalibur™ or FACSVerse™ flow cytometer using FL1/FITC channel. The data collection was based on the mean fluorescence signal for 10,000 cells. All assays were carried out in triplicate. 5(6)-Carboxyfluorescein (FAM) was used as the negative control.

11.2. Mechanistic study of cellular uptake by removing energy sources. To examine the cellular uptake mechanism F'-[KW₄E]-(β -Ala)-[KR₅] at low temperature, the uptake assay was carried out at 4 °C to inhibit the energy-dependent cellular uptake. SK-OV-3 cells were preincubated at 4 °C for 15 min, and incubated with the fluorescein-labeled bicyclic peptide for 1 h at 4 °C. Cells were collected and assessed with the same protocol described in cellular uptake of fluorescein-labeled bicyclic peptide. The data collected at 37 °C were used for control. For the ATP-depletion assay, cells were incubated with 10 mM sodium azide and 50 mM 2-deoxy-D-glucose for 1 h before adding the fluorescein-labeled bicyclic peptide. During 1 h incubation, the 50 μ M of fluorescein-labeled bicyclic peptide was prepared in the Opti-MEM® I reduced serum medium in the presence of 10 mM sodium azide and 50 mM 2-deoxy-D-glucose. Then the cells were incubated with this solution for 1 h. The protocol for

sample preparation and flow cytometry analysis was same with the protocol described in cellular uptake of fluorescein-labeled bicyclic peptide.

11.3. Cellular uptake pathway study using endocytosis inhibitors. The cellular uptake studies were also conducted in the presence of several endocytosis inhibitors. Chloroquine (100 μM), chlorpromazine (30 μM), methyl β -cyclodextrin (2.5 mM), nystatin (50 $\mu\text{g/mL}$), and 5-(*N*-ethyl-*N*-isopropyl)amiloride (EIPA, 50 μM) were used. SK-OV-3 cells were incubated with each inhibitor for 30 min before 1 h incubation with F'-[KW₄E]-(β -Ala)-[KR₅]. The protocol for sample preparation and flow cytometry analysis was same with the protocol described in cellular uptake of fluorescein-labeled bicyclic peptide.

12. Cytotoxicity assay by MTS assay. MTS proliferation assays were performed against two human cancer cell lines (SK-OV-3 and CCRF-CEM) and one human normal cell line (HEK 293T). Cells were seeded on 96-well plates (5×10^3 cells for SK-OV-3, 1×10^5 cells for CCRF-CEM, and 1×10^4 cells for HEK 293T) and incubated with 100 μL of complete media for overnight. The various concentrations (0– 600 μM) of the bicyclic peptide solution (10 μL) were added to cells, and kept at 37 °C with 5% CO₂ for 24 h. Then 20 μL of CellTiter 96 aqueous solution were added on each well and incubated at 37 °C with 5% CO₂ for 1-4 h. The absorbance was obtained at 490 nm using microplate reader. The cells without any peptide were used as control.

We carried out cytotoxic assay of all peptides against two adherent cell lines (SK-OV-3 and HEK 293T) using above protocol (Figure S1). In case of [W₅E]-(β -Ala)-[KR₅], we examined further cytotoxicity against non-adherent cell line (human leukemia CCRF-CEM). The result of cytotoxicity against CCRF-CEM was presented at Figure S2.

13. Cellular uptake of a phosphopeptide, F'-GpYEEI in the presence of peptides.

To evaluate and compare the molecular transporter property of the bicyclic peptides, their analogues, and other representative CPPs ([WR]₅, TAT, CR₇), the following procedure was employed. SK-OV-3 cells were seeded in 6-well plates (2×10^5 cells/well) and grown with complete EMEM media for overnight. A fluorescein-labeled phosphopeptide, F'-GpYEEI (5 μ M), and synthesized peptides (10 μ M) were premixed in OPTI-MEM I® reduced serum medium at room temperature for 30 min. Then the cells were incubated with the premixed solution at 37 °C with 5% CO₂ for 1 h. The sample preparation for FACS analysis was carried out with the same protocol described for cellular uptake for fluorescein-labeled bicyclic peptide. DMSO and F'-GpYEEI were used as a negative control (Figure S3).

14. Cellular uptake of doxorubicin (DOX).

DOX uptake in the presence of the bicyclic peptide was performed in SK-OV-3 cells. Dox (5 μ M) and the bicyclic peptide (10 μ M) were premixed in OPTI-MEM I® reduced serum medium. The premixed solution was added to cells and kept for 1 h at 37 °C with 5% CO₂. Then the media were replaced by fresh complete media and incubated for 24 h. The sample

preparation and FACS analysis were the same as described above except using FL2/PE channel.

15. Antiproliferative assay of doxorubicin in the presence of the bicyclic peptide.

The antiproliferative activity of DOX alone and in the presence of [W₅E]-(β -Ala)-[KR₅] against SK-OV-3 cells was determined by MTS assay. All cells were plated overnight in 96-well plates with a density of 5000 cells per well in 0.1 mL of appropriate growth medium at 37 °C. DOX alone (1 μ M) or a combination of DOX (1 μ M) and [W₅E]-(β -Ala)-[KR₅] (10 μ M) were incubated with the cells for 24 h. After 24 h incubation, the treatment was replaced by fresh media. The cells were kept in an incubator for 24-72 h. The cells without compounds were included in each experiment as controls. After each incubation period of time, 20 μ L of MTS solution was added and incubated for 2 h. The absorbance of the formazan product was measured at 490 nm using a microplate reader. The percentage of cell viability was calculated as (OD value of untreated cells – OD value of treated cells)/OD value of untreated cells \times 100%.

Figures for supporting information

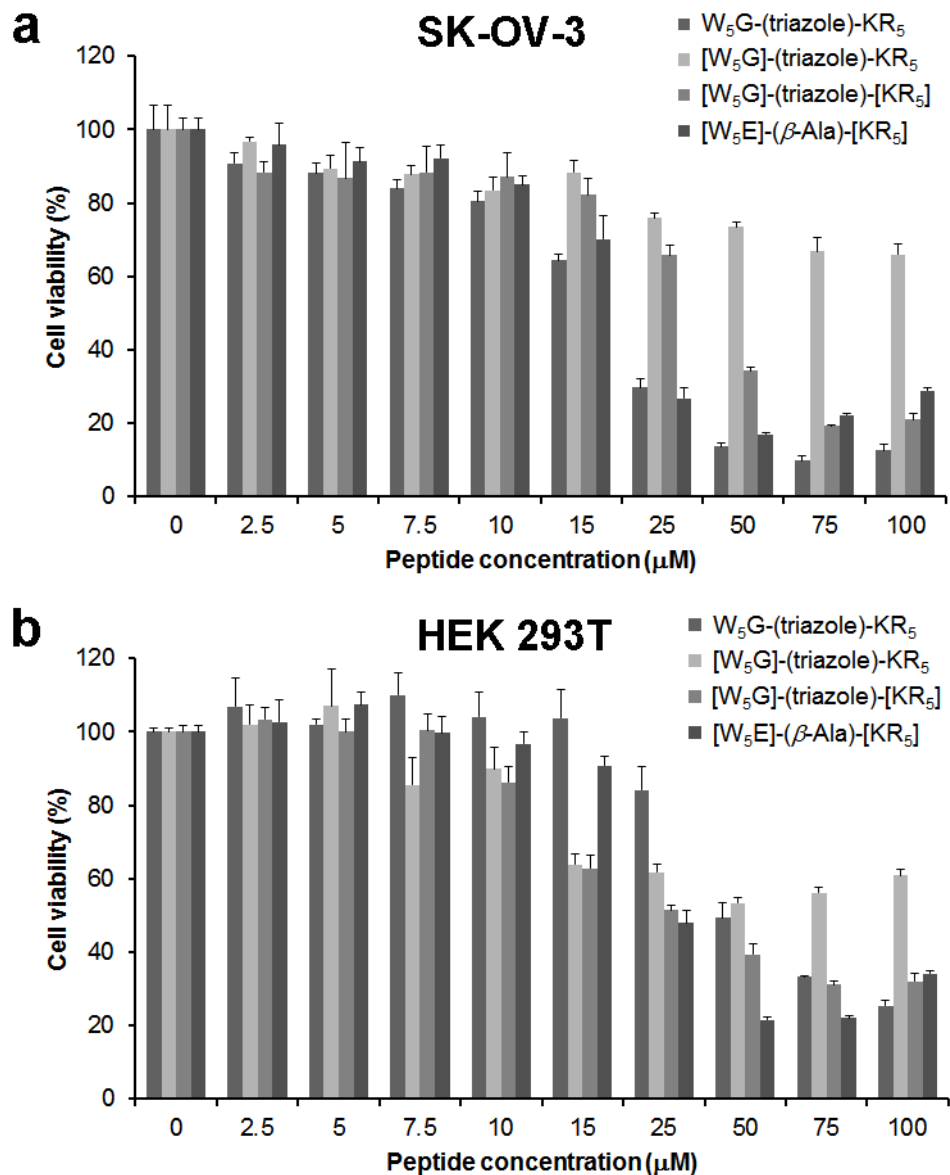


Figure S1. Cytotoxicity of amphiphilic peptides in human ovarian adenocarcinoma SK-OV-3 and human embryonic kidney HEK 293T cells after 24 h incubation.

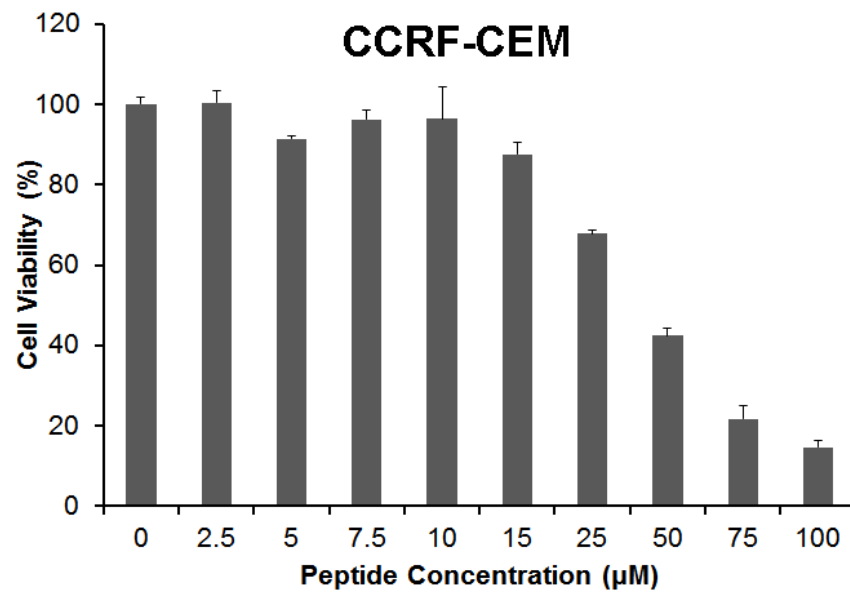


Figure S2. Cytotoxicity of $[W_5E]-(\beta\text{-Ala})-[KR_5]$ against human leukemia CCRF-CEM cell after 24 h incubation.

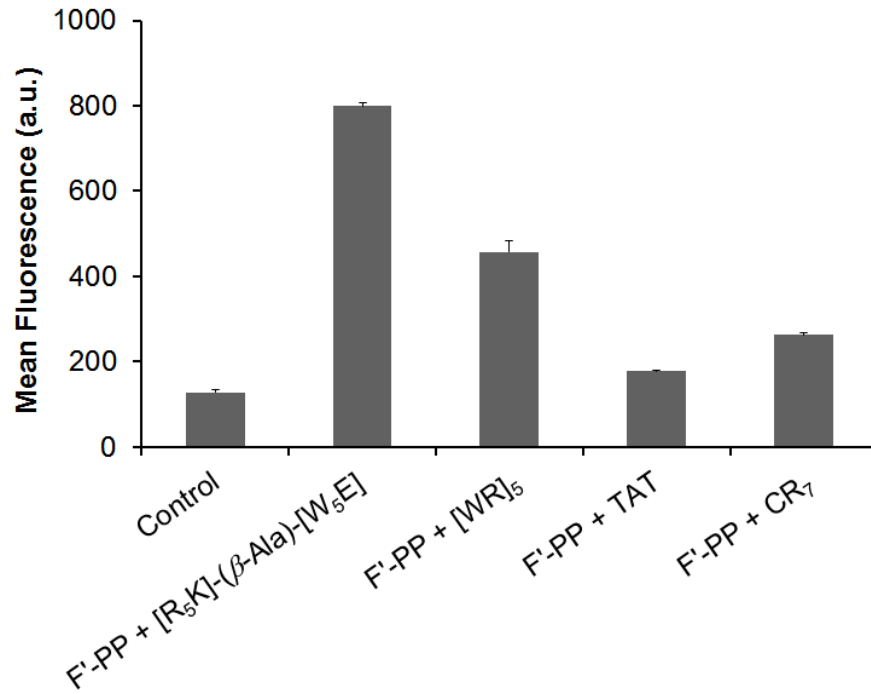
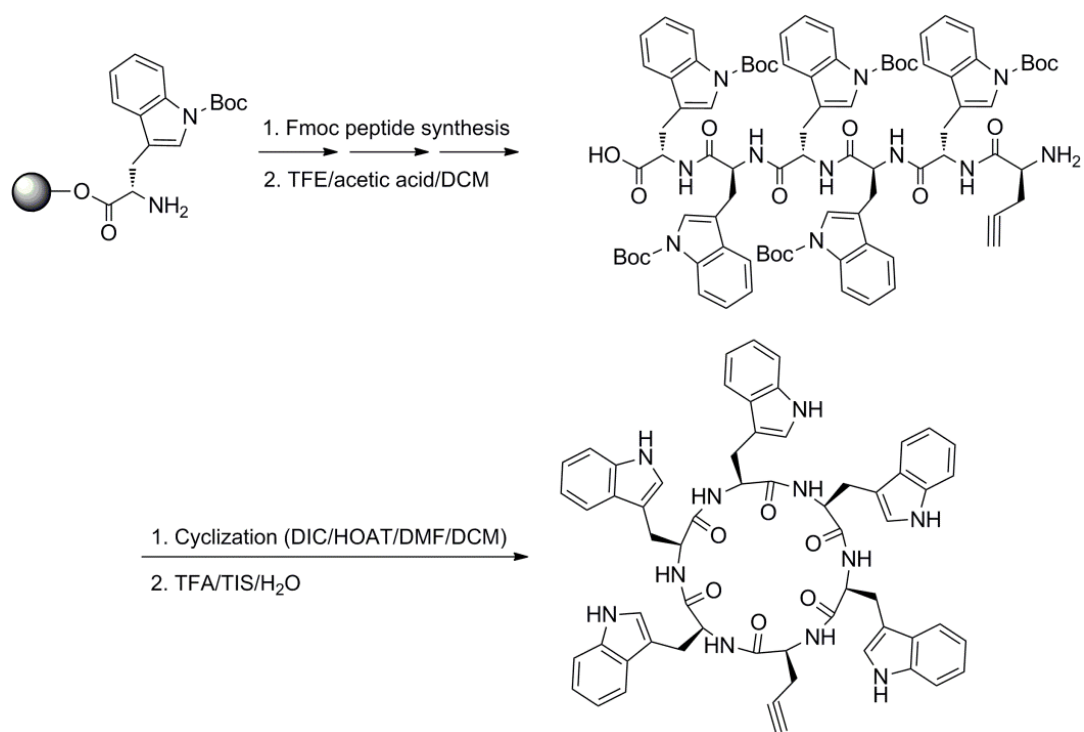
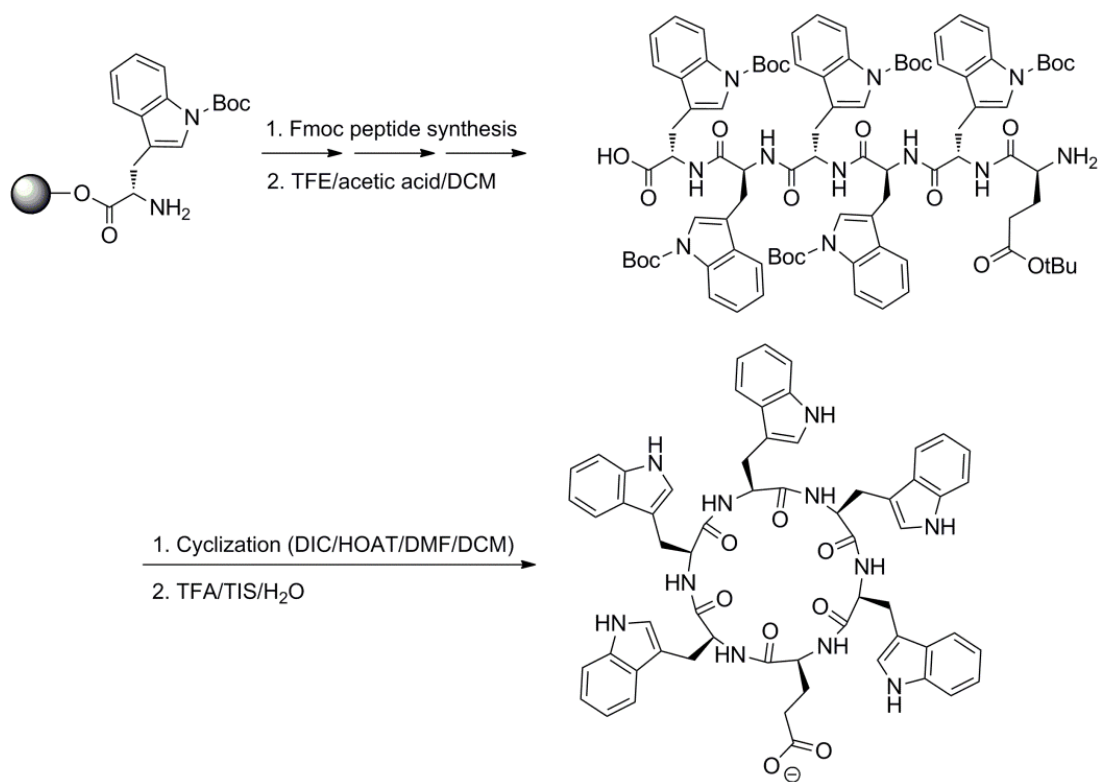


Figure S3. Cellular uptake of F'-GpYEEI (F'-PP, 5 μ M) in SK-OV-3 cells in the presence of cell-penetrating peptides (10 μ M). The sequences of CR₇ and TAT are CRRRRRRR-NH₂ and YGRKKRRQRRR-NH₂, respectively.

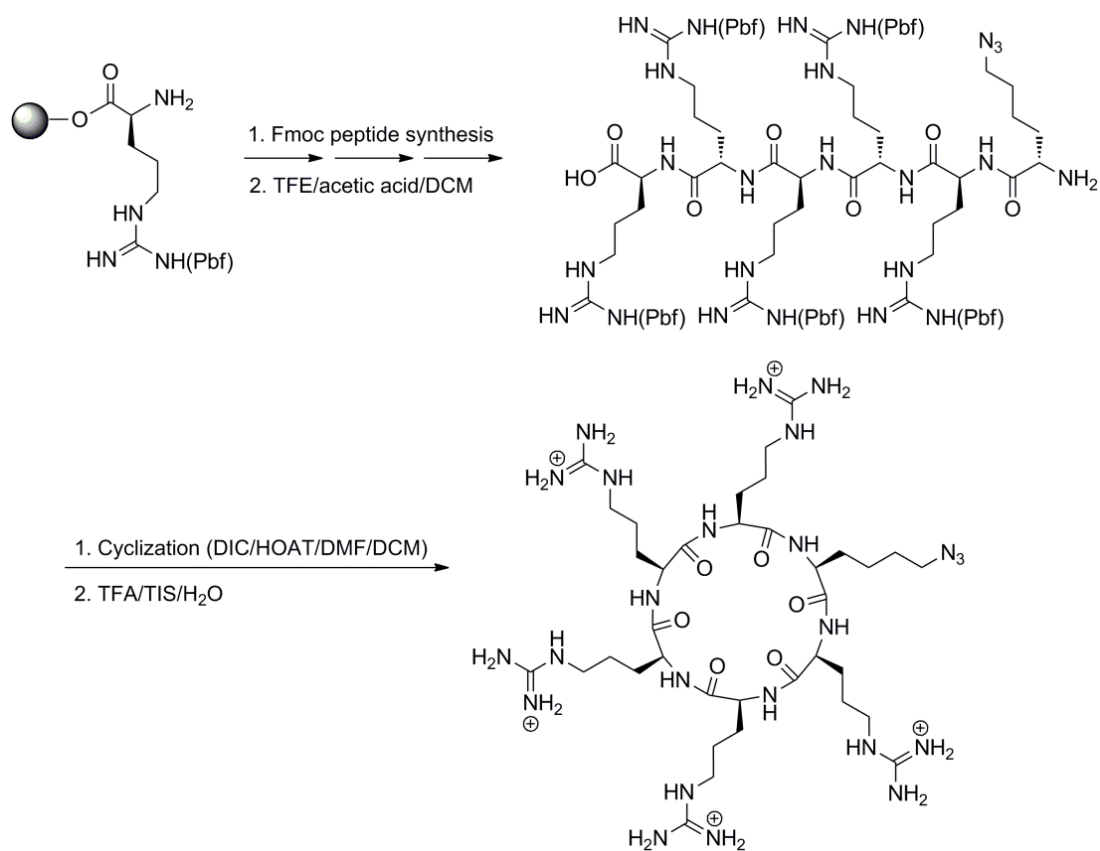
Schemes for supporting information



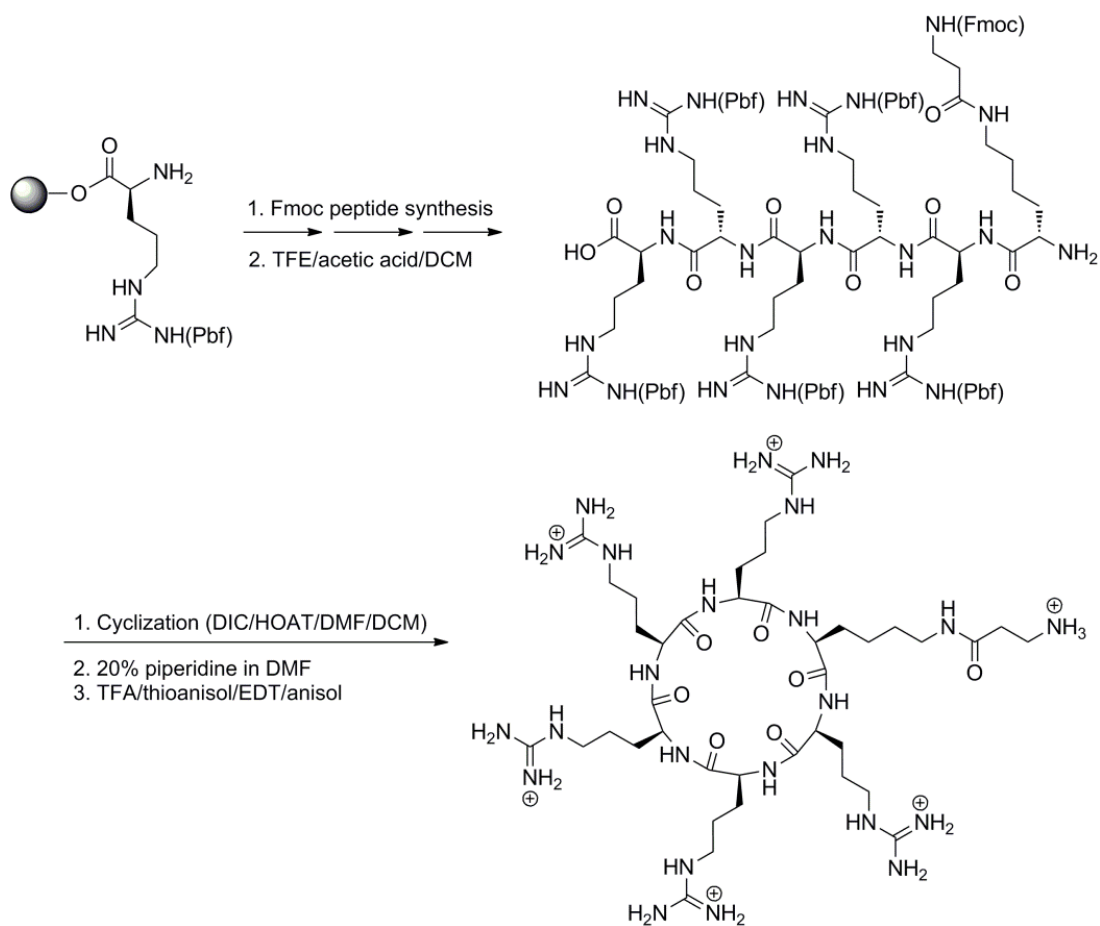
Scheme S1. The synthesis of monocyclic peptide [W₅G(propargyl)].



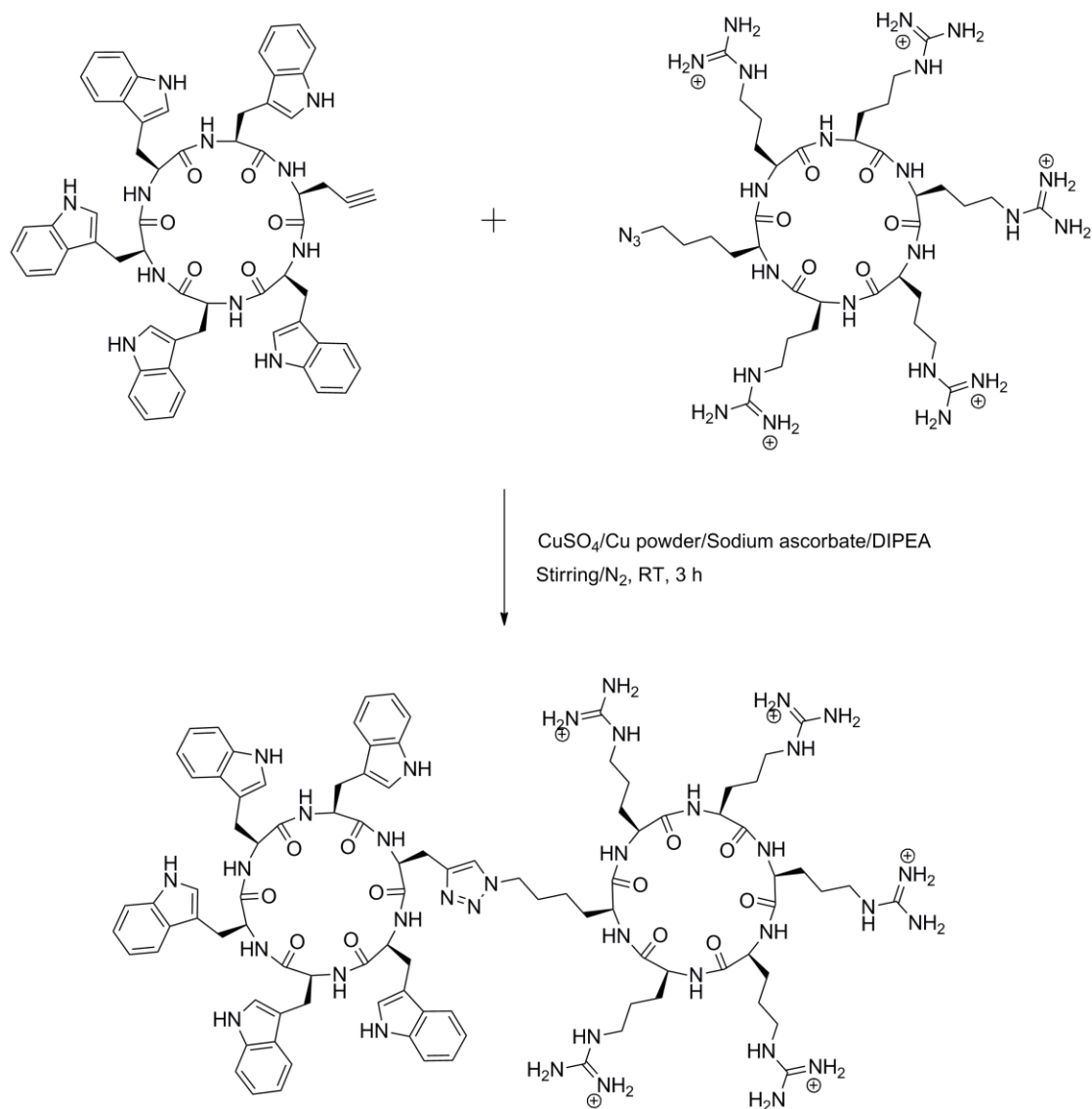
Scheme S2. The synthesis of monocyclic peptide [W₅E].



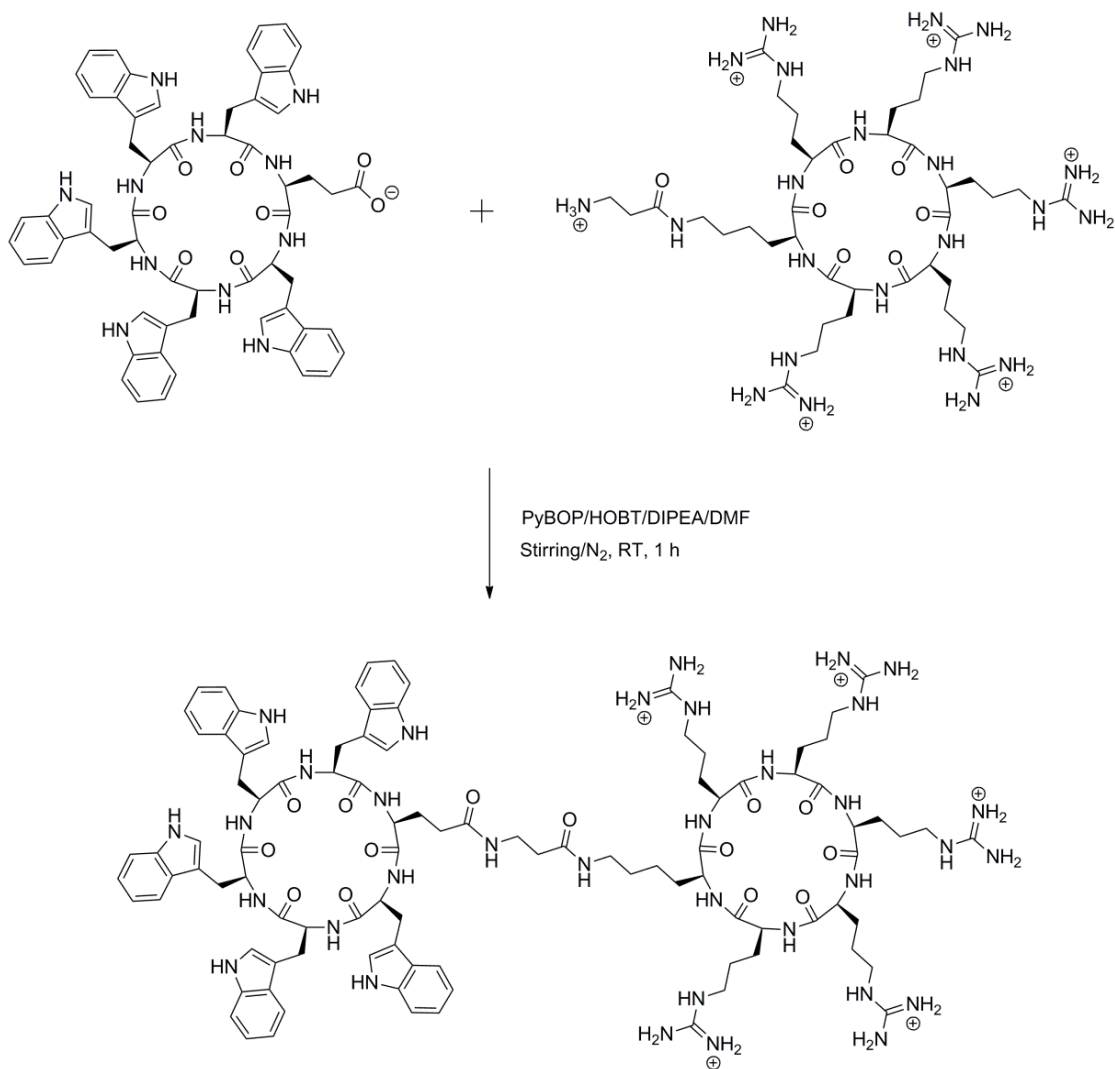
Scheme S3. The synthesis of monocyclic peptide [K(N₃)R₅].



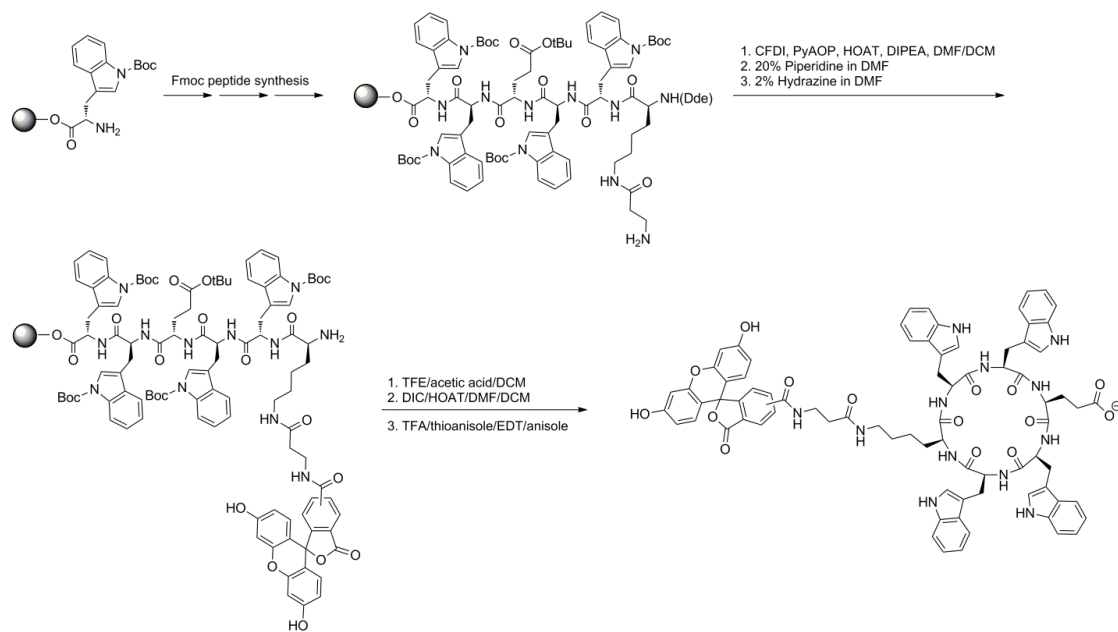
Scheme S4. The synthesis of monocyclic peptide (β -Ala)-[KR₅].



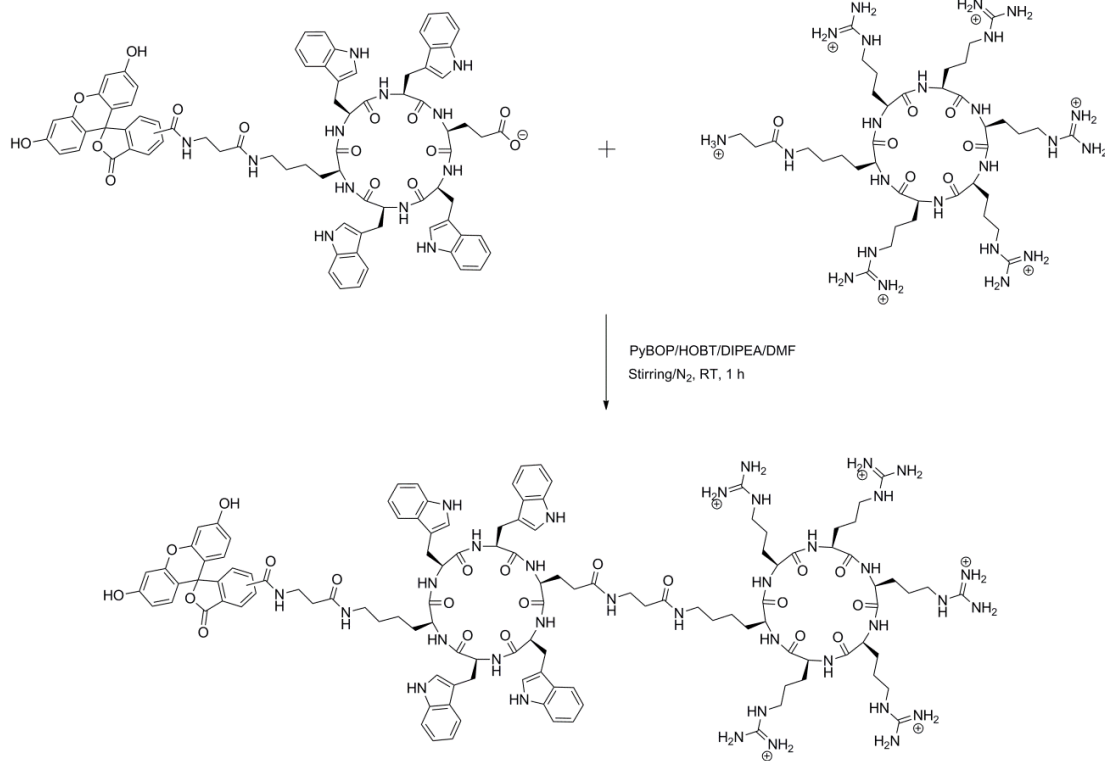
Scheme S5. The conjugation of two monocyclic peptides for the synthesis of [W₅G]-
(triazole)-[KR₅] peptide.



Scheme S6. The conjugation of two monocyclic peptides for the synthesis of [W₅E]-(β -Ala)-[KR₅] peptide.



Scheme S7. The synthesis of monocyclic F'-[KW₄E] peptide.



Scheme S8. The synthesis of fluorescein-labeled bicyclic peptide F'-[KW₄E]-(β-Ala)-[KR₅].

MANUSCRIPT II

Submitted to *Molecular Pharmaceutics* in March 2014

Enhanced Cellular Uptake of Short Polyarginine Peptides through Fatty Acylation and Cyclization

Donghoon Oh,^a Amir Nasrolahi Shirazi,^{a,b} Kevin Northup,^a Brian Sullivan,^a Rakesh
Kumar Tiwari,^{a,b} Keykavous Parang^{a,b,*}

^aDepartment of Biomedical and Pharmaceutical Sciences, College of Pharmacy,
University of Rhode Island, Kingston, RI 02881, United States

^bSchool of Pharmacy, Chapman University, Irvine, CA, 92866, United States

kparang@uri.edu

TITLE RUNNING HEAD. Fatty Acylated Cyclic Polyarginine as Molecular
Transporter

*Corresponding author:

K. Parang: 7 Greenhouse Road, Department of Biomedical and Pharmaceutical
Sciences, College of Pharmacy, University of Rhode Island, Kingston, Rhode Island,

02881, United States; Tel.: +1-401-874-4471; Fax: +1-401-874-5787; E-mail address:
kparang@uri.edu

Harry and Diane Rinker Health Science Campus, 9401 Jeronimo Road, School of
Pharmacy, Chapman University, Irvine, California 92618, United States; Tel.: +1-714-
516-5489; Fax: +1-714-516-5481; Email: parang@chapman.edu

ABSTRACT

The majority of the reported arginine-rich cell-penetrating peptides (CPPs) for the enhanced delivery of drugs are linear peptides. Moreover, they are usually composed of more than seven arginine residues to retain the cell penetration properties. Herein, we synthesized a class of eight polyarginine peptides containing 5 and 6 arginines namely R₅ and R₆. We further explored the effect of acylation with long chain fatty acids (i.e., octanoic acid, dodecanoic acid, hexadecanoic acid), and cyclization of amino acids on the cell penetrating properties of the peptides. The fluorescence-labeled acylated cyclic peptide dodecanoyl-[R₅] and linear peptide dodecanoyl-(R₅) showed approximately 13.7- and 10.2-fold higher cellular uptake than that of control 5(6)-carboxyfluorescein, respectively. The mechanism of the peptide internalization into cells was found to be energy-dependent endocytosis. The molecular transporter ability of fatty acylated cyclic peptides was evaluated using a flow cytometry method. Dodecanoyl-[R₅] and dodecanoyl-[R₆] enhanced the intracellular uptake of a fluorescence-labeled cell impermeable negatively charged phosphopeptide (F'-GpYEEI) in human ovarian cancer cells (SK-OV-3) by 3.4-fold and 5.5-fold, respectively. The cellular uptake of F'-GpYEEI in the presence of hexadecanoyl-[R₅] was 9.3- and 6.0-fold higher than that of in the presence of octanoyl-[R₅] and dodecanoyl-[R₅], respectively. A comparative FACS results showed that dodecanoyl-[R₅] enhanced the cellular uptake of the phosphopeptide by 1.4-2.5 fold higher than the corresponding linear peptide dodecanoyl-(R₅) and those of representative CPPs, such as hepta-arginine (CR₇) and TAT peptide. Our findings showed that a combination of acylation by long chain fatty acids and cyclization on short arginine-

containing peptides can improve their cell-penetrating property, possibly through efficient interaction of rigid positively charged R and hydrophobic dodecanoyl moiety with the corresponding residues in the cell membrane phospholipids.

Keywords: Acylation, Cyclic Peptide, Cyclization, Drug Delivery, Polyarginine.

INTRODUCTION

Polyarginine peptides are known as one of the widely used classes of cell-penetrating peptides (CPPs) and cellular delivery tools.¹ It has been reported that the presence of the guanidine group in the side chain of arginine plays a key role for improved ability of arginine-rich peptides to cross the cell membrane.^{2,3} Various systematic structural investigations have been performed to determine the required number of arginine residues and the length of the peptide for the optimization of cellular uptake.^{2,4} Short polyarginine peptides containing less than six arginine residues did not exhibit significant cellular uptake in several previously reported investigations.^{2,4,5} Thus, the presence of more than six arginine residues in the structure of polyarginine peptides is critical for their efficient cell-penetrating functions.

On the other hand, several investigations were conducted to increase the cellular uptake of polyarginines by attaching the fatty acid to the *N*-terminal of the peptide. It has been previously reported that the acylation of the *N*-terminal by fatty acids can facilitate the intracellular uptake of polyarginines.⁶⁻⁸ For instance, Katayama et al. synthesized acylated octa-arginines and discovered that the introduction of hydrophobic fatty acid enhanced the intracellular uptake of octa-arginine peptide and its conjugated ubiquitin.⁸ Furthermore, Lee et al. designed a class of lipopeptides carrying 7-15 arginine residues. Among them, myristoylated-hendeca-arginine (C₁₄R₁₁) was found to be the most efficient cell-penetrating peptide.⁷ However, the fatty acylated polyarginine peptides that contain 7-15 arginine residues can potentially cause toxicity, and they can be easily degraded by proteases.

Moreover, linear peptides carrying L-form are not stable in serum and therefore have a limited application for *in vivo* studies.⁹ Replacing L-form amino acids with D-form to improve the peptide stability leads to high cost production. On the other hand, cyclic peptides show more proteolytic stability than linear counterparts. Thus, the synthesis and development of cyclic CPPs containing short amino acid sequence with less toxicity is desired.

Herein, we designed acylated cyclic polyarginine peptides (ACPPs) containing five arginine residues and investigated their ability as cell-penetrating peptides. We compared ACPPs with a corresponding acylated linear polyarginine peptide (ALPP) and a nonacylated cyclic polyarginine as controls. We hypothesize that the combination of acylation and cyclization of short polyarginine peptides having less than six arginine residues will increase the intracellular uptake and can generate peptides with molecular transporter properties. For convenience, square brackets [] and parentheses () were used to represent cyclic and linear peptides, respectively.

EXPERIMENTAL SECTION

Peptide Synthesis. All peptides were synthesized by Fmoc/*t*Bu solid-phase peptide synthesis strategy either manually or using Rainin PS3™ synthesizer (Protein Technologies Inc.). Manual reactions were carried out in a glass reaction vessel with a sintered glass frit by mixing under nitrogen bubbling at room temperature. Fmoc-L-amino acid building blocks, fatty acids, and single Arg(Pbf) loaded 2-chlorotrityl resin were used as starting materials. 2-(1*H*-Benzotriazole-1-yl)-1,1,3,3-tetramethyluronium hexafluorophosphate (HBTU), hydroxybenzotriazole (HOBT), and *N,N*-

diisopropylethylamine (DIPEA) in *N,N*-dimethylformamide (DMF) were used as coupling and activating reagents, respectively for manual synthesis. In case of using peptide synthesizer, 0.4 M *N*-methylmorpholine in DMF was used instead of DIPEA. Piperidine in DMF (20%) was employed to deprotect Fmoc group at each step.

To cleave the linear peptide from the resin, a mixture of trifluoroacetic acid (TFA)/triisopropylsilane (TIS)/water (92.5/5/2.5, v/v/v) was used. However, in the synthesis of cyclic peptides, the side chain protected linear peptides were first cleaved from the resin by using a cleavage cocktail, containing 2,2,2-trifluoroethanol (TFE)/acetic acid/dichloromethane (DCM) (2:1:7, v/v/v). Cyclization reaction was performed by employing a mixture of 1-hydroxy-7-azabenzotriazole (HOAT) and *N,N'*-diisopropylcarbodiimide (DIC) in anhydrous DMF/DCM for 12 h. After solvent evaporation, the peptide was deprotected and cleaved from the resin by using a cleavage cocktail reagent "R", containing TFA/thioanisole/1,2-ethanedithiol (EDT)/anisole (90:5:3:2, v/v/v/v) for 2-3 h. The crude peptides were precipitated and washed with cold diethyl ether. To purify the crude peptides, we used a reversed-phase high pressure liquid chromatography (RP-HPLC) system using Shimadzu LC-8A preparative liquid chromatography on a Phenomenex Gemini C18 column (10 μ m, 250 \times 21.2 mm) with a gradient 0-100% of acetonitrile (CH₃CN) containing 0.1% TFA (v/v) and water containing 0.1% TFA (v/v) for 1 h with a flow rate at 15.0 mL/min at the wavelength of 214 nm.

As a representative example, the synthesis of dodecanoyl-[R₅] is described here. H-Arg(Pbf)-2-chlorotrityl resin (660 mg, 0.35 mmol, 0.53 mmol/g) was swelled in DMF for 40 min by N₂. Fmoc-Arg(Pbf)-OH (681 mg, 1.05 mmol, 3 equiv) was

coupled to the *N*-terminal of the resin, using HBTU (398 mg, 1.05 mmol, 3 equiv), HOBT (142 mg, 1.05 mmol, 3 equiv), and DIPEA (366 μ L, 2.1 mmol, 6 equiv) in DMF (15 mL) by agitating the resin for 1 h using N₂. After the coupling, the resin was washed with DMF, followed by Fmoc-deprotection with piperidine in DMF (20%). The subsequent three Fmoc-Arg(Pbf)-OH couplings and one Dde-Lys(Fmoc)-OH (559 mg, 1.05 mmol, 3 equiv; Dde = 1-(4,4-dimethyl-2,6-dioxocyclohex-1-ylidene)ethyl) coupling was carried out in the same manner, respectively. After removing the Fmoc group in side chain of lysine, dodecanoic acid (210 mg, 1.05 mmol, 3 equiv) was coupled using HBTU, HOBT, and DIPEA. Then Dde protection group at *N*-terminal of peptide was removed by 2% hydrazine in DMF, followed by washing with DMF and DCM. The side chain protected linear peptides were cleaved from the resin by using a cleavage cocktail, TFE/acetic acid/DCM (2:1:7, v/v/v) for 1 h. The filtrate was evaporated, and the residue was dried overnight in a vacuum. The cyclization was conducted under a dilute condition with anhydrous DMF/DCM (5:3, v/v, 250 mL), using HOAT (190 mg, 1.4 mmol, 4 equiv) and DIC (240 μ L, 1.54 mmol, 4.4 equiv), and stirred for 12 h under nitrogen atmosphere. After cyclization, the solvent was evaporated, and the side chain deprotection was carried out by the addition of reagent "R" for 2 h. The crude dodecanoyl-[R₅] was precipitated and washed with cold diethyl ether, and purified by preparative RP-HPLC system as described above.

Fluorescein-labeled peptides were synthesized with the same protocol before the attachment of fatty acid. We used Fmoc-12-aminododecanoic acid instead of dodecanoic acid, and after removing Fmoc group, 5(6)-carboxyfluorescein

diisobutyrate (CFDI) was attached using 7-azabenzotriazol-1-yl-oxytris(pyrrolidino)phosphonium hexafluorophosphate (PyAOP), HOAT, and DIPEA. As an example, we started fluorescein-labeled peptide synthesis in smaller scale with H-Arg(Pbf)-2-chlorotrityl resin (208 mg, 0.11 mmol, 0.53 mmol/g). Fmoc-Arg(Pbf)-OH (214 mg, 0.33 mmol, 3 equiv), Dde-Lys(Fmoc)-OH (176 mg, 0.33 mmol, 3 equiv), and Fmoc-12-aminododecanoic acid (144 mg, 0.33 mmol, 3 equiv) were used to couple each building block to the resin using HBTU (125 mg, 0.33 mmol, 3 equiv), HOBT (45 mg, 0.33 mmol, 3 equiv), and DIPEA (115 μ L, 0.66 mmol, 6 equiv) in DMF. CFDI (170 mg, 0.33 mmol, 3 equiv) was coupled with amino group of 12-aminododecanoic chain using PyAOP (172 mg, 0.33 mmol, 3 equiv), HOAT (45 mg, 0.33 mmol, 3 equiv), and DIPEA. The reaction mixture was agitated for 3 h using N_2 . After removal of Dde protecting group with 2% hydrazine in DMF and washing with DMF and DCM, side chain protected fluorescein linear peptides were cleaved from resin using TFE/acetic acid/DCM (2:1:7, v/v/v). The following cyclization and purification steps were same as above. The molecular weights of final products were confirmed by an AXIMA performance matrix-assisted laser desorption/ionization-time of flight (MALDI-TOF) mass spectrometer (Shimadzu Corporation).

Dodecanoyl-[R₅]: MALDI-TOF (m/z): C₄₈H₉₄N₂₂O₇ calcd. 1090.7676; found 1091.7576 [M + H]⁺. **Dodecanoyl-[R₆]:** MALDI-TOF (m/z): C₅₄H₁₀₆N₂₆O₈ calcd. 1246.8687; found 1247.7397 [M + H]⁺. **Dodecanoyl-(R₆):** MALDI-TOF (m/z): C₄₈H₉₆N₂₂O₈ calcd. 1108.7781; found 1109.7308 [M + H]⁺. **[R₅]:** MALDI-TOF (m/z): C₃₆H₇₂N₂₂O₆ calcd. 908.6005; found 909.6772 [M + H]⁺. **F'-Dodecanoyl-[R₅]:**

MALDI-TOF (m/z): C₆₉H₁₀₅N₂₃O₁₃ calcd. 1463.8262; found 1464.6556 [M + H]⁺. **F'-Dodecanoyl-(R₅)**: MALDI-TOF (m/z): C₆₉H₁₀₇N₂₃O₁₄ calcd. 1481.8368; found 1482.7586 [M + H]⁺. **W-Dodecanoyl-[R₅]**: MALDI-TOF (m/z): C₆₁H₁₀₇N₂₅O₉ calcd. 1333.8684; found 1334.8713 [M + H]⁺. **W₄-[R₅]**: MALDI-TOF (m/z): C₈₂H₁₁₄N₃₀O₁₁ calcd. 1694.9283; found 1696.3111 [M + H]⁺. **Octanoyl-[R₅]**: MALDI-TOF (m/z): C₄₄H₈₆N₂₂O₇ calcd. 1034.7050; found 1035.7084 [M + H]⁺. **Hexadecanoyl-[R₅]**: MALDI-TOF (m/z): C₅₂H₁₀₂N₂₂O₇ calcd. 1146.8302; found 1147.8404 [M + H]⁺.

Cell Culture. Human ovarian adenocarcinoma (SK-OV-3), leukemia (CCRF-CEM), and embryonic kidney (HEK 293T) cells were purchased from American Type Culture Collection. The SK-OV-3 and HEK 293T cells were grown in eagle's minimum essential medium (EMEM), and RPMI-1640 medium (ATCC, Manassas, VA) was used for CCRF-CEM cells. Both medium were supplemented with fetal bovine serum (FBS, 10%) and penicillin-streptomycin solution (1%, 10,000 units of penicillin and 10 mg of streptomycin in 0.9% NaCl) in a humidified atmosphere of 5% CO₂ at 37 °C.

Cytotoxicity Assay. Cytotoxicity of peptides was examined by MTS proliferation assay in two human cancer cell lines (SK-OV-3 and CCRF-CEM) and one human normal cell line (HEK 293T). Cells were seeded into 96-well plates (SK-OV-3 (5 × 10³ cells/well), CCRF-CEM (1 × 10⁵ cells/well), and HEK 293T (1 × 10⁴ cells/well)). Then, the cells were incubated with complete media (100 μL) for overnight. Different concentration (0–600 μL) of peptide solution (10 μL) were added to cells and incubated at 37 °C with 5% CO₂ for 24 h. Then, CellTiter 96 aqueous solution (20 μL)

was added to each well and incubated for 1-4 h. The absorbance was measured at 490 nm using microplate reader. The cells without any peptide were used as the control.

Flow Cytometry

Cellular Uptake of Fluorescein-Labeled Peptide. SK-OV-3 cells were grown in 6-well plates (2×10^5 cells/well) with complete EMEM media 24 h prior to the experiment. The fluorescein-labeled peptide stock solution (1 mM) was prepared in water and diluted in Gibco® Opti-MEM® I reduced serum medium to obtain the final concentration of 5 μ M. The media were removed and the mixture containing fluorescein-labeled peptide solution (5 μ M) was added. After 1 h incubation, trypsin-EDTA solution was added to detach cells from plate's surface and remove cell surface binding peptides. After 5 min, the complete media (2 mL) was added to neutralize the trypsin. The cells were collected and centrifuged at 2500 rpm for 5 min. Then they were washed with PBS (without calcium and magnesium) twice. Samples were prepared in FACS buffer for analysis. Finally, the cells were analyzed by BD FACSCalibur™ or FACSVerse™ flow cytometer using FITC channel. The data collection was based on the mean fluorescence signal for 10,000 cells. All assays were carried out in triplicate. 5(6)-Carboxyfluorescein (FAM) was used as a negative control.

Mechanism Study of Cellular Uptake by Removing Energy Sources. For examination of the cellular uptake mechanism of F'-dodecanoyl-[R₅] at low temperature, the assay was carried out at 4 °C to inhibit the energy-dependent cellular

uptake pathways. The SK-OV-3 cells were preincubated at 4 °C for 15 min and incubated with the fluorescein-labeled peptide for 1 h at 4 °C. Cells were collected and analyzed using flow cytometry with the previously described protocol above. The data collected at 37 °C were used as the control. To perform the ATP-depletion assay, cells were incubated with sodium azide (10 mM) and 2-deoxy-D-glucose (50 mM) for 1 h before adding the fluorescein-labeled peptide. During the incubation time (1 h), the fluorescein-labeled bicyclic peptide (5 μM) was prepared in the Opti-MEM® I reduced serum medium in the presence of sodium azide (10 mM) and 2-deoxy-D-glucose (50 mM). Then, the cells were incubated with this solution for 1 h. The following sample preparation and flow cytometry analysis protocol was same as described above.

Confocal Laser Scanning Microscopy (CLSM). SK-OV-3 cells were seeded with complete EMEM on coverslips in 6-well plate (1×10^5 cells/well) and kept until 50% confluency. The media were removed, and cells were incubated with F'-dodecanoyl-[R₅] (10 μM) and F'-dodecanoyl-(R₅) (10 μM) in Gibco® Opti-MEM® I reduced serum medium (Life Technologies, Grand Island, NY) for 1 h at 37 °C. Then cells were washed with $1 \times$ phosphate buffered saline with calcium and magnesium (PBS⁺) for three times. The coverslips were mounted on microscope slides, and images were obtained using Carl Zeiss LSM 700 system with a 488 nm argon ion laser excitation and a BP 505-530 nm band pass filter.

Intracellular Uptake of a Phosphopeptide, F'-GpYEEI. SK-OV-3 and CCRF-CEM cells were seeded in 6-well plates (2×10^5 cells/well for SK-OV-3 and 1×10^6 cells/well for CCRF-CEM) and grown with complete EMEM media (RPMI-1640 for CCRF-CEM) for overnight. A mixture of fluorescein-labeled phosphopeptides F'-GpYEEI (5 μ M) and peptides (10 μ M) were prepared in OPTI-MEM I® reduced serum medium at room temperature and incubated for 15 min. Then the cells were incubated with the premixed solution at 37 °C with 5% CO₂ for 1 h. The sample preparation for FACS analysis was carried out by previously mentioned protocol described before. In this assay, DMSO and F'-GpYEEI were used as the negative controls.

RESULTS AND DISCUSSION

Chemistry

The acylated cyclic polyarginine peptides were synthesized by Fmoc/t-Bu solid-phase peptide synthesis method. Fmoc-L-Arg(Pbf)-OH was coupled on H-Arg(Pbf) loaded 2-chlorotrityl resin in the presence of HBTU, HOBT, and DIPEA in DMF. Then Dde-Lys(Fmoc)-OH was attached, and a fatty acid was coupled to the side chain of lysine. Dde protecting group was removed by 2% hydrazine in DMF, and a cleavage cocktail containing TFE/acetic acid/DCM (2:1:7 v/v/v) was used for 1 h to cleave the side-chain protected linear peptides from the resin. Cyclization of linear peptides was carried out in the presence of a mixture of HOAT and DIC in anhydrous DMF/DCM for 6-24 h. The side-chain deprotection of cyclic peptide were carried out by a cleavage cocktail reagent "R" for 2 h. The crude peptides were precipitate and

purified with RP-HPLC as described above. As a representative example, the synthesis of dodecanoyl-[R₅] is shown in Scheme 1.

A corresponding acylated linear polyarginine peptide (ALPP) was synthesized for comparative studies with the cyclic peptide (ACPP). Moreover, a cyclic polyarginine without fatty acid [R₅] was also synthesized to investigate the effect of the fatty acid on cyclic peptide and its effect on molecular transporting efficiency. To investigate whether the peptide alone can enter into cells, fluorescein-labeled F'-dodecanoyl-[R₅], and F'-dodecanoyl-(R₅), where F' = fluorescein, were synthesized for FACS and microscopy investigations. All synthesized peptides are shown in Figure 1.

Cytotoxicity Assay of Synthetic Peptides

The cytotoxicity of all peptides were tested in two different cancer cell lines, adherent (SK-OV-3) and non-adherent (CCRF-CEM) cells and a normal cell line (HEK 293T) using MTS assay (Figure 2). Cyclic polyarginine [R₅] without fatty acid was used to explore the effect of *N*-terminal acylation on cytotoxicity and cellular uptake. ALPP (dodecanoyl-(R₅)) and [R₅] peptides showed consistently less cytotoxicity in all three cells compared to ACPPs (dodecanoyl-[R₅] and dodecanoyl-[R₆]). After 24 h incubation, ACPPs showed approximately 20% toxicity in cells at a concentration of 25 μM in CCRF-CEM cells. However, linear dodecanoyl-(R₅) and cyclic [R₅] did not exhibit significant cytotoxicity at 25 μM and showed less than 20% toxicity at the concentration of 100 μM. In SK-OV-3 cells, dodecanoyl-(R₅) and [R₅] showed more than 80% cell viability at the concentration of 25 μM. In normal cells (HEK 293T), all peptides exhibited less than 5% toxicity at 25 μM. This differential

behavior of the peptides in normal and cancer cells can be possibly rationalized through the interaction between polyarginine peptides and cell membranes. The membrane of cancer cells holds more negative charges compared to that in normal cells because of the presence of anionic lipids such as phosphatidylserine.¹⁰ Therefore, polyarginine peptides can be interacted with cancer cells more effectively compared to normal cells. Consequently, higher cell viability was observed in normal cells. These data indicated that ACPPs are more toxic than ALPP and a non-acylated cyclic peptide [R₅], especially at concentration of $\geq 25 \mu\text{M}$. Thus, a non-cytotoxic concentration of 5-10 μM was used in cell-based assays.

Cellular Uptake of Fluorescein-labeled Acylated Cyclic and Linear Polyarginine Peptides

The intracellular uptake studies of fluorescein-labeled acylated cyclic and linear PP, F'-dodecanoyl-[R₅] and F'-dodecanoyl-(R₅), was carried out in SK-OV-3 cells by using flow cytometry and confocal laser scanning microscopy (CLSM) methods. Fluorescein (FAM, F') alone was selected as a negative control. As it is shown in Figure 3, The F'-dodecanoyl-[R₅] and F'-dodecanoyl-(R₅) showed approximately 13.7- and 10.3-fold higher cellular uptake than that of control 5,6-carboxyfluorescein (FAM), respectively, in SK-OV-3 cells. F'-dodecanoyl-[R₅] showed 1.3-fold higher cellular uptake compared to that of F'-dodecanoyl-(R₅). The cellular uptake of F'-dodecanoyl-[R₅] was confirmed by CLSM images (Figure 4). F'-Dodecanoyl-[R₅] showed higher fluorescence intensity compared to that of F'-dodecanoyl-(R₅) in SK-OV-3 cells. Therefore, ACPP F'-dodecanoyl-[R₅] was found to be more efficient cell-

penetrating peptide compared to the linear counterpart. As shown in Figure 4, the fluorescence signal is extended through the whole cells, suggesting that F'-dodecanoyl-[R₅] can get localized in the nucleus as well as cytoplasm.

Cellular Uptake Mechanistic Study of F'-Dodecanoyl-[R₅]

The mechanism of the cellular internalization of F'-dodecanoyl-[R₅] was investigated by a temperature control assay at 4 °C along with ATP depletion assay. These two assays have been widely used to examine the energy-dependent endocytosis.¹¹ FACS results showed that the intracellular uptake of F'-dodecanoyl-[R₅] was significantly reduced at 4 °C, indicating that the mechanism of internalization was mainly dependent on the endocytosis pathways (Figure 5).¹² Furthermore, ATP depletion assay was performed to investigate receptor-mediated endocytosis.¹³ To induce ATP depletion, SK-OV-3 cells were pre-incubated with sodium azide (10 mM) and 2-deoxy-D-glucose (50 mM) for 1 h prior to the experiment, and a similar concentration was maintained during the incubation (1 h) with F'-dodecanoyl-[R₅]. The results showed that the cellular uptake of F'-ACPP was inhibited in the presence of sodium azide and 2-deoxy-D-glucose, suggesting that receptor-mediated endocytosis is involved for the cellular uptake of F'-ACPP. In ATP depletion assay, the basic cellular uptake of FAM was higher compared to that in temperature control assay. However, this is evident that the intracellular uptake of F'-dodecanoyl-[R₅] was inhibited, and there was no significant difference between the cells treated with FAM compared to those treated with F'-dodecanoyl-[R₅] in

temperature control and ATP depletion assays, suggesting that endocytosis is the major pathway for the cellular uptake of F'-dodecanoyl-[R₅].¹⁴

Molecular Transporter Property of Peptides

The ability of ACPPs as a molecular transporter was evaluated and compared by selecting a fluorescein-labeled phosphopeptide, F'-GpYEEI, as a molecular cargo. The phosphopeptide, pYEEI (pTyr-Glu-Glu-Ile) is an optimal peptide template for the SH2 domain of Src tyrosine kinase. Several analogues of this peptide have been synthesized as potent ligands for this target.¹⁵⁻¹⁷ Due to the presence of the negatively charged amino acid residues in the structure of the phosphopeptide including phosphorylated tyrosine, it does not cross the cell membrane easily. Moreover, the internalization of the negatively charged phosphopeptide in cancer cells by diffusion is more difficult because cancer cell membranes are composed of more negatively charged lipids. Thus, cellular delivery of cell-impermeable negatively charged phosphopeptides is significantly challenging. We have previously reported different peptide-based carriers for the intracellular delivery of negatively charged phosphopeptides as model cell-impermeable drugs in several cell lines.¹⁸

In this study, the intracellular uptake of F'-GpYEEI was monitored in the presence and absence of synthetic peptides after 1 h incubation by flow cytometry. As it is exhibited in Figure 6, the ACPPs (dodecanoyl-[R₅] and dodecanoyl-[R₆]) delivered the phosphopeptide more efficiently compared to ALPPs, dodecanoyl-(R₅) and [R₅]. The intracellular uptake of F'-GpYEEI in the presence of dodecanoyl-[R₅] and dodecanoyl-[R₆] was enhanced by 3.4- and 5.5-fold higher than the uptake in the

absence of ACPPs. However, dodecanoyl-(R₅) and [R₅] only improved 1.3- and 1.4-fold intracellular uptake, respectively. The results showed that acylated and cyclized polyarginine peptides can deliver the phosphopeptide effectively. However, the intracellular uptake of the phosphopeptide did not improve significantly in the presence of either acylated linear polyarginine peptide or cyclic [R₅]. These data suggest that a combination of acylation and cyclization would improve the molecular transporting efficiency of the polyarginine-based peptide (containing less than six arginines) for the intracellular delivery of a cell-impermeable phosphopeptide. It has been previously reported that the acylated linear octa-arginine increased the cellular uptake of molecular cargoes by just adding fatty acid to the *N*-terminal of octa-arginine.⁸ However, we discovered that both cyclization and acylation in a short penta-arginine can significantly improve the delivery of a cell-impermeable phosphopeptide in SK-OV-3 cells.

The major driving forces for the intracellular delivery are presumed to be structural rigidity through cyclization of the peptide and the interaction of the fatty acid with the cell membrane. It has been previously reported that the cellular uptake of the peptide can be increased due to the structural rigidity by cyclization of arginine-rich peptides.³ They proposed that the maximal distance between guanidine groups of arginine residue can lead to an efficient transduction of arginine-rich peptides. Our investigations showed that dodecanoyl-[R₆] is able to deliver more efficiently by 1.6-fold higher F'-GpYEEI uptake compared to that of dodecanoyl-[R₅]. Increasing the number of positively charged arginine residues can enhance the cellular uptake through ionic interactions with the negatively charged phosphopeptide and/or

phospholipid in the cell membrane through ionic interactions. However, the higher number of arginine residue is not the only responsible element for the efficient cellular internalization. For example, it has been reported that polyarginine containing eleven amino acids (R_{11}) showed higher cellular uptake compared to the polyarginine containing thirteen amino acids (R_{13}). At the same time, R_{11} was found to be more potent transporter compared to R_9 in prostate cancer cells.¹⁹ These investigations showed that an optimal number of arginine residues are required for the highest degree of functionality. However, the more number of amino acid residues in cyclic peptides can decrease the structural rigidity, which lower the ability of the peptide to get into cells.

Dodecanoyl- $[R_5]$ was also compared with several commonly CPPs, such as CR_7 and TAT (YGRKKRRQRRR) peptides. The ACP improved the cellular uptake of the phosphopeptide by 1.4- and 1.8-fold higher than those of CR_7 and TAT, respectively (Figure 6B). Thus, these results revealed that ACP dodecanoyl- $[R_5]$ can be used as an efficient molecular transporter even it has shorter peptide sequence than CR_7 and TAT.

The Effect of Fatty Acid Chain Length on the Cellular Uptake of ACPs

To investigate the effect of the chain length on the cell penetration potency, we synthesized octanoyl- $[R_5]$, dodecanoyl- $[R_5]$, and hexadecanoyl- $[R_5]$ (Figure 8). The cytotoxicity of the peptides was examined in SK-OV-3 cells. ACPs showed less than 20% toxicity in cells at the concentration of 25 μ M. The *in vitro* toxicity results showed that increasing the fatty acid chain length caused enhanced toxicity in cells as

hexadecanoyl-[R₅] was more cytotoxic than dodecanoyl-[R₅] and octanoyl-[R₅]. These data indicate that the fatty acid chain length could alter the interaction with the cell membrane and disturb the membrane integrity. Based on the cytotoxicity data, a concentration of 10 μM was selected for further cell-based assays.

It has been previously reported that there was a relationship between the length of fatty acid in polyarginines and their cellular uptake,⁷ meaning that the optimal length of fatty acid is required for optimal functionality based on the peptide sequence and cell type. The results exhibited that the cellular uptake of F'-GpYEEI was improved in the order of octanoyl-[R₅] < dodecanoyl-[R₅] < hexadecanoyl-[R₅]. The cellular uptake of F'-GpYEEI in the presence of hexadecanoyl-[R₅] was 9.3- and 6.0-fold higher than that of in the presence of octanoyl-[R₅] and dodecanoyl-[R₅], respectively. These data suggest that among the synthesized peptides, hexadecanoyl-[R₅] containing a fatty acid with sixteen-carbon chain length (C₁₆) is an optimized length for the intracellular delivery of F'-GpYEEI in SK-OV-3 cells.

Effect of Addition of Tryptophan Residues in Molecular Transporter Property

After ACPPs were found to act as CPP and molecular transporter, a systematic investigation was performed to modify the fatty acid to another hydrophobic moiety. Two other conjugates were synthesized. In the first conjugate, W₄-[R₅], the whole fatty acid chain was replaced with four tryptophan residues. The second conjugate W-dodecanoyl-[R₅] had one more tryptophan at the end of the dodecanoyl fatty acid chain. W₄-[R₅] enhanced intracellular delivery of F'-GpYEEI by 4.1-fold higher compared to that of dodecanoyl-[R₅] in SK-OV-3. However, W-dodecanoyl-[R₅]

improved the uptake of F'-GpYEEI by 1.3-fold higher compared to that of W₄-[R₅] in CCRF-CEM cells (Figure 9). The cellular uptake is affected by the cell lines. Thus, it is not straightforward to compare the cellular uptakes in SK-OV-3 and CCRF-CEM. However, the results could be assessed indirectly by relative comparison with the cellular uptake by W₄-[R₅]. These data suggest that the presence of hydrophobic tryptophan moieties could enhance the molecular transporting efficiency. In other words, appropriate modification of hydrophobic moiety in CPPs can increase the drug delivery ability of ACPP. Existing a balance between the cyclization of short polyarginine and the presence of hydrophobic moiety is critical to obtain the optimal intracellular transportation ability.

CONCLUSION

In conclusion, acylated cyclic polyarginine peptides were synthesized and examined as CPPs and potential molecular transporters. ACPPs showed higher potency as molecular transporter compared to the corresponding linear counterpart and cyclic polyarginine without fatty acid. The mechanism of the peptide internalization was found to be energy-dependent endocytosis. Cyclization and acylation reactions on the structure of the peptide enhanced the intracellular uptake of polyarginine peptides although they carry a short length of sequence. This intracellular delivery property of ACPPs can be optimized by modifying the length of fatty acid chain. To the best of our knowledge, this is the first report of fatty acylated cyclic polyarginine peptide as molecular transporter of a cell-impermeable phosphopeptide. This study provided insights about how a combination of the cyclic nature and acylation can improve the

cell internalization of polyarginines. Further investigations are undergoing to determine whether conjugation of cell-impermeable hydrophobic drugs to acylated cyclic polyarginines can be an efficient method for designing novel drug delivery systems.

ACKNOWLEDGMENTS

We acknowledge the American Cancer Society, Grant No. RSG-07-290-01-CDD for the financial support. We thank National Center for Research Resources, NIH, and Grant Number 8 P20 GM103430-12 for sponsoring the core facility. This material is based upon work conducted at a research facility at the University of Rhode Island supported in part by the National Science Foundation EPSCoR Cooperative Agreement #EPS-1004057.

ABBREVIATIONS

ACPP, acylated cyclic polyarginine peptides; ALPP, acylated linear polyarginine peptide; ATP, adenosine triphosphate; CCRF-CEM, human leukemia carcinoma cell line; CFDI, 5(6)-carboxyfluorescein diisobutyrate; CLSM, confocal laser scanning microscopy; CPPs, cell-penetrating peptides; DCM, dichloromethane; Dde, 1-(4,4-dimethyl-2,6-dioxocyclohex-1-ylidene)ethyl; DIC, *N,N'*-diisopropylcarbodiimide; DIPEA, *N,N*-diisopropylethylamine; DMF, *N,N*-dimethylformamide; EDT, 1,2-ethanedithiol; EMEM, eagle's minimum essential medium; FAM, 5(6)-carboxyfluorescein; FBS, fetal bovine serum; Fmoc, 9-fluorenylmethoxycarbonyl; FACS, fluorescence activated cell sorter; HBTU, 2-(1*H*-Benzotriazole-1-yl)-1,1,3,3-tetramethyluronium hexafluorophosphate; HEK 293T, human embryonic kidney cell line; HOAT, 1-hydroxy-7-azabenzotriazole; HOBT, hydroxybenzotriazole; MALDI-TOF, matrix-assisted laser desorption/ionization-time of flight; MTS, (3-(4,5-dimethylthiazol-2-yl)-5-(3-carboxymethoxyphenyl)-2-(4-sulfophenyl)-2*H*-tetrazolium); NMP, *N*-methylmorpholine); PBS, phosphate buffered saline; PyAOP, 7-azabenzotriazol-1-yl-oxytris(pyrrolidino)phosphonium hexafluorophosphate; RP-HPLC, reversed-phase high pressure liquid chromatography; SK-OV-3, human ovarian adenocarcinoma cell line; TFA, trifluoroacetic acid; TFE, 2,2,2-trifluoroethanol ; TIS, triisopropylsilane.

REFERENCES

- (1) Deshayes, S.; Morris, M. C.; Divita, G.; Heitz, F. Cell-penetrating peptides: tools for intracellular delivery of therapeutics. *Cell. Mol. Life Sci. CMLS* **2005**, *62*, 1839–1849.
- (2) Mitchell, D. J.; Kim, D. T.; Steinman, L.; Fathman, C. G.; Rothbard, J. B. Polyarginine enters cells more efficiently than other polycationic homopolymers. *J. Pept. Res. Off. J. Am. Pept. Soc.* **2000**, *56*, 318–325.
- (3) Lättig-Tünnemann, G.; Prinz, M.; Hoffmann, D.; Behlke, J.; Palm-Apergi, C.; Morano, I.; Herce, H. D.; Cardoso, M. C. Backbone rigidity and static presentation of guanidinium groups increases cellular uptake of arginine-rich cell-penetrating peptides. *Nat. Commun.* **2011**, *2*, 453.
- (4) Futaki, S.; Suzuki, T.; Ohashi, W.; Yagami, T.; Tanaka, S.; Ueda, K.; Sugiura, Y. Arginine-rich peptides: an abundant source of membrane-permeable peptides having potential as carriers for intracellular protein delivery. *J. Biol. Chem.* **2001**, *276*, 5836–5840.
- (5) Wender, P. A.; Mitchell, D. J.; Pattabiraman, K.; Pelkey, E. T.; Steinman, L.; Rothbard, J. B. The design, synthesis, and evaluation of molecules that enable or enhance cellular uptake: peptoid molecular transporters. *Proc. Natl. Acad. Sci.* **2000**, *97*, 13003–13008.
- (6) Futaki, S.; Ohashi, W.; Suzuki, T.; Niwa, M.; Tanaka, S.; Ueda, K.; Harashima, H.; Sugiura, Y. Stearylated arginine-rich peptides: a new class of transfection systems. *Bioconjug. Chem.* **2001**, *12*, 1005–1011.

- (7) Lee, J. S.; Tung, C.-H. Lipo-oligoarginines as effective delivery vectors to promote cellular uptake. *Mol. Biosyst.* **2010**, *6*, 2049.
- (8) Katayama, S.; Hirose, H.; Takayama, K.; Nakase, I.; Futaki, S. Acylation of octaarginine: implication to the use of intracellular delivery vectors. *J. Controlled Release* **2011**, *149*, 29–35.
- (9) Youngblood, D. S.; Hatlevig, S. A.; Hassinger, J. N.; Iversen, P. L.; Moulton, H. M. Stability of cell-penetrating peptide–morpholino oligomer conjugates in human serum and in cells. *Bioconjug. Chem.* **2007**, *18*, 50–60.
- (10) Riedl, S.; Rinner, B.; Asslaber, M.; Schaidler, H.; Walzer, S.; Novak, A.; Lohner, K.; Zweghtick, D. In search of a novel target – phosphatidylserine exposed by non-apoptotic tumor cells and metastases of malignancies with poor treatment efficacy. *Biochim. Biophys. Acta* **2011**, *1808*, 2638–2645.
- (11) Richard, J. P.; Melikov, K.; Vives, E.; Ramos, C.; Verbeure, B.; Gait, M. J.; Chernomordik, L. V.; Lebleu, B. Cell-penetrating peptides: a reevaluation of the mechanism of cellular uptake. *J. Biol. Chem.* **2003**, *278*, 585–590.
- (12) Saraste, J.; Palade, G. E.; Farquhar, M. G. Temperature-sensitive steps in the transport of secretory proteins through the golgi complex in exocrine pancreatic cells. *Proc. Natl. Acad. Sci.* **1986**, *83*, 6425–6429.
- (13) ATP is required for receptor-mediated endocytosis in intact cells. *J. Cell Biol.* **1990**, *111*, 2307–2318.
- (14) Richard, J. P.; Melikov, K.; Vivès, E.; Ramos, C.; Verbeure, B.; Gait, M. J.; Chernomordik, L. V.; Lebleu, B. Cell-penetrating peptides. *J. Biol. Chem.* **2003**, *278*, 585–590.

- (15) Bibbins, K. B.; Boeuf, H.; Varmus, H. E. Binding of the Src SH2 domain to phosphopeptides is determined by residues in both the SH2 domain and the phosphopeptides. *Mol. Cell. Biol.* **1993**, *13*, 7278–7287.
- (16) Ye, G.; Nam, N.-H.; Kumar, A.; Saleh, A.; Shenoy, D. B.; Amiji, M. M.; Lin, X.; Sun, G.; Parang, K. Synthesis and evaluation of tripodal peptide analogues for cellular delivery of phosphopeptides. *J. Med. Chem.* **2007**, *50*, 3604–3617.
- (17) Ye, G.; Schuler, A. D.; Ahmadibeni, Y.; Morgan, J. R.; Faruqui, A.; Huang, K.; Sun, G.; Zebala, J. A.; Parang, K. Synthesis and evaluation of phosphopeptides containing iminodiacetate groups as binding ligands of the Src SH2 domain. *Bioorganic Chem.* **2009**, *37*, 133–142.
- (18) Nasrolahi Shirazi, A.; Tiwari, R. K.; Oh, D.; Banerjee, A.; Yadav, A.; Parang, K. Efficient delivery of cell impermeable phosphopeptides by a cyclic peptide amphiphile containing tryptophan and arginine. *Mol. Pharm.* **2013**, *10*, 2008–2020.
- (19) Zhou, J.; Liu, W.; Pong, R.-C.; Hao, G.; Sun, X.; Hsieh, J.-T. Analysis of oligo-arginine cell-permeable peptides uptake by prostate cells. *Amino Acids* **2012**, *42*, 1253–1260.

Figure legends

Figure 1: Chemical structures of synthetic peptides used in this study. (F': fluorescein-labeled; []: cyclic peptide; (): linear peptide)

Figure 2: Comparison of cytotoxicity between cyclic and linear acylated polyarginine peptides, and non-acylated cyclic peptide [R₅] at various concentrations against CCRF-CEM, SK-OV-3, and HEK 293T after 24 h.

Figure 3: Comparative cellular uptake of F'-dodecanoyl-[R₅] and F'-dodecanoyl-(R₅) (5 μM) in SK-OV-3 cells (1 h).

Figure 4: Confocal laser scanning microscope image of (A) F'-dodecanoyl-[R₅] and (B) F'-dodecanoyl-(R₅). The peptides were incubated for 1 h in SK-OV-3 cells at 10 μM concentration.

Figure 5: Cellular uptake of F'-dodecanoyl-[R₅] (5 μM) in SK-OV-3 cells in temperature control assay at 37 °C and 4 °C, and ATP depletion assay with NaN₃ (10 mM) and 2-deoxy-D-glucose (50 mM) analyzed by flow cytometry.

Figure 6: Cellular uptake of F'-GpYEEI (5 μM) in the presence of dodecanoyl-[R₅], [R₅], dodecanoyl-(R₅), and dodecanoyl-[R₆] (10 μM) in SK-OV-3 cell line. Phosphopeptide delivery efficiency of dodecanoyl-[R₅] were compared with known CPPs (R₇: CRRRRRRR; TAT: YGRKKRRQRRR). The mean fluorescence of F'-GpYEEI taken by dodecanoyl-[R₅] was set as 100%.

Figure 7: Chemical structures of ACPPs with different length of fatty acid chains (C₈, C₁₂, and C₁₆).

Figure 8: (A) Cytotoxicity assay of cyclic polyarginine peptide-fatty acid conjugates against SK-OV-3 cells (24 h incubation). (B) Cellular uptake of a phosphopeptide, F'-

GpYEEI (5 μM) in the presence of peptide-fatty acid conjugates (10 μM) in SK-OV-3 cells.

Figure 9: Cellular uptake assay of a phosphopeptides, F'-GpYEEI (5 μM) in the presence of W₄-[R₅] and W-dodecanoyl-[R₅] (10 μM) against SK-OV-3 and CCRF-CEM cell lines (1 h incubation). The mean fluorescence of F'-GpYEEI by W₄-[R₅] was set as 100%.

Scheme legends

Scheme 1. Synthesis of dodecanoyl-[R₅] as a representative example.

Figure 1

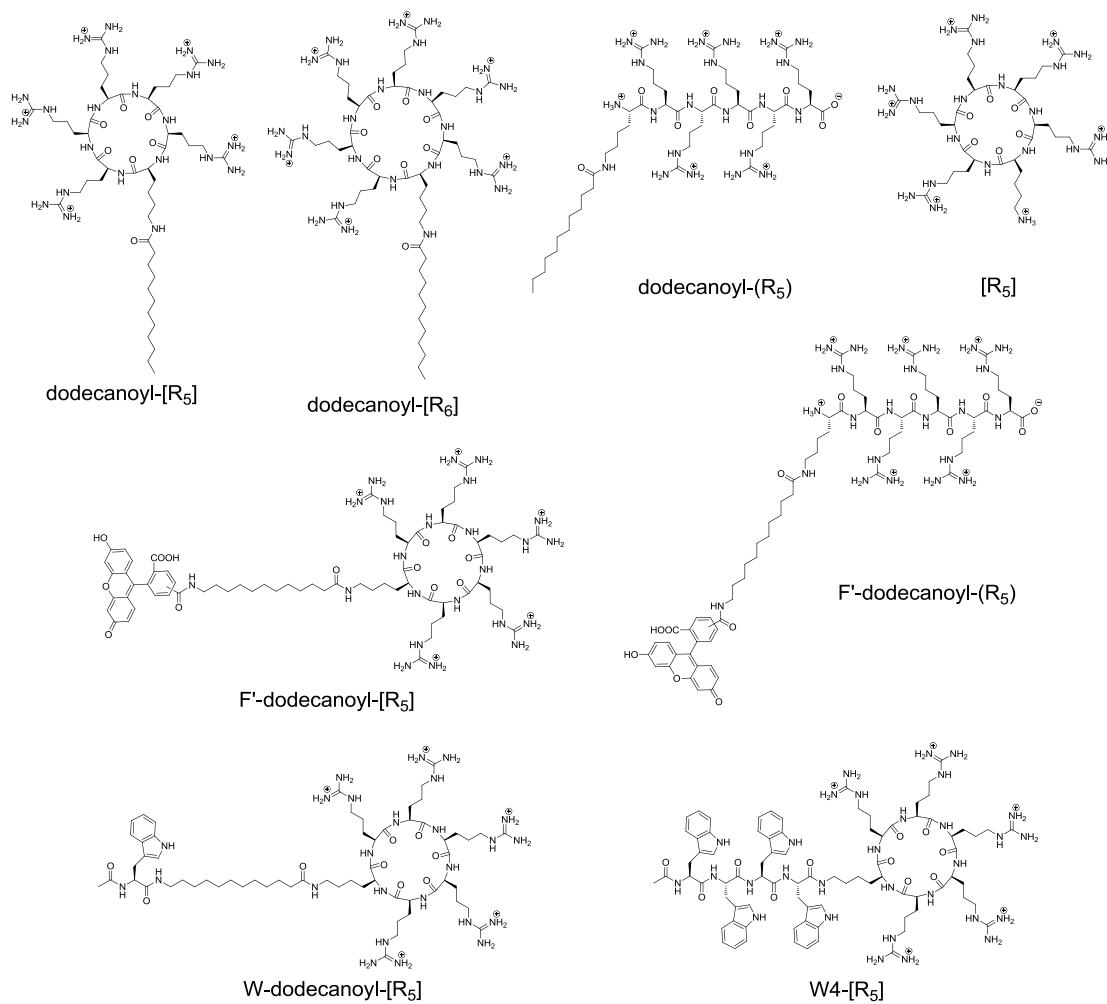


Figure 2

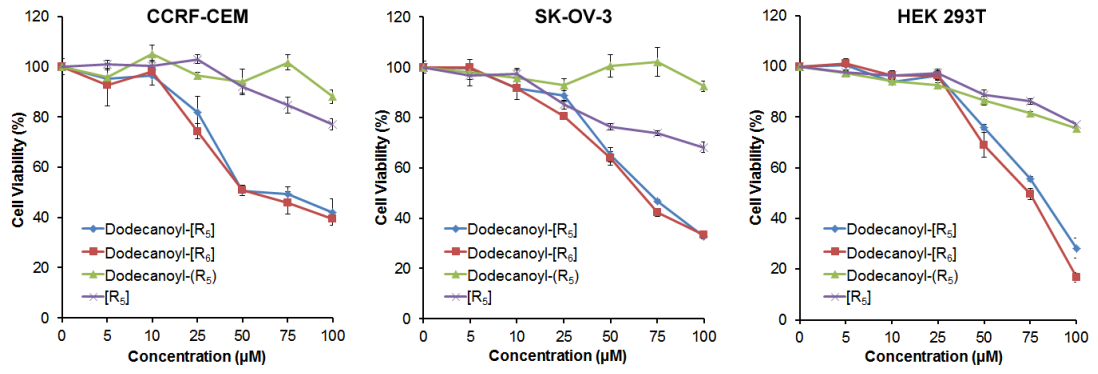


Figure 3

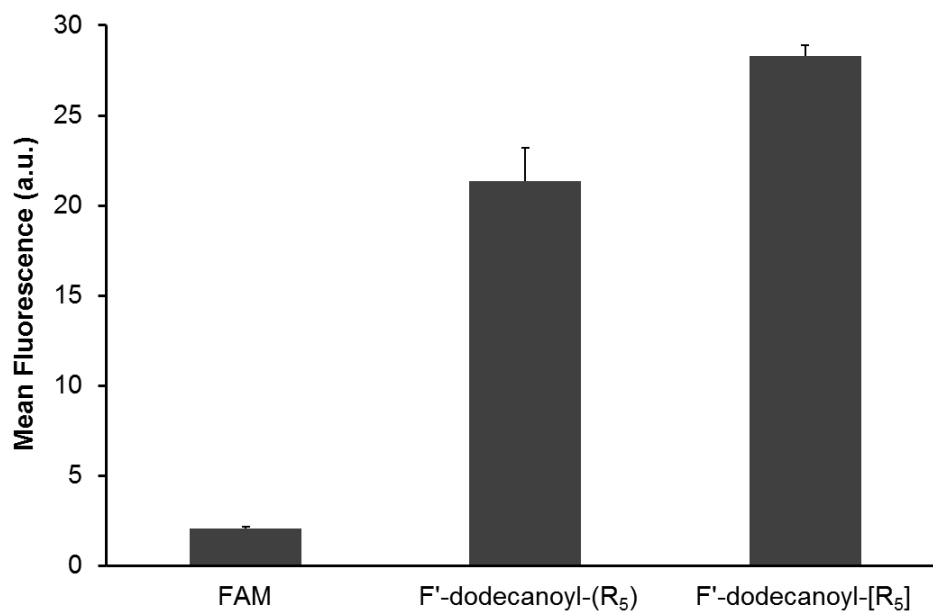


Figure 4

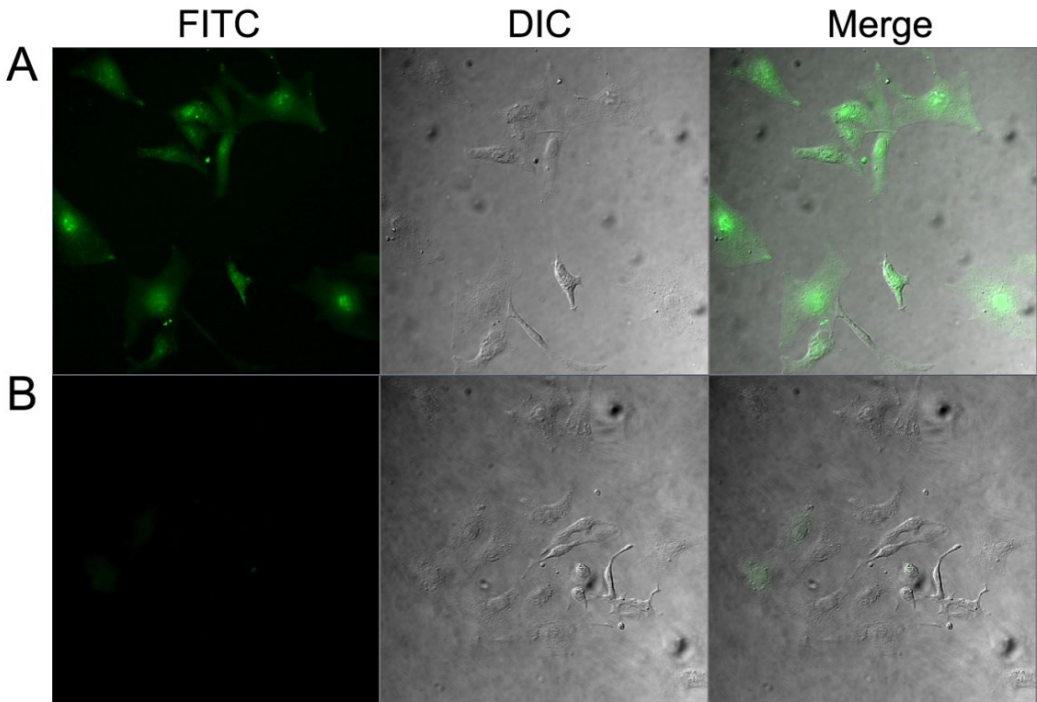


Figure 5

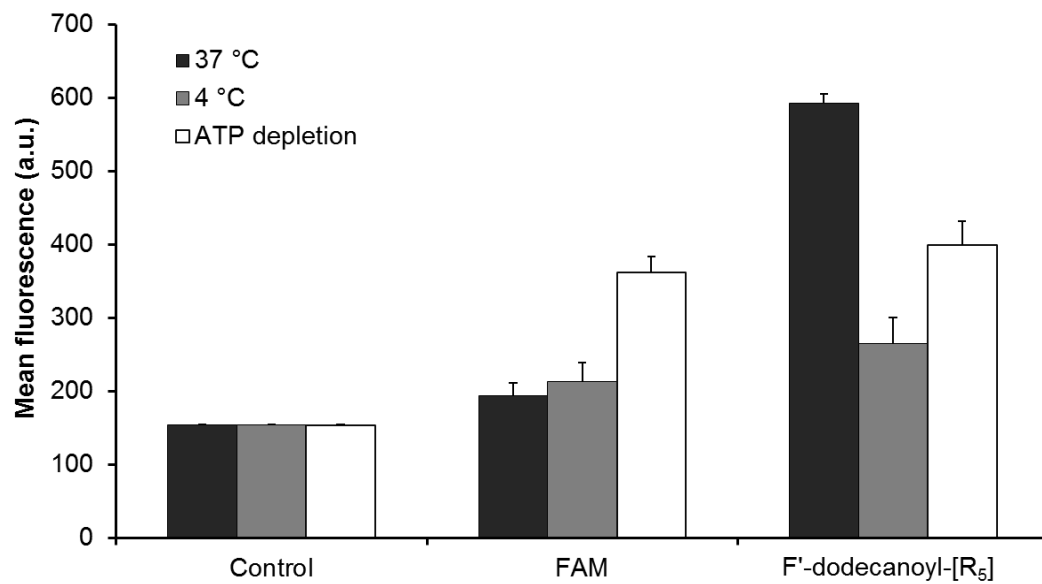


Figure 6

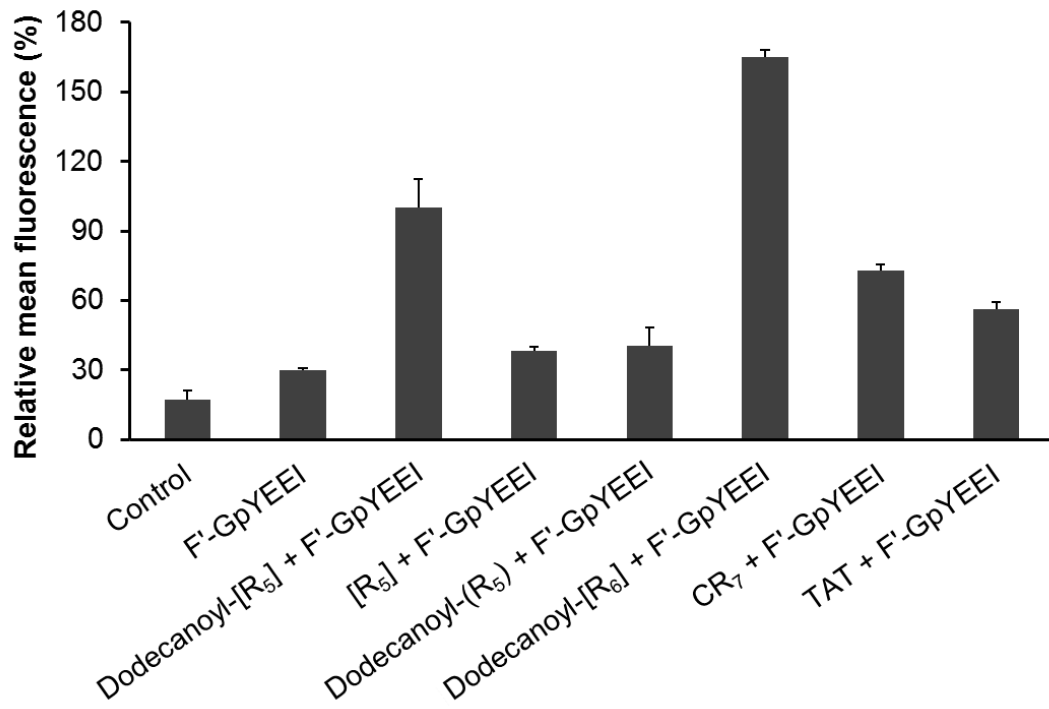


Figure 7

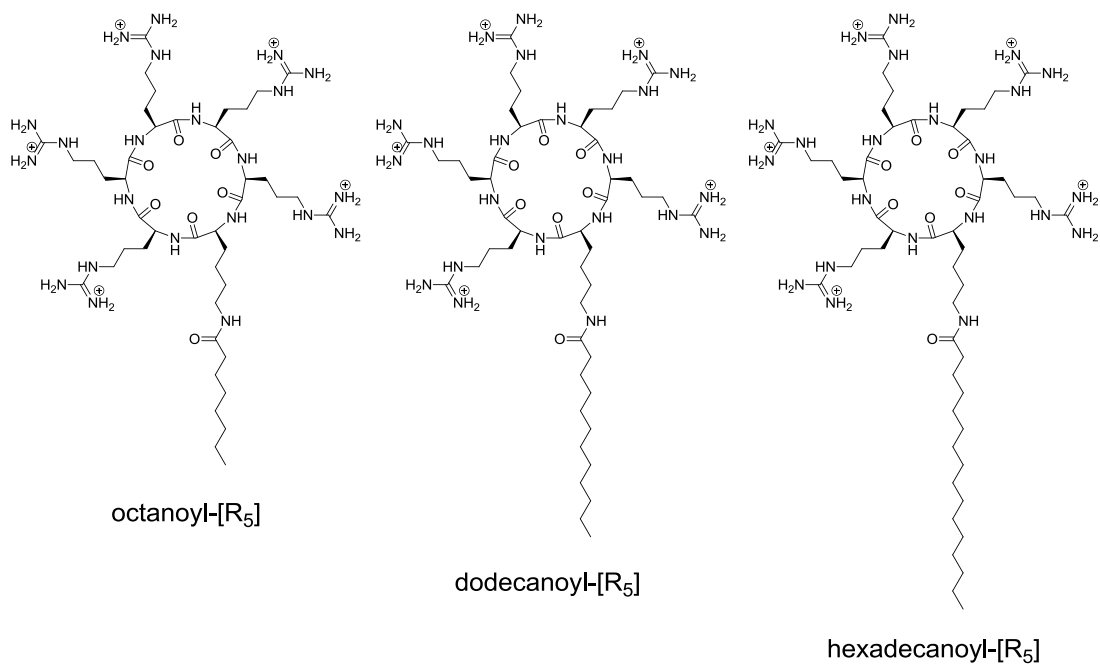


Figure 8

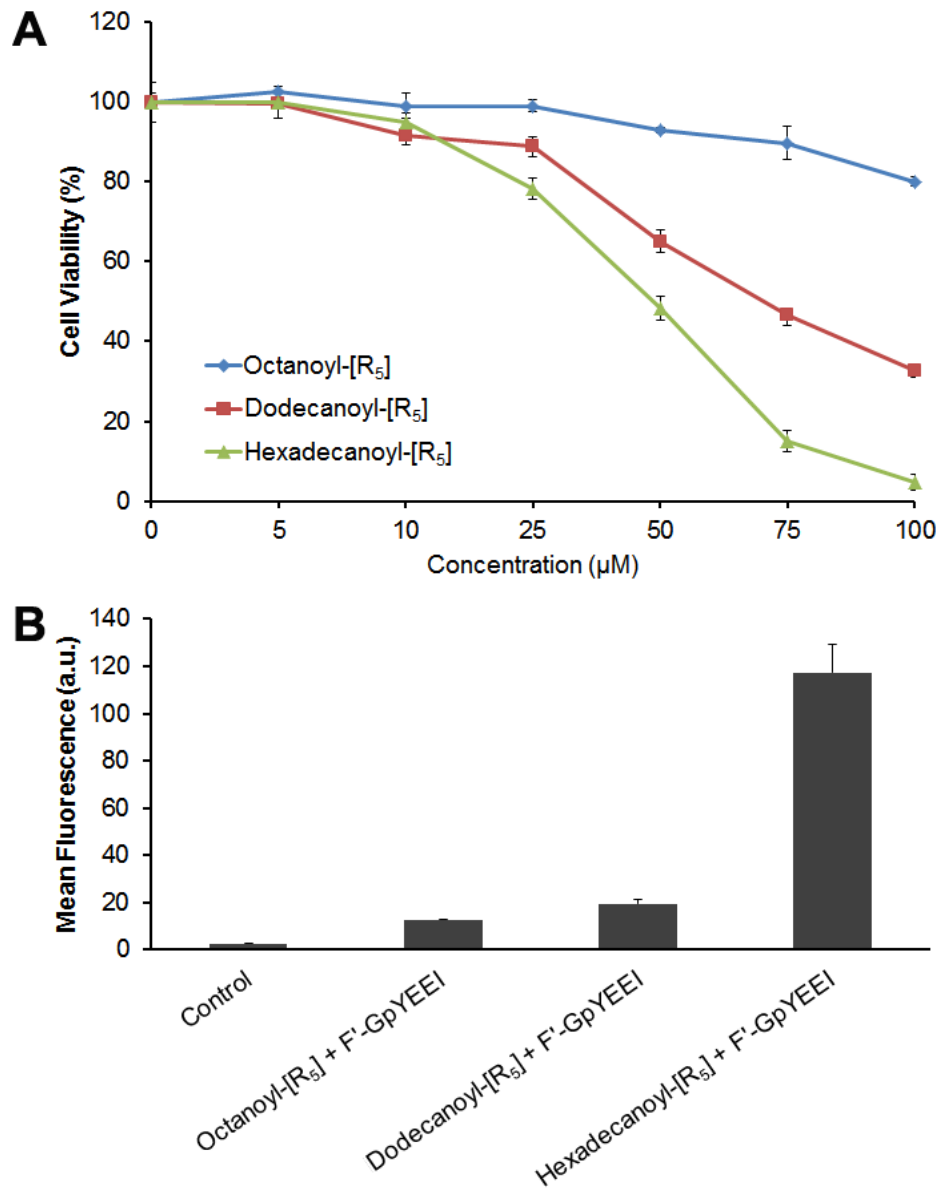
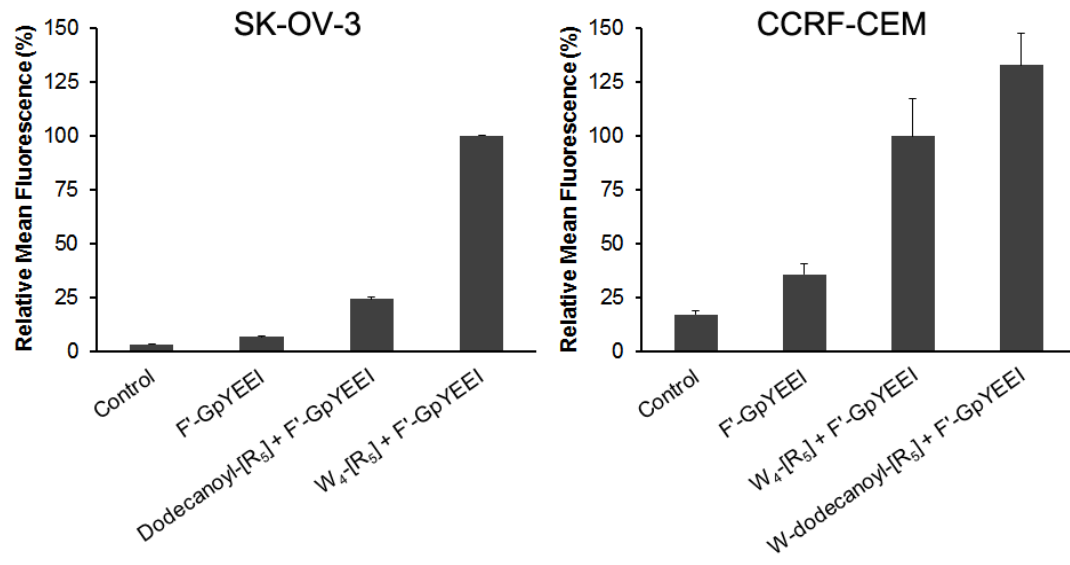
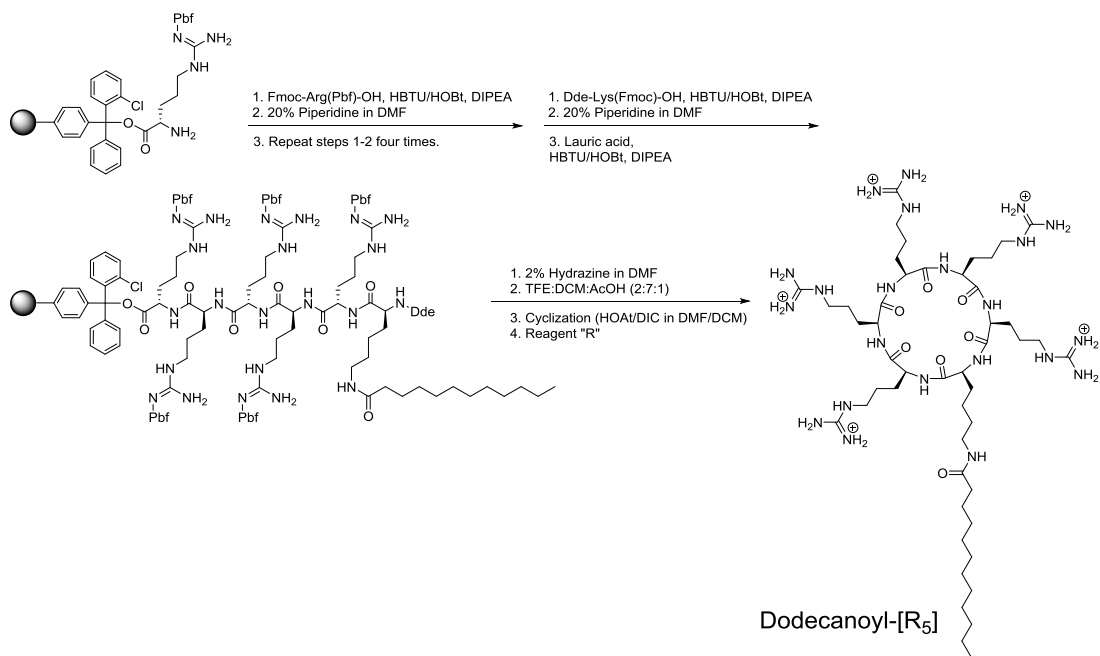


Figure 9



Scheme 1



MANUSCRIPT III

Prepared to be submitted in *Molecular Pharmaceutics*

Antibacterial Activities of Amphiphilic Cyclic Cell-Penetrating Peptides against Multidrug Resistant Pathogens

Donghoon Oh,^a Jiadong Sun,^a Amir Nasrolahi Shiraz,^{a,b} Kerry L. LaPlante,^{c,*} David C.
Rowley,^{a,*} Keykavous Parang^{a,b,*}

^aDepartment of Biomedical and Pharmaceutical Sciences, College of Pharmacy, University of Rhode Island, Kingston, RI 02881, United States; ^bSchool of Pharmacy, Chapman University, Irvine, CA, 92866, United States; ^cDepartment of Pharmacy Practice, College of Pharmacy, University of Rhode Island, Kingston, RI 02881, United States

kparang@uri.edu

TITLE RUNNING HEAD. Antibacterial Activities of Cyclic CPPs

*Corresponding authors:

K. Parang, D. Rowley, K. LaPlante: 7 Greenhouse Road, Department of Biomedical and Pharmaceutical Sciences, College of Pharmacy, University of Rhode Island,

Kingston, Rhode Island, 02881, United States; Tel.: +1-401-874-4471; Fax: +1-401-874-5787; E-mail address: kparang@uri.edu, drowley@mail.uri.edu, kerrylaplante@uri.edu

Harry and Diane Rinker Health Science Campus, 9401 Jeronimo Road, School of Pharmacy, Chapman University, Irvine, California 92618, United States; Tel.: +1-714-516-5489; Fax: +1-714-516-5481; Email: parang@chapman.edu

ABSTRACT

Multidrug resistant pathogens have become a major public health concern. There is a great need for the development of novel antibiotics with alternative mechanisms of action the treatment of life-threatening bacterial infections. Antimicrobial peptides (AMPs), a major class of antibacterial agents, share amphiphilicity and cationic structural properties with cell-penetrating peptides (CPPs). We have previously reported that a number of amphiphilic cyclic peptides have enhanced cellular uptake properties in eukaryotic cells versus their linear counterparts. Herein, several amphiphilic cyclic CPPs and their analogs were synthesized and exhibited potent antibacterial activities against multidrug resistant pathogens. Among them, cyclic peptide [R₄W₄] (peptide **1**) showed the most potent antibacterial activity against methicillin-resistant *Staphylococcus aureus* (MRSA, exhibiting a minimum inhibitory concentration (MIC) of 2.67 µg/mL). Cyclic [R₄W₄] and the linear counterpart R₄W₄ exhibited MIC values of 42.8 and 21.7 µg/mL, respectively, against *Pseudomonas aeruginosa*. [R₄W₄] in combination with tetracycline enhanced the potency, by decreasing the MIC 4 fold (0.12 µg/mL) presenting partial synergistic effect of the combination between peptide **1** and tetracycline against MRSA. Twenty-four hour time-kill studies evaluating [R₄W₄] with 2× the MIC in combination with tetracycline demonstrated bactericidal activity at 4 and 8× the MIC of tetracycline against MRSA and 2-8× the MIC against *E. coli*, respectively. Peptide **1** presented its cell-penetrating properties as expected, and showed more than 84% cell viability at 15 µM (20.5 µg/mL) concentration against in three different human cell lines. This study suggests

that amphiphilic cyclic CPPs, when used in combination with antimicrobials may provide additional benefit to defeat multi-drug resistant pathogens.

Keywords: Antimicrobial Peptide, Cell-Penetrating Peptide, Combination, Drug Delivery, MRSA.

INTRODUCTION

The emergence of Methicillin-resistant *Staphylococcus aureus* (MRSA) threatens public health worldwide. Despite a half century of efforts to find effective treatments, healthcare practitioners are still challenged to cure infections caused by MRSA.¹ MRSA is widespread in hospitals, and community-associated MRSA has continued to emerge since the mid-1990s.² In 2009, 463,017 infections were attributed to MRSA, which corresponds to 11.74 infections per 1,000 hospitalizations in the United States.³ Approximately 19,000 of human death were attributed to invasive MRSA in 2005.⁴ Moreover, MRSA rapidly evolves resistance against new commercial antibiotics.

Currently, vancomycin is employed commonly for the treatment of MRSA. However, vancomycin-resistant *Staphylococcus aureus* was reported in 1996.⁵ Daptomycin is a cyclic lipopeptide having a broad spectrum against Gram-positive bacteria, and it shows fast antibacterial responses. Its novel mechanism of action involves membrane depolarization resulting in efflux of potassium ions, followed by bacterial cell death.⁶ Despite its novelty of the mechanism, daptomycin-resistance by MRSA was reported in 2005, only two years after FDA approval. The resistance mechanism against daptomycin remains to be determined.⁷ Thus, new classes of antibiotics with different mechanisms of action are urgently needed.

Antimicrobial peptides (AMPs) have emerged as alternative therapeutics against antibiotic resistant pathogens because they can act as effectors and regulators of the immune system as well as inhibitors of bacterial cell growth.⁸ Cationic AMPs target negatively charged bacterial membrane lipids, which may reduce the occurrence of bacterial resistance.⁹ AMPs have been found as host defense peptides in various

organisms, such as insects, amphibians, and mammals.^{10,11} AMPs such as magainin and omiganan are in clinical trials or in development.¹²

Cell-penetrating peptides (CPPs) are short hydrophilic and/or amphiphilic peptides. Because of their ability to translocate across the eukaryotic cell membrane, they have been studied as molecular vehicles to deliver other drugs intracellularly.^{13,14} Some AMPs and CPPs share similar physical properties, such as amphiphilicity and cationic properties. Thus, CPPs have potential application as AMPs with dual actions as both antibiotics and possible molecular transporter properties.

We have synthesized and evaluated several cyclic CPPs as molecular transporters of other cargo drugs. For example, we recently reported that synthetic cyclic peptides [WR]₄ and [WR]₅ enhanced the cellular uptake of phosphopeptides, doxorubicin, and anti-HIV drugs.¹⁵ These peptides are expected to be more stable than linear peptides towards human serum because the cyclization decreases proteolytic degradation.¹⁶ It has been previously reported that the rigidity in the peptides can enhance the cell-penetrating property.¹⁷ According to our recent study, the acylation and cyclization of short polyarginine peptides enhance the intracellular delivery of cell-impermeable phosphopeptides.

In general, AMPs contain hydrophobic and hydrophilic portions that interact with the lipid part and hydrophilic negatively charged heads in bacteria membranes, respectively. Many linear AMPs adopt amphipathic α -helix conformations with the hydrophobic side chains arranged along one side of the helical structure and the hydrophilic side chains organized on the opposite side. This arrangement results in the ideal amphipathic helical structures.¹⁸ Some AMPs form amphipathic β -sheet

conformation to interact with cell membranes.¹⁸ We hypothesized that amphiphilic cyclic peptides with cell-penetrating property can have potential antibacterial and synergistic activity with other antibiotics. Herein, we report two classes of amphiphilic cyclic CPPs: (a) cyclic peptides containing tryptophan and arginine amino acids and (b) fatty acylated cyclic polyarginine peptides (ACPPs). The antimicrobial activities of synthesized peptides were evaluated against multidrug-resistant bacterial pathogens.

EXPERIMENTAL SECTION

Peptide Design and Synthesis. The peptides were synthesized by Fmoc/*t*Bu solid-phase peptide synthesis. Single amino acid (tryptophan or arginine) preloaded trityl resins were employed for the synthesis of cyclic peptides. Fmoc-L-amino acid building blocks were coupled to the resin using the 2-(1*H*-benzotriazole-1-yl)-1,1,3,3-tetramethyluronium hexafluorophosphate (HBTU), hydroxybenzotriazole (HOBT), and *N,N*-diisopropylethylamine (DIPEA) in *N,N*-dimethylformamide (DMF). Fmoc protecting groups were removed by treatment with 20% (v/v) piperidine in DMF after each coupling. The side chain protected peptides were detached from the resin by 2,2,2-trifluoroethanol (TFE)/acetic acid/dichloromethane (DCM) (2:1:7, v/v/v), and cyclized using 1-hydroxy-7-azabenzotriazole (HOAT), *N,N'*-diisopropylcarbodiimide (DIC) in anhydrous DMF/DCM. Then all protecting groups were removed with trifluoroacetic acid/thioanisole/1,2-ethanedithiol/anisole (90:5:3:2, v/v/v/v) mixture, and crude peptides were collected by precipitation with cold diethyl ether. The crude cyclic peptides were purified by a reversed-phase high pressure liquid chromatography (RP-HPLC) system using a preparative Phenomenex Gemini C18 column (10 μ m, 250

× 21.2 mm) with a gradient 0-100% of acetonitrile (CH₃CN) containing 0.1% TFA (v/v) and water containing 0.1% TFA (v/v) for 1 h with a flow rate of 15.0 mL/min at the wavelength of 214 nm.

As a representative example, the synthesis of peptide **1** ([R₄W₄]) is described here. After swelling of H-Trp(Boc)-2-chlorotrityl resin (449 mg, 0.35 mmol, 0.78 mmol/g) in DMF for 40 min by N₂, three consecutive coupling of Fmoc-Trp(Boc)-OH (553 mg, 1.05 mmol, 3 equiv) with the resin was carried out using HBTU (398 mg, 1.05 mmol, 3 equiv), HOBT (142 mg, 1.05 mmol, 3 equiv), and DIPEA (366 μL, 2.1 mmol, 6 equiv) in DMF (15 mL). In each coupling step, the mixture of resin and reaction solution was agitated using N₂ for 1 h. Piperidine in DMF (20% v/v) was used to remove Fmoc group after each coupling. The subsequent Fmoc-Arg(Pbf)-OH (681 mg, 1.05 mmol, 3 equiv) coupling was conducted four times in a similar manner. The linear peptide with protected side chain was cleaved from the resin in the presence of TFE/acetic acid/DCM (2:1:7, v/v/v) for 1 h. After evaporation and overnight drying of the filtrate in a vacuum, the cyclization was carried out under a dilute condition. The linear peptide was dissolved in anhydrous DMF/DCM (5:3, v/v, 250 mL). HOAT (190 mg, 1.4 mmol, 4 equiv), and DIC (240 μL, 1.54 mmol, 4.4 equiv) were added to the solution. The reaction mixture was stirred for 12 h under nitrogen atmosphere. Then, the solvent was evaporated. Reagent "R", trifluoroacetic acid/thioanisole/1,2-ethanedithiol/anisole (90:5:3:2, v/v/v/v), was added, and the solution was mixed for 2 h to remove side chain protecting groups. The crude peptide **1** was precipitated and washed with cold diethyl ether, and purified by a preparative RP-HPLC system as described above.

The peptide structures were confirmed by an AXIMA performance matrix-assisted laser desorption/ionization-time of flight (MALDI-TOF) spectrometer. The sequence of synthesized fourteen peptides is shown in Table 1. Fluorescein-labeled peptide **1** (F'-[KR₄W₄]) was synthesized by conjugation of a cyclic peptide (β -Ala)-[KR₄W₄] and 5(6)-carboxyfluorescein *N*-hydroxysuccinimide ester in solution phase. A cyclic peptide (β -Ala)-[KR₄W₄] was synthesized using the same protocol described above but Dde-Lys(Fmoc)-OH was added for attachment of Boc- β -Ala-OH on the side chain of lysine.

[RRRRWWWW] (1): MALDI-TOF (m/z): C₆₈H₈₈N₂₄O₈ calcd. 1368.7217; found 1369.6412 [M + H]⁺. **RRRRWWWW-COOH (2):** MALDI-TOF (m/z): C₆₈H₉₀N₂₄O₉ calcd. 1386.7323; found 1387.3780 [M + H]⁺. **[RRRRWWWW] (3):** MALDI-TOF (m/z): C₅₇H₇₈N₂₂O₇ calcd. 1182.6424; found 1183.5685 [M + H]⁺. **RRRRWWWW-COOH (4):** MALDI-TOF (m/z): C₅₇H₈₀N₂₂O₈ calcd. 1200.6529; found 1201.5652 [M + H]⁺. **[EEEEWWWW] (5):** MALDI-TOF (m/z): C₆₄H₆₈N₁₂O₁₆ calcd. 1260.4876; found 1261.3981 [M + H]⁺, 1283.4336 [M + Na]⁺, 1299.4365 [M + K]⁺. **[EEEEWWWW] (6):** MALDI-TOF (m/z): C₅₃H₅₈N₁₀O₁₅ calcd. 1074.4083; found 1075.4027 [M + H]⁺, 1113.4099 [M + K]⁺. **[KRRRRR] (7):** MALDI-TOF (m/z): C₃₆H₇₂N₂₂O₆ calcd. 908.6005; found 909.6772 [M + H]⁺. **Dodecanoyl-[KRRRRR] (8):** MALDI-TOF (m/z): C₄₄H₈₆N₂₂O₇ calcd. 1034.7050; found 1035.7084 [M + H]⁺. **Dodecanoyl-[KRRRRR] (9):** MALDI-TOF (m/z): C₄₈H₉₄N₂₂O₇ calcd. 1090.7676; found 1091.7576 [M + H]⁺. **Hexadecanoyl-[KRRRRR] (10):** MALDI-TOF (m/z): C₅₂H₁₀₂N₂₂O₇ calcd. 1146.8302; found 1147.8404 [M + H]⁺. ***N*-Acetyl-L-**

tryptophanyl-12-aminododecanoyl-[KRRRRR] (11): MALDI-TOF (m/z): $C_{61}H_{107}N_{25}O_9$ calcd. 1333.8684; found 1334.8713 $[M + H]^+$. ***N*-Acetyl-**WWWW-[KRRRRR]**** (12): MALDI-TOF (m/z): $C_{82}H_{114}N_{30}O_{11}$ calcd. 1694.9283; found 1696.3111 $[M + H]^+$. **Dodecanoyl-[KRRRRR]** (13): MALDI-TOF (m/z): $C_{54}H_{106}N_{26}O_8$ calcd. 1246.8687; found 1247.7397 $[M + H]^+$. **Dodecanoyl-KRRRRR-COOH** (14): MALDI-TOF (m/z): $C_{48}H_{96}N_{22}O_8$ calcd. 1108.7781; found 1109.7308 $[M + H]^+$.

F'-[KR₄W₄]. Fluorescein-labeled peptide F'-[KR₄W₄] was synthesized using the same protocol, but a lysine residue was added to attach a fluorescein. First, (β -Ala)-[KR₄W₄] was synthesized in 0.10 mmol scale. H-Trp(Boc)-2-chlorotrityl resin (128 mg, 0.10 mmol, 0.78 mmol/g), Fmoc-Trp(Boc)-OH (158 mg, 0.30 mmol, 3 equiv), Fmoc-Arg(Pbf)-OH (195 mg, 0.30 mmol, 3 equiv), Dde-Lys(Fmoc)-OH (160 mg, 0.30 mmol, 3 equiv), and Boc- β -Ala-OH (57 mg, 0.30 mmol, 3 equiv) were used to couple each building block to the resin using HBTU (114 mg, 0.30 mmol, 3 equiv), HOBT (41 mg, 0.30 mmol, 3 equiv), and DIPEA (105 μ L, 0.60 mmol, 6 equiv) in DMF. Dde protecting group was removed with 2% hydrazine in DMF, and side chain protected linear peptides were cleaved from the resin using TFE/acetic acid/DCM (2:1:7, v/v/v). The subsequent cyclization and purification steps were the same as described above.

The (β -Ala)-[KR₄W₄] peptide (8.00 mg, 5.10 μ mol) and 5(6)-carboxyfluorescein *N*-hydroxysuccinimide ester (FAM-NHS, 3.14 mg, 6.63 μ mol, 1.3 equiv) was coupled using PyAOP (3.46 mg, 6.63 μ mol, 1.3 equiv), and DIPEA (8.9 μ L, 51.0 μ mol, 10

equiv) in anhydrous DMF (200 μ L) and a few drops of anhydrous DCM. The reaction mixture was stirred for 3.5 h under N₂. After evaporation of the solvent, the residue was purified using a preparative RP-HPLC system using the same condition described above. After removal of Dde protecting group with 2% hydrazine in DMF and washing with DMF and DCM, side chain protected fluorescein linear peptides were cleaved from the resin using TFE/acetic acid/DCM (2:1:7, v/v/v). The subsequent cyclization and purification steps were described above. **F'-[KW₄R₄]**: MALDI-TOF (m/z): C₉₈H₁₁₅N₂₇O₁₆ calcd. 1925.9015; found 1926.8654 [M + H]⁺.

Bacterial Strains. Methicillin-resistant *Staphylococcus aureus* (MRSA; ATCC 43300), *Pseudomonas aeruginosa* (PAO1), and *Escherichia coli* (ATCC 35218) were employed for antimicrobial activities of peptides alone and in the combination with tetracycline.

Antibacterial Activities against MRSA and *P. aeruginosa*. MRSA and *P. aeruginosa* were inoculated into tryptic soy broth (TSB, BD™) at 37 °C and shaken at 175 rpm overnight. The cultured suspension (1×10^8 CFU/mL) was immediately diluted into 1×10^5 CFU/mL. All fourteen peptides were dissolved in distilled water (except for peptides **5** and **6**, dissolved in 50 mM NH₄HCO₃ solution to increase solubility) to make 5 mM solutions, respectively. Tetracycline and tobramycin were used as positive control and prepared as 0.10 mg/mL solution and 0.094 mg/mL. Minimal inhibitory concentration (MIC) was determined by the two-fold broth microdilution method according to National Committee for Clinical Laboratory

Standards (NCCLS) guidelines.¹⁹ Briefly, in a 96-well microtiter plate, all tested peptides and control were mixed well with bacteria suspension (1:39, v/v). After a series of two-fold dilution, the microtiter plates were then incubated statically at 37 °C overnight. Absorbance was read at 600 nm by plate reader (SpectraMax M2, Molecular Devices). MIC of each peptide was determined as the minimum concentration where no visible bacterial growth was present. Additionally, combination activity of peptide **1**, **7**, **9**, **10**, and **13** were assessed by mixing with tetracycline and bacteria suspension (1:1:38, v/v/v). MICs were determined as the same procedures described above. All experiments were triplicated.

Time-Kill Studies. Time-kill studies were performed using MRSA (ATCC 43300) and *E. coli* (ATCC 35218). Strains were incubated at 37 °C for 18-24 h on tryptic soy agar (TSA; Difco, Becton Dickinson Co., Sparks, MD) and a McFarland standard was diluted in Mueller Hinton Broth (MHB; Becton Dickinson Co., Sparks, MD) supplemented with 25 mg/L calcium and 12.5 mg/L magnesium, to a final concentration of $\sim 5.5 \log_{10}$ CFU/mL.²¹ Peptide **1** ([R₄W₄]) and tetracycline were evaluated at one, two, four, and eight times their respective MICs. Peptide **1** at two times the MIC was also combined with tetracycline at one, two, four and eight times the MIC to evaluate for synergy, defined as $>2 \log_{10}$ CFU/mL reduction over the most active agent alone. Each bacterial-antimicrobial combination was run in triplicate. Runs in the absence of antimicrobials ensured adequate growth of the organisms in the model. Each culture was incubated in a shaking incubator (Excella E24, New Brunswick Scientific, Enfield, CT) at 37°C for an additional 24 h. Samples were taken

at 0, 4, and 24 h, serially diluted, and plated on TSA for colony count enumeration, where the limit of detection was $2.0 \log_{10}$ CFU/mL.²¹ Bactericidal activity (99.9% kill) was defined as a $\geq 3 \log_{10}$ CFU/mL reduction at 24 h in colony count from the initial inoculum. Bacteriostatic activity was defined as a $< 3 \log_{10}$ CFU/mL reduction.

Cellular Cytotoxicity Assays. MTS proliferation assays were carried out against three cell lines (human ovarian adenocarcinoma SK-OV-3, human leukemia CCRF-CEM, and human embryonic kidney HEK 293T). Cells were seeded into 96-well plates (5×10^3 cells for SK-OV-3, 1×10^5 cells for CCRF-CEM, and 1×10^4 cells for HEK 293T) and incubated overnight with 100 μ L of complete media for overnight at 37 °C with 5% CO₂. Various concentrations (0 – 600 μ M) of the peptide solution (10 μ L) were added to cells. The cells were kept in an incubator (37 °C, 5% CO₂) for 24 h. Then CellTiter 96 aqueous solution (20 μ L) was added into each well and incubated for 1-4 h at the same condition. The absorbance was obtained at 490 nm using a microplate reader. Wells containing cells in the absence of any peptide were used as control.

Cellular Uptake of Fluorescein-labeled Peptide 1 (F'-[KW₄R₄]). SK-OV-3 cells were grown in 6-well plates (2×10^5 cells/well) with complete EMEM media prior 24 h to cellular uptake assay. A 1 mM of fluorescein-labeled peptide stock solution was prepared in water and diluted in Gibco® Opti-MEM® I reduced serum medium to prepare a 5 μ M final concentration. The culture media were removed from 6-well plates, and the 5 μ M fluorescein-labeled peptide solution was added. After 1 h incubation, trypsin-EDTA solution was added to detach cells from plate's surface and

remove cell surface binding peptides. After 5 min. treatment with trypsin-EDTA, a portion of complete media was added to stop the activity of trypsin. The cell lines were collected and centrifuged at 2500 rpm. Then cells were washed twice using PBS without calcium and magnesium, and prepared in FACS buffer for cell sorting. The cells were analyzed by BD FACSVerse™ flow cytometer using FITC channel. The data collection was based on the mean fluorescence signal for 10,000 cells. All assays were carried out in triplicate. 5(6)-Carboxyfluorescein (FAM) was used as a negative control.

Mechanism Study of Cellular Uptake by Removing Energy Sources. To examine the cellular uptake mechanism F'-[KR₄W₄] at low temperature, the uptake assay was carried out at 4 °C to inhibit the energy-dependent cellular uptake. SK-OV-3 cells were preincubated at 4 °C for 15 min and then incubated with the fluorescein-labeled peptide for 1 h at 4 °C. Cells were collected and assessed with the same protocol described in cellular uptake of the fluorescein-labeled peptide. The data collected at 37 °C were used for control. For the ATP-depletion assay, cells were incubated with 10 mM sodium azide and 50 mM 2-deoxy-D-glucose for 1 h before adding the fluorescein-labeled peptide. During 1 h incubation, the 5 μM of F'-[KR₄W₄] was prepared in the Opti-MEM® I reduced serum medium in the presence of 10 mM sodium azide and 50 mM 2-deoxy- D-glucose. Then the cells were incubated with this solution for 1 h. The subsequent sample preparation and flow cytometry analysis protocol were similar to the protocol described above.

Confocal Laser Scanning Microscopy (CLSM). SK-OV-3 cells were seeded with complete EMEM on coverslips in 6-well plate (1×10^5 cells/well) and kept until 50% confluency. The media were removed, and cells were incubated with 10 μ M F'-[KR₄W₄] in Gibco® Opti-MEM® I reduced serum medium (Life Technologies, Grand Island, NY) for 1 h at 37 °C. Then cells were washed with 1× phosphate buffered saline with calcium and magnesium (PBS⁺) three times. The coverslips were mounted on microscope slides, and images were obtained using Carl Zeiss LSM 700 system with a 488 nm argon ion laser excitation and a BP 505-530 nm band pass filter.

RESULTS AND DISCUSSION

Chemistry

All fourteen peptides **1-14** (Table 1) were synthesized by Fmoc/*t*Bu solid-phase peptide synthesis as described above. Peptides **1-6** were synthesized for this study and peptides **7-14** have already been reported in Manuscript II for cellular uptake. Peptides **1-4** were designed to have positive charge and hydrophobic moieties. On the other hand, peptides **5** and **6** were designed to have negative charge and hydrophobic moieties for comparative studies. Peptides **7-13** have cyclic polyarginines and hydrophobic fatty acids or tryptophan. Peptide **14** was synthesized as linear counterpart of peptide **13**. The chemical structures of synthesized peptides are shown in Figure 1.

As a representative example, the synthesis of [R₄W₄] is described here (Scheme 1). Fmoc-Trp(Boc)-OH was coupled on H-Trp(Boc)-2-chlorotrityl resin three times using HBTU, HOBT, and DIPEA in DMF. Piperidine in DMF (20% v/v) was used to

remove Fmoc group after each coupling. The subsequent coupling of Fmoc-Arg(pbf)-OH was conducted four times in a similar manner. The linear peptide with protected side chain was cleaved from the resin using TFE/acetic acid/DCM (2:1:7, v/v/v) and cyclized in the presence of HOAT and DIC. Reagent "R", trifluoroacetic acid/thioanisole/1,2-ethanedithiol/anisole (90:5:3:2 v/v/v/v), was added to remove side chain protecting groups to yield crude peptide **1**. The peptide was purified by a preparative RP-HPLC system as described in the experimental section.

Antibacterial Activities

MIC and IC₅₀ values were measured for the fourteen peptides against MRSA and *P. aeruginosa* (Table 2). These two bacterial strains are the representative strains of Gram-positive and Gram-negative pathogens. MRSA is the most common Gram-positive pathogen that causes life-threatening infection, while *Pseudomonas aeruginosa* is a Gram-negative multi-drug resistant pathogen which can use multidrug efflux pumps and gene mutations.²² Overall, these peptides were more potent against the Gram-positive MRSA than the Gram-negative *P. aeruginosa*. The lowest MIC values against *P. aeruginosa* was 21.7 µg/mL (15.6 µM) of peptide **2** while other compounds showed MICs more than 37.0 µg/mL (31.3 µM). Peptide **1** was the most potent peptide against MRSA with a MIC value 2.67 µg/mL (1.95 µM). Cyclic peptides **1**, **3**, **9**, **10**, and **13** showed better antibacterial activities compared to linear peptides **2**, **4**, and **14**. Acylated cyclic peptides **9**, **10**, and **13** exhibited more potent activity than the non-acylated cyclic peptide **7**. These data are consistent with the cell-penetrating property of amphiphilic peptides described in Manuscript II. The

correlation between antimicrobial activity and cell-penetrating property is presumably due to the interaction between positively charged amphiphilic peptides and bacterial membranes that have negatively charged components. These data explain why negatively charged peptides **5** and **6** did not show any antibacterial activities. Peptide **1** showed promising results as an antimicrobial peptide against MRSA. Thus, it was selected for further synergistic studies.

Combination effect of peptides and tetracycline against MRSA

Based on antibacterial activity screening, peptides **1**, **9**, **10**, and **13** were selected to determine whether they could increase the antibacterial activity when co-incubated with tetracycline. Non-acylated cyclic peptide **7** was used as a control since it showed the lowest potency and was structurally different from other cyclic peptides. Peptide **1** in combination with tetracycline showed the most potent antibacterial activity with a MIC value of 0.12 µg/mL against MRSA (Table 3). Peptides **9**, **10**, and **13** exhibited MIC values of 0.19-0.22 µg/mL. Among all peptides, control non-acylated peptide **7** exhibited the lowest potency (MIC = 0.31 µg/mL).

Fraction inhibitory concentration (FIC) index has been widely used to examine the interaction between two antibiotics.²³ When drug A and drug B are applied in combination, FIC index can be calculated by the equation 'FIC index = MIC (A in combination with B)/MIC (A alone) + MIC (B in combination with A)/ MIC (B alone)'.^{24,25} The FIC index values are interpreted as 'synergy' with FIC ≤ 0.5, 'partial synergy' with FIC between 0.5 and 1, 'indifference' with FIC 1-4, and 'antagonism'

with $FIC > 4$.^{23,26,27} According to this definition, the combination of peptide **1** and tetracycline can be defined as partial synergy (Table 3).

Time-kill Studies against MRSA and *E. coli*

Time-kill studies were conducted to evaluate the antimicrobial activity of peptide **1** alone and in combination with tetracycline against MRSA and *E. coli* over 24 h. Peptide **1** and tetracycline alone did not demonstrate bactericidal ($>3 \log_{10}$ CFU/mL reduction) activity against MRSA. Combinations of two times the MIC of peptide **1** with four and eight times the MIC of tetracycline demonstrated bactericidal activity against MRSA by 24 h. Thus, combinations of peptide **1** and tetracycline did not meet the definition for synergy against MRSA. However, the combination of the two compounds turned the bacteriostatic activities of tetracycline and peptide **1** into the bactericidal activity.

Peptide **1** alone was able to produce bactericidal activity alone against *E. coli* only at the highest concentration tested ($8\times$ the MIC). All combinations of peptide **1** and tetracycline demonstrated bactericidal activity at 24 h. The combination of eight times the MIC of tetracycline and $2\times$ the MIC of peptide **1** also demonstrated synergy at 24 h. More studies are required to determine the mechanism of synergism. One assumption is that amphiphilic peptide **1** acts as cell-penetrating peptide and can deliver tetracycline at higher concentration. The fluorescence studies using peptide **1** and tetracycline were challenging because emission and excitation range for tetracycline were outside the range determined by the flow cytometer.

Cytotoxicity Assay of Peptide 1

The cytotoxicity of peptide **1** was evaluated by MTS proliferation assay against human ovarian adenocarcinoma SK-OV-3, human leukemia CCRF-CEM, and human embryonic kidney HEK 293T cell lines. In both cancer and normal cell lines, the compound showed more than 84% cell viability at 15 μ M (20.5 μ g/mL) concentration (Figure 3). Peptide **1** alone showed 2.67 μ g/mL MIC against MRSA that is significantly lower than the cytotoxic concentration of peptide **1**. Furthermore, the therapeutic index peptide **1** was increased when was combined with tetracycline showing a MIC value of 0.12 μ g/mL, exhibiting partial synergistic effect. Therefore, the combination of peptide **1** with tetracycline can be used to enhance the therapeutic index.

Cell-Penetrating Property of Peptide 1 ([R₄W₄])

Peptide **1** was originally designed as a CPP to have cell-penetrating property. Thus, we synthesized fluorescein-labeled peptide **1** (F'-[KR₄W₄]) for cellular uptake assays, where F' is fluorescein. The fluorescein-labeled peptide, F'-[KR₄W₄] (10 μ M) was added to SK-OV-3 cells and incubated for 1 h at 37 °C. Confocal laser scanning microscope (CLSM) images showed that the fluorescein-labeled peptide was dispersed into the nucleus and cytosol (Figure 4), but no significant fluorescence was observed in the cells treated with fluorescein alone under the similar condition (data not shown).

The mechanism of cellular uptake was investigated by a temperature control assay at 4 °C and ATP depletion assay. The cellular uptake of peptide **1** was decreased about 59% at 4 °C, indicating that the cellular uptake occurred by both endocytotic

and nonendocytotic pathways (Figure 5). ATP depletion assay also supports this mixed pathways because there was 80% intracellular transportation even though all energy source was blocked by sodium azide and 2-deoxy-D-glucose. These results were consistent with the previous studies that indicated that intracellular transportation can be controlled by several mixed pathways.²⁸

CONCLUSION

Amphiphilic cyclic CPPs (peptides **1**, **9**, **10**, and **13**) exhibited potent antibacterial activities against Gram-positive MRSA in the range of 2.67–9.75 µg/mL. Cyclic peptides showed better antibacterial activities compared to the corresponding linear counterparts. Fatty acylated cyclic peptides exhibited more potency versus non-acylated cyclic peptide. The antibacterial activity correlates well with cell-penetrating property of the same peptides. These data suggest that amphiphilic cyclic CPPs with improved cellular uptake leads to more potent antibacterial activity. Moreover, we found the combination of amphiphilic cyclic CPPs with tetracycline can be partially synergistic and thus may be more effective in the treatment of multidrug-resistant pathogens. Time-kill study showed both peptide **1** and tetracycline had bacteriostatic activities for MRSA and *E. coli*. However, the combination of those two compounds exhibited bactericidal activities in both pathogens. The data provide insights in exploring the combination of amphiphilic cyclic peptides with other antibiotics. This study suggests that amphiphilic cyclic CPPs could provide alternative strategy in defeating life-threatening infectious diseases.

ACKNOWLEDGMENTS

We acknowledge the American Cancer Society, Grant No. RSG-07-290-01-CDD for the financial support. We thank National Center for Research Resources, NIH, and Grant Number 8 P20 GM103430-12 for sponsoring the core facility. This material is based upon work conducted at a research facility at the University of Rhode Island supported in part by the National Science Foundation EPSCoR Cooperative Agreement #EPS-1004057.

ABBREVIATIONS

AMPs, antimicrobial peptides; ACPPs, acylated cyclic polyarginine peptides; ATP, adenosine triphosphate; Boc, tert-Butoxycarbonyl; CCRF-CEM, human leukemia carcinoma cell line; CFU, colony-forming unit; CLSM, confocal laser scanning microscopy; CPPs, cell-penetrating peptides; DCM, dichloromethane; Dde, 1-(4,4-dimethyl-2,6-dioxocyclohex-1-ylidene)ethyl; DIC, *N,N'*-diisopropylcarbodiimide; DIPEA, *N,N*-diisopropylethylamine; DMF, *N,N*-dimethylformamide; EDT, 1,2-ethanedithiol; EDTA, ethylenediaminetetraacetic acid; EMEM, eagle's minimum essential medium; FAM, 5(6)-carboxyfluorescein; FAM-NHS, 5(6)-carboxyfluorescein *N*-hydroxysuccinimide ester; FBS, fetal bovine serum; Fmoc, 9-fluorenylmethoxycarbonyl; FACS, fluorescence activated cell sorter; HBTU, 2-(1*H*-Benzotriazole-1-yl)-1,1,3,3-tetramethyluronium hexafluorophosphate; HEK 293T, human embryonic kidney cell line; HOAT, 1-hydroxy-7-azabenzotriazole; HIV, human immunodeficiency virus; HOBT, hydroxybenzotriazole; MALDI-TOF, matrix-assisted laser desorption/ionization-time of flight; MHB, Mueller Hinton

Broth; MIC, minimum inhibitory concentration; MRSA, methicillin-resistant *Staphylococcus aureus*; MTS, (3-(4,5-dimethylthiazol-2-yl)-5-(3-carboxymethoxyphenyl)-2-(4-sulfophenyl)-2H-tetrazolium); Pbf, 2,2,4,6,7-pentamethyldihydrobenzofuran-5-sulfonyl; PBS, phosphate buffered saline; PyAOP, 7-azabenzotriazol-1-yl-oxytris(pyrrolidino)phosphonium hexafluorophosphate; RP-HPLC, reversed-phase high pressure liquid chromatography; SK-OV-3, human ovarian adenocarcinoma cell line; TFA, trifluoroacetic acid; TFE, 2,2,2-trifluoroethanol; TIS, triisopropylsilane; TSB, tryptic soy broth.

REFERENCES

- (1) Moellering, R. C. MRSA: The first half century. *J. Antimicrob. Chemother.* **2012**, *67*, 4–11.
- (2) David, M. Z.; Daum, R. S. Community-associated methicillin-resistant *Staphylococcus aureus*: epidemiology and clinical consequences of an emerging epidemic. *Clin. Microbiol. Rev.* **2010**, *23*, 616–687.
- (3) Klein, E. Y.; Sun, L.; Smith, D. L.; Laxminarayan, R. The changing epidemiology of methicillin-resistant *Staphylococcus aureus* in the United States: A national observational study. *Am. J. Epidemiol.* **2013**, *177*, 666–674.
- (4) Klevens, R. M.; Morrison, M. A.; Nadle, J.; Petit, S.; Gershman, K.; Ray, S.; Harrison, L. H.; Lynfield, R.; Dumyati, G.; Townes, J. M.; et al. Invasive methicillin-resistant *Staphylococcus aureus* infections in the United States. *JAMA J. Am. Med. Assoc.* **2007**, *298*, 1763–1771.
- (5) Hiramatsu, K. Vancomycin-resistant *Staphylococcus aureus*: A new model of antibiotic resistance. *Lancet Infect. Dis.* **2001**, *1*, 147–155.
- (6) Steenbergen, J. N.; Alder, J.; Thorne, G. M.; Tally, F. P. Daptomycin: A lipopeptide antibiotic for the treatment of serious Gram-positive infections. *J. Antimicrob. Chemother.* **2005**, *55*, 283–288.
- (7) Hayden, M. K.; Rezai, K.; Hayes, R. A.; Lolans, K.; Quinn, J. P.; Weinstein, R. A. Development of daptomycin resistance in vivo in methicillin-resistant *Staphylococcus aureus*. *J. Clin. Microbiol.* **2005**, *43*, 5285–5287.
- (8) Fjell, C. D.; Hiss, J. A.; Hancock, R. E. W.; Schneider, G. Designing antimicrobial peptides: Form follows function. *Nat. Rev. Drug Discov.* **2012**, *11*, 37–51.

- (9) Lohner, K. New strategies for novel antibiotics: Peptides targeting bacterial cell membranes. *Gen. Physiol. Biophys.* **2009**, *28*, 105–116.
- (10) Lehrer, R. I.; Ganz, T. Antimicrobial peptides in mammalian and insect host defence. *Curr. Opin. Immunol.* **1999**, *11*, 23–27.
- (11) Rinaldi, A. C. Antimicrobial peptides from amphibian skin: An expanding scenario: commentary. *Curr. Opin. Chem. Biol.* **2002**, *6*, 799–804.
- (12) Fox, J. L. Antimicrobial peptides sage a comeback. *Nat. Biotechnol.* **2013**, *31*, 379–382.
- (13) Snyder, E. L.; Dowdy, S. F. Cell penetrating peptides in drug delivery. *Pharm. Res.* **2004**, *21*, 389–393.
- (14) Vivès, E.; Schmidt, J.; Pèlerin, A. Cell-penetrating and cell-targeting peptides in drug delivery. *Biochim. Biophys. Acta* **2008**, *1786*, 126–138.
- (15) Mandal, D.; Nasrolahi Shirazi, A.; Parang, K. Cell-penetrating homochiral cyclic peptides as nuclear-targeting molecular transporters. *Angew. Chem. Int. Ed.* **2011**, *50*, 9633–9637.
- (16) Nguyen, L. T.; Chau, J. K.; Perry, N. A.; de Boer, L.; Zaat, S. A. J.; Vogel, H. J. Serum Stabilities of short tryptophan- and arginine-rich antimicrobial peptide analogs. *PLoS ONE* **2010**, *5*, e12684.
- (17) Lättig-Tünnemann, G.; Prinz, M.; Hoffmann, D.; Behlke, J.; Palm-Apergi, C.; Morano, I.; Herce, H. D.; Cardoso, M. C. Backbone rigidity and static presentation of guanidinium groups increases cellular uptake of arginine-rich cell-penetrating peptides. *Nat. Commun.* **2011**, *2*, 453.

- (18) Epanand, R. M.; Vogel, H. J. Diversity of antimicrobial peptides and their mechanisms of action. *Biochim. Biophys. Acta* **1999**, *1462*, 11–28.
- (19) Clinical and Laboratory Standards Institute. *Methods for dilution antimicrobial susceptibility tests for bacteria that grow aerobically; Approved standard M7-A7*; National Committee for Clinical Laboratory Standards: Wayne, PA, 1997.
- (20) Clinical and Laboratory Standards Institute. *Methods for dilution antimicrobial susceptibility tests for bacteria that grow aerobically; Approved standard - ninth edition. M07-A9*; Clinical and Laboratory Standards Institute: Wayne, PA, 2012.
- (21) LaPlante, K. L.; Rybak, M. J. Clinical glycopeptide-intermediate Staphylococci tested against arbekacin, daptomycin, and tigecycline. *Diagn. Microbiol. Infect. Dis.* **2004**, *50*, 125–130.
- (22) Aeschlimann, J. R. The role of multidrug efflux pumps in the antibiotic resistance of *Pseudomonas aeruginosa* and other Gram-negative bacteria. Insights from the society of infectious diseases pharmacists. *Pharmacotherapy* **2003**, *23*, 916–924.
- (23) Hall, M. J.; Middleton, R. F.; Westmacott, D. The fractional inhibitory concentration (FIC) index as a measure of synergy. *J. Antimicrob. Chemother.* **1983**, *11*, 427–433.
- (24) Berenbaum, M. C. A method for testing for synergy with any number of agents. *J. Infect. Dis.* **1978**, *137*, 122–130.
- (25) Koneman, E. W. *Diagnostic microbiology: Color atlas and textbook of*; J.B. Lippincott, 1997.
- (26) López-Brea, M.; Domingo, D.; Sánchez, I.; Prieto, N.; Alarcón, T. Study of the Combination of ranitidine bismuth citrate and metronidazole against metronidazole-

resistant *Helicobacter pylori* clinical isolates. *J. Antimicrob. Chemother.* **1998**, *42*, 309–314.

(27) Eliopoulos, G. M.; Moellering, R. C. Antimicrobial combinations. In *antibiotics in laboratory medicine*; Williams & Wilkins, Co.: Baltimore, MD USA, 2000; pp. 432–449.

(28) Madani, F.; Lindberg, S.; Langel, U.; Futaki, S.; Gräslund, A. Mechanisms of cellular uptake of cell-penetrating peptides. *J. Biophys. Hindawi Publ. Corp. Online* **2011**, *2011*, 414729.

Table legends

Table 1: Synthetized peptides list used for antimicrobial activity

Table 2: Antibacterial activities of synthetic peptides against Gram-positive and Gram-negative strains

Table 3: Antimicrobial activity of peptides in combination with tetracycline against MRSA

Figure legends

Figure 1: Chemical structures of synthetic peptides examined for antimicrobial activity

Figure 2: Time-kill curves of peptide 1, tetracycline, and combination for MRSA (ATCC 43300) and *E. coli* (ATCC 35218) at 37 °C for 24 h. Peptide 1 at two times the MIC was combined with tetracycline at one, two, four and eight times (MICs of peptide 1: 4 µg/mL for MRSA and 16 µg/mL for *E. coli*; tetracycline (TC): 0.5 µg/mL for MRSA and 2 µg/mL for *E. coli*).

Figure 3: Cytotoxicity assay of peptide 1 by MTS-PMS assay (24 h incubation)

Figure 4: Confocal laser scanning microscope image of F'-[KR₄W₄] (10 µM) in SK-OV-3 cells (1 h incubation).

Figure 5: Energy-dependent mechanistic study of intracellular uptake for F'-[KW₄R₄]. Cellular uptake was investigated under 4 °C and ATP depletion conditions.

Scheme legends

Scheme 1: The synthesis of peptide 1 ([R₄W₄])

Table 1

Peptide No.	Peptide sequence	Abbreviation
1	[RRRRWWWW]	[R ₄ W ₄]
2	RRRRWWWW-COOH	R ₄ W ₄
3	[RRRRWWW]	[R ₄ W ₃]
4	RRRRWWW-COOH	R ₄ W ₃
5	[EEEEWWWW]	[E ₄ W ₄]
6	[EEEEWWW]	[E ₄ W ₃]
7	[KRRRRR]	[KR ₅]
8	Octanoyl-[KRRRRR]	C ₈ -[R ₅]
9	Dodecanoyl-[KRRRRR]	C ₁₂ -[R ₅]
10	Hexadecanoyl-[KRRRRR]	C ₁₆ -[R ₅]
11	<i>N</i> -Acetyl-L-tryptophanyl-12-aminododecanoyl-[KRRRRR]	W-C ₁₂ -[R ₅]
12	<i>N</i> -Acetyl-WWWW-[KRRRRR]	W ₄ -[R ₅]
13	Dodecanoyl-[KRRRRR]	C ₁₂ -[R ₆]
14	Dodecanoyl-KRRRRR-COOH	C ₁₂ -(R ₅)

Table 2

Peptide No.	Methicillin-resistant <i>Staphylococcus aureus</i>		<i>Pseudomonas aeruginosa</i>	
	MIC ($\mu\text{g/mL}$) ^a	IC ₅₀ (μM) \pm SD ^b	MIC ($\mu\text{g/mL}$)	IC ₅₀ (μM) \pm SD
1	2.67 (1.95)	NA	42.8 (31.3)	3.1 \pm 0.7
2	43.4 (31.3)	16.3 \pm 1.7	21.7 (15.6)	9.6 \pm 1.2
3	18.5 (15.6)	10.3 \pm 1.0	37.0 (31.3)	9.8 \pm 2.7
4	150 (125)	82.5 \pm 30.9	150 (125)	33.1 \pm 3.1
5	>158 (>125)	NA	>158 (>125)	NA
6	>134 (>125)	NA	>134 (>125)	NA
7	>114 (>125)	NA	>114 (>125)	NA
8	129 (125)	81.1 \pm 2.9	>129 (>125)	NA
9	8.53 (7.81)	4.4 \pm 0.3	136 (125)	41.0 \pm 6.2
10	8.97 (7.81)	4.7 \pm 1.6	>143 (>125)	NA
11	83.4 (62.5)	26.2 \pm 10.0	167 (125)	44.0 \pm 3.9
12	53.0 (31.3)	19.5 \pm 3.5	>212 (>125)	NA
13	9.75 (7.81)	3.9 \pm 0.02	156 (125)	45.3 \pm 5.6
14	69.3 (62.5)	27.7 \pm 3.0	>139(>125)	NA
Control ^c	0.156 (0.352)	0.13 \pm 0.01	0.731 (1.56)	NA

^aValue in parenthesis presents MIC in micromolar concentration; ^bData are presented as means \pm standard deviation where applicable; ^cTetracycline and tobramycin were used as control for MRSA and *P. aeruginosa*, respectively.

Table 3

Compounds	MIC ($\mu\text{g/mL}$)	IC₅₀ (μM) \pm SD^a	FIC index^b
1 + TC^c	0.12	0.08	0.8
7 + TC	0.31	0.11 \pm 0.01	NA
9 + TC	0.20	0.10 \pm 0.01	1.2
10 + TC	0.22	0.13 \pm 0.04	1.3
13 + TC	0.19	0.13 \pm 0.02	1.4
TC	0.15	0.15 \pm 0.02	-

^aData are presented as means \pm standard deviation where applicable; ^bFraction inhibitory concentration (FIC) index = MIC (A in combination with B)/MIC (A alone) + MIC (B in combination with A)/MIC (B alone). Synergy: FIC \leq 0.5; partial synergy: 0.5 < FIC \leq 1; indifference: 1 < FIC \leq 4; antagonism: FIC > 4; ^cTC stands for tetracycline.

Figure 1

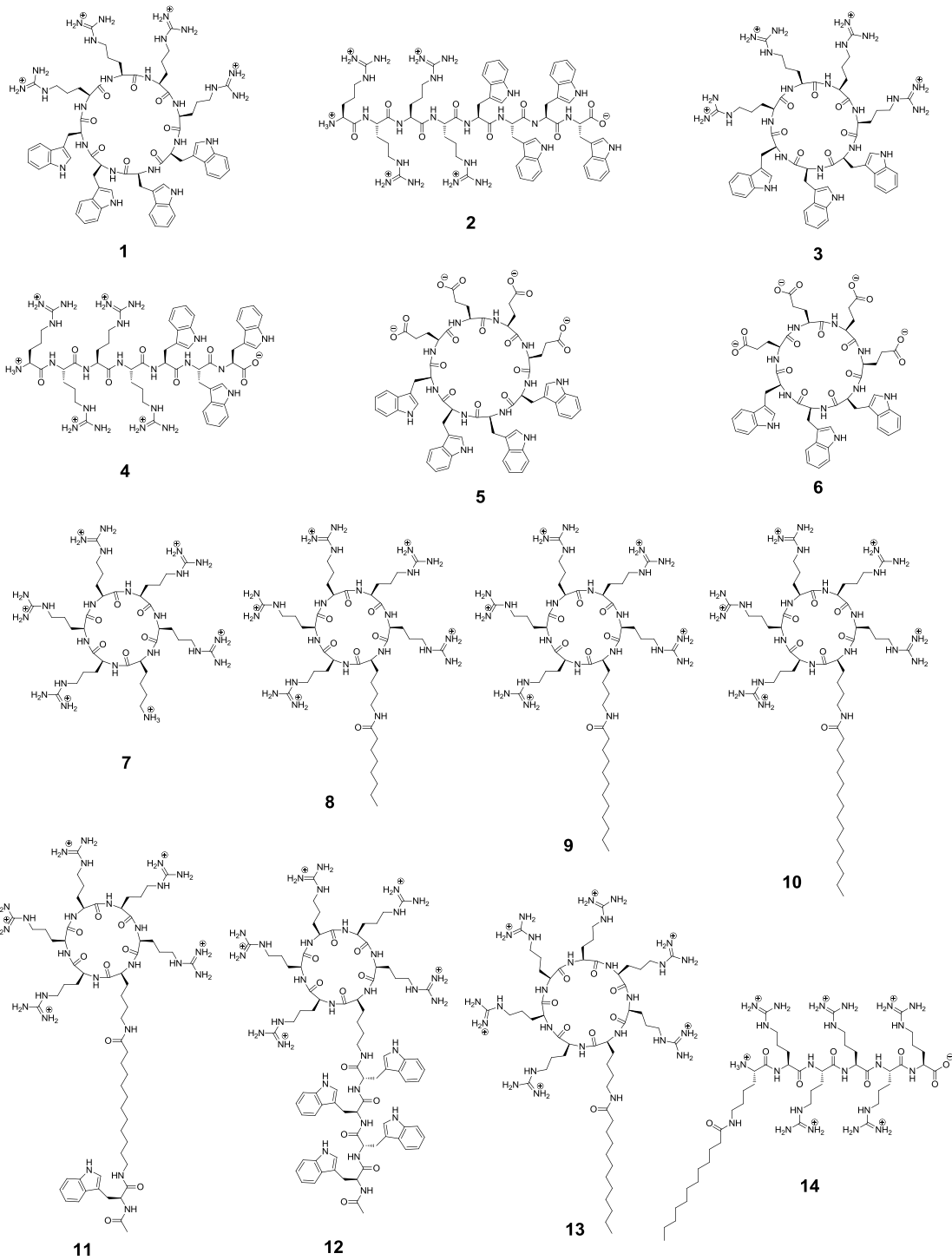


Figure 3

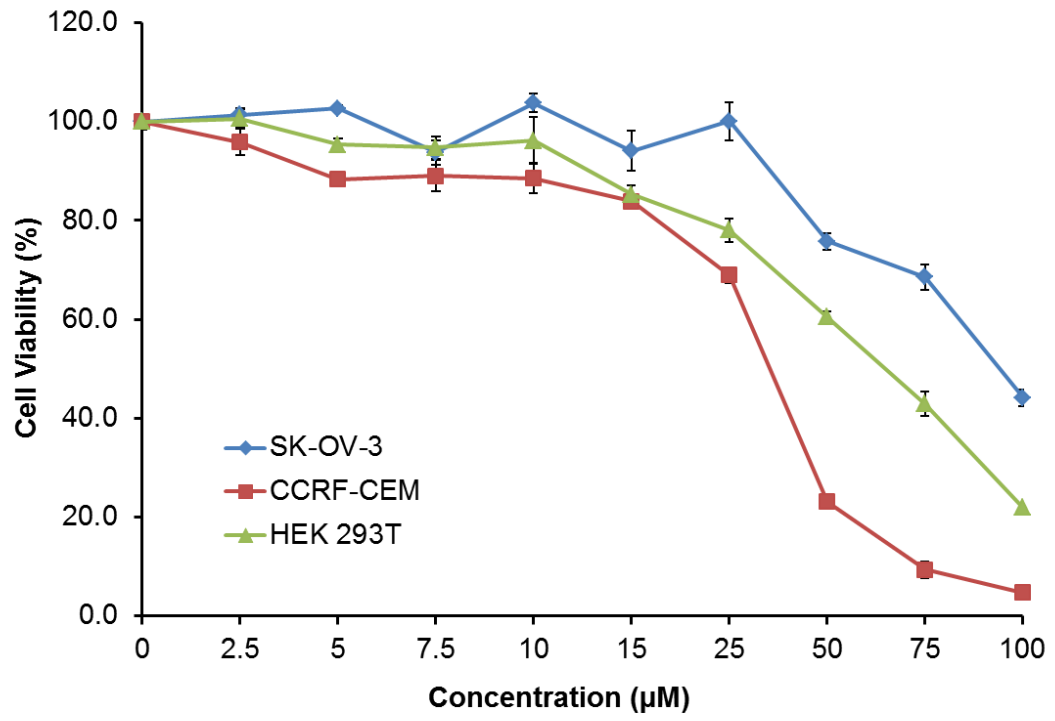


Figure 4

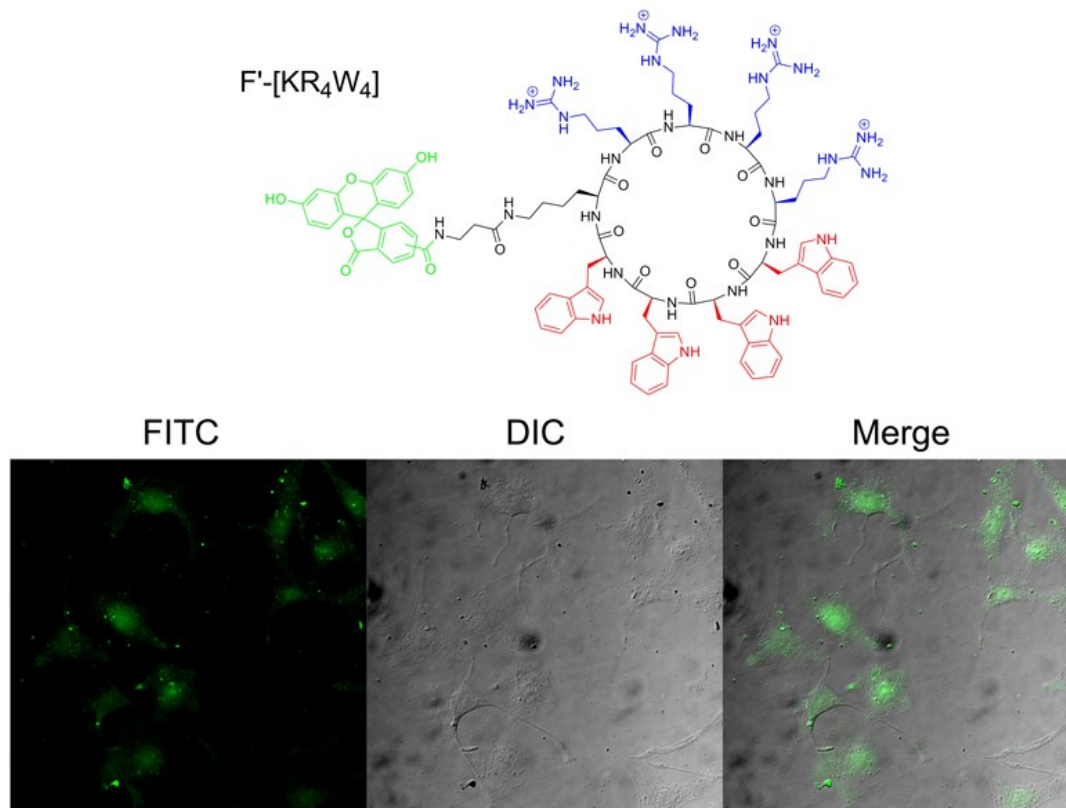
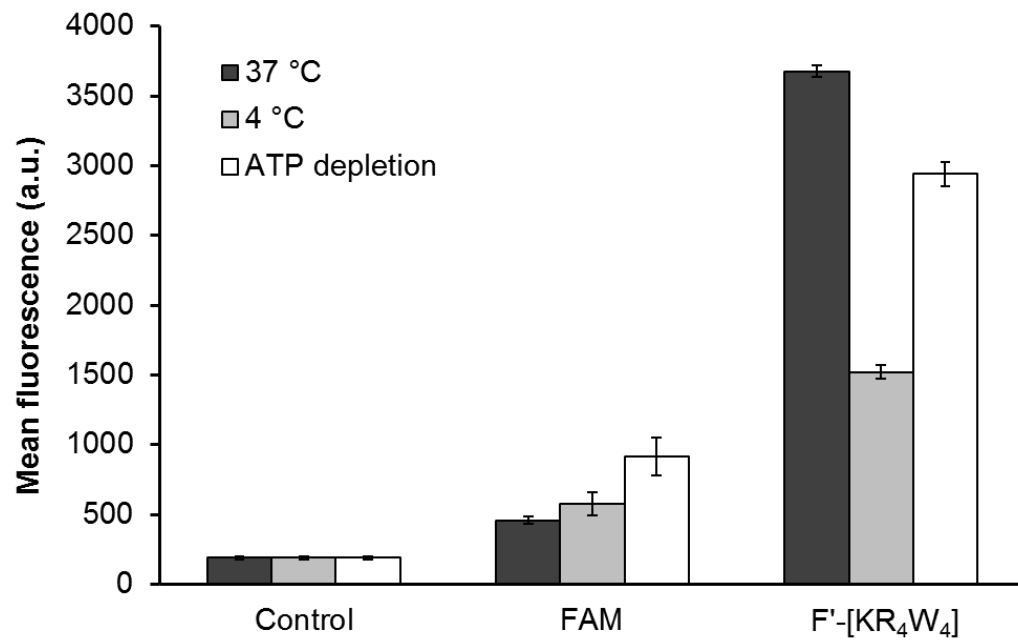


Figure 5



Scheme 1

